

Replies to review comments

We thank the reviewers and the co-editor for the time and effort spent on the manuscript. Please find our point-by-point replies below (in blue color and italics). A revised manuscript with tracked changes will be uploaded.

In the revision of the manuscript, we made the following major changes:

1. The term “SO₂ emission rate” in the manuscript was changed into “SO₂ emission time series”.
2. Equation (1) was added to Section 2.1 to define the AIRS SO₂ index used in this paper. Equations (2)-(4) are added to Section 2.3 to explain the MIPAS aerosol detections used in this paper and a brief comment on the MIPAS aerosol data is added too.
3. A brief explanation on the “1.5-day forward and backward trajectories” that we calculated to generate more aerosol data points based on the MIPAS aerosol detections is added in Section 4.2.
4. A brief explanation on the water vapor recorder is added in Section 4.3.
5. A further discussion on the robustness of the percentage of SO₂ that entered the tropical stratosphere is added in Section 5.
6. In the discussion and summary, we changed the estimated amount of sulfate aerosol added to the tropical stratosphere to “0.06±0.01 Tg”, instead of 0.07 Tg in the original version. This estimate was made based on the “1.2±0.2 Tg” of SO₂ injected into the upper troposphere and lower stratosphere (Haywood et al., 2010).
6. The wind vector scale is added in Fig. 1.
7. A dashed line is added in the middle and bottom panels of Fig.5 to show the time of the end of the model simulation. In the bottom panel of Fig. 5, time series of the number of MIPAS aerosol detections above the 380 K and the 400 K isentropic surfaces between 30°N and 30°S are added. The explanation of Fig.5 is changed accordingly in Section 4.1.
8. Languages errors have been fixed.

Anonymous Referee #1

Received and published: 16 June 2017

Wu et al. present a case study of the dispersion of the volcanic plume from the Mt. Sarachev eruption in 2009. They effectively demonstrate the use of AIRS SO₂ observations and a back-trajectory methodology to provide time- and altitude-dependent volcanic SO₂ emission rates for their transport simulations. The authors make good use of AIRS and MIPAS observations to judge the fidelity of their trajectory based transport simulations, which demonstrate the role of the Asian monsoon anticyclone in steering a small but significant contribution of the Sarachev plume to stratospheric aerosol in the tropics.

The paper is generally well written, and will be a useful addition to the literature on this subject. I have some minor points of clarification, below, which should be addressed.

p.3, line 23: ref “NASA operational data products” Please clarify what products are referred to (OMI?), and why the SO₂ index used here is considered “better”.

According to the AIRS Version 6 Release Level 2 Product User Guide, the operational SO₂ index in the operational AIRS Level-1B and Level-2 data products uses the channels of 1361.44 cm⁻¹ and 1433.06 cm⁻¹. The SO₂ index used in this study is calculated based on the brightness temperature differences of 1407.21 cm⁻¹ and 1371.52 cm⁻¹. After comparing with the operational AIRS SO₂ index, the SO₂ index used here was found to be more sensitive and better at suppressing emissions of interfering species (Hoffmann et al., 2014).

We replaced “NASA operational data products” by “AIRS operational SO₂ index products” to clarify.

p.4, line 16: what about Dx in the stratosphere and Dz in the troposphere? I note that Hoffman et al. (2016) uses the same values in the stratosphere and troposphere.

Dx and Dz is assigned to be 50 m² s⁻¹ and 0 m² s⁻¹ in the troposphere and 0 m² s⁻¹ and 0.1 m² s⁻¹ in the stratosphere. We have made a change in this sentence to clarify.

p.4, line 19: do you mean constituent (i.e. SO₂) mass here?

Yes, it has been clarified as “the mass of SO₂” in this sentence.

p.5, line 16: Units of emission rate are given in kg m⁻¹ s⁻¹. Why m⁻¹, not m⁻³?

In our study, we considered the SO₂ emission within a column with a radius of 75 km over the location of Sarychev. So the unit of the SO₂ emission kg m⁻¹ s⁻¹ can be simply converted to kg m⁻³ s⁻¹ by dividing by the area. In Fig. 2, we decide to group the SO₂ emission only by time and altitude instead of showing the area-averaged value.

“kg m⁻¹ s⁻¹” may not be a reasonable unit for “rate”, so we decide to change the “SO₂ emission rate” in this paper to “SO₂ emission time series”.

p.5, line 36: split (sp)

Fixed. Thank you.

p.7, line 15: the ASM anticyclone

Fixed. Thank you.

p.7, lines 19-20: sentence is unclear. Many more aerosol detections are found N of the subtropical jet between 360-400K.

Fixed. Thank you.

Figures 8, 9, 10, and 11: the PV (black) and geopotential height (red) contours shown appear to be identical for July 10th, July 20th and July 31st. This would appear to be a mistake. The flow fields should change.

Based on the explanation and calculation method of the PV-based transport barrier (Ploeger et al., 2015), it is not always possible to define a transport barrier on each day or in any month when the Asian summer monsoon is not strong. So we have to show the monthly mean PV-based transport barrier in our figures. That is why the black contours in our figures, which denote the PV-based transport barrier, are identical. And in June, a PV-based transport barrier is not found, so there is no black contour for the top-left panel in Fig.8–11.

To make it consistent, we also used the monthly mean geopotential height. So the red contours in our figures are identical too.

Thank you for pointing this out. We have added a sentence in the caption of Fig. 8 to clarify.

p.8, lines 24-25: I see very few MIPAS aerosol detections south of 30N in Fig. 11 (number of detections above 400K), or for the simulated air parcels (Fig.10) so where is “the increased aerosol in the tropical stratosphere above 400K” the authors referring to here?

Here we refer to the MIPAS aerosol detections with altitude higher than ~18 km shown in the original Fig.5. A sentence has been added here to clarify. And we have revised the Fig.5 in the revised manuscript, so the aerosol above 380 K and above 400 K is shown clearer.

p.8, lines 28-37, ref - Figure 13: as above, none of the earlier figures demonstrate Sarachev aerosol in the tropics above 400K. Is this then, the first evidence shown of Sarachev aerosol ascending in the tropics? Maybe Fig.13 should be introduced earlier.

In the revised Fig.5, the altitudes and aerosol and number of MIPAS aerosol detections in the tropical stratosphere above 400K are added. Actually it is in the Fig. 5 was the evidence of Sarychev aerosol in the tropics first shown.

p.9, line 18, ASM anticyclone

Fixed. Thank you.

Anonymous Referee #2

Received and published: 16 June 2017

Wu et al. studied the dispersion of volcanic aerosols after Sarychev eruption in 2009. The study mainly uses trajectory model, and observations from AIRS and MIPAS. It shows a fairly good model-observation comparison on the SO₂ plumes. Wu et al. suggests a 4% of Sarychev aerosol goes to the Tropical Stratosphere with the help of ASM circulations. In general the topic is interesting, however many issues need to be resolved.

Main Concern:

1. Is your “4%” significant statistics? What is the confidence interval? How is the 4% of volcanic aerosols from Sarychev compared with local background aerosol?

The “4%” is roughly calculated by dividing the number of SO₂ parcels between 30°N and 30°S above the 380 K isentropic surface by the total number of SO₂ parcels released into the upper troposphere and lower stratosphere. A brief explanation has been added in Section 4.1.

In the revised manuscript, we included the time series of the number of MIPAS aerosol detection in the stratosphere between 30°N and 30°S in the bottom panel of Fig. 5. These time series show that the number of MIPAS aerosol detections at the end of July 2009, when this “4%” is calculated, is increased by about six times compared with the number before the Sarychev eruption occurred.

In the discussion section, we also estimated the mass of sulfate aerosol entering the tropics after the Sarychev eruption. Although the “4%” seems to be small, but the mass of sulfate aerosol is several times larger than the background aerosol.

2. I believe one of the evidence for your equator-ward is MIPAS aerosol detection number data (Figure 5C). The color scale makes it quite difficult to tell the numbers, look like there is a factor of 5+ more detections between May 2009 and May 2010. Is it consistent with your estimate? 4% of volcanic aerosol vs. background?

We have revised Fig. 5. In the bottom panel, the number of MIPAS aerosol detections in the tropical stratosphere above 380 K and above 400 K is shown. We hope that this revision makes the numbers clear to readers.

The “4%” is a proportion to the total number of air parcels we have released in the model simulation, but not to the background aerosol layer. Based on the “4%”, we have estimated the mass of sulfate aerosol and the comparison to the background is discussed in the discussion section.

3. Please also comment on uncertainties/noises from observations (MIPAS). Are the signals robust?

Several sentences have been added to Section 2.2 to address the quality of the MIPAS aerosol observations. And the retrieval method is briefly explained in Section 2.2 too.

The MIPAS aerosol observations have been used to show the spatial distribution of volcanic aerosols from three strong volcanic eruptions. Two of them are characterized by large SO₂ emissions (Grímsvötn, Nabro), and one is characterized with volcanic ash (Puyehue–Cordón Caulle). The MIPAS observations for these three cases were compared with horizontal high-resolution AIRS SO₂ and ash index, which verified the capacity of the MIPAS aerosol retrievals in differentiating the aerosol, clear sky, clouds, and ashes (Griessbach et al., 2016).

4. Figure 13, you argue the gap between 2009.10 and 2010.2 is due to temperature perturbation. Are you suggesting H₂SO₄-H₂O aerosol gets evaporated? I don't think so, the reason is at such low temp, the vapor pressure is super low. Graves may lead to some evaporation, but I assume a few months gap is not expected. Any other reasons? What is the green in early 2009 and late 2010? Any more analysis/evidence suggests they are actually from Sarychev volcanic aerosols for the period of 2009.7-2010.5?

Actually, the gap is due to an aerosol detection method artefact.

The aerosol detection is based on an aerosol-cloud-index (ACI) method described in Griessbach et al. (2016). An analysis of the entire ACI time series shows that there is a very regular gap pattern: every 6 months in about January and July there is a gap. The periodic (semi-annual) changes in the ACI are caused by the radiances in the 960 cm⁻¹ window of the AI. At 960 cm⁻¹ an impact of CO₂ hot bands (at around 50 km) is the most likely explanation for the detection artefact. We added a brief explanation in the revised manuscript.

5. Any chance to expand your study to other high-latitude volcanoes? What is the equator-ward transport sensitive to? E.g. injection latitude, altitude, season, location (in/out of ASM), etc? If you move the

location north/south, do you expect to get different higher/lower fraction than 4%? I assume if injection is too close to ASM, then you parcels will be trapped in ASM anticyclone instead of going further south?

The Sarychev case in our study is a reprehensive case to study how a high-latitude eruption can have a notable influence on the tropical and global stratospheric aerosol layer. After this study, it is also a meaningful work to extend our modelling approach and satellite data to other mid- and high-latitude eruptions that have influenced the tropical stratospheric aerosol loading, e.g., Kasatochi (52 °N, August, 2008) and Calbuco (41 °S, April, 2015), to study the efficiency of transport, transport pathway, and further evaluate the role of high-latitude eruption.

6. I assume your trajectory model doesn't have aerosol microphysics. Will coagulation and some loss terms that happened in real atmosphere affect your results (i.e. 4%)?

Thank you very much for pointing this out. The MPTRAC model does not resolve aerosol microphysics processes. We admit that meteorological conditions (like wind fields, humidity and temperature) will affect the fate of the SO₂ injected into the atmosphere, and of the subsequently formed sulfate aerosols.

The "4%" from our model simulation could be affected by many possible mechanisms of the aerosol loss, like the interaction of sulfate aerosol and clouds, and coagulation with other particles. Larger particle size may result in quicker sedimentation rate, especially at higher altitudes where the mean free path between air molecules far exceeds the particle size and particles fall more rapidly than they would otherwise. The scavenging efficiency of SO₂ could be increased if it is incorporated into growing ice (Textor et al., 2003). Also, SO₂ is slightly soluble in liquid water and it may have a small chance to be washed out during the transport process. But as revealed in our study, the efficient pathway of the transport is approximately between the 360 and 400 K isentropic surfaces, where the atmosphere is relatively dryer, cooler and cleaner than the lower troposphere. So our model results can be considered as an approximate value.

We will add this discussion in our manuscript.

Minor:

1. Define latitude range for tropics in the abstract/beginning of the paper

Added in the introduction. Thank you.

Anonymous Referee #3

Received and published: 19 June 2017

Fundamentally, this paper is about transport of a small amount of Sarychev aerosol into the tropics in the summer of 2009. This is not a new result, and that there is an anticyclone over the Asian summer monsoon that could have provided the circulation that did this, but would not do so in winter, is also quite obvious and well-known.

I cannot understand the units the authors use. 4% of what? Of what parcels? And is this small amount significant? What is the error associated with the calculation of this number? If more than 95% of the aerosols did NOT go to the tropics, isn't that the conventional standard to prove that they did not go to the tropics?

In other words, what is the error bar on this 4%? What is the mass of aerosols that went into the tropics? What difference did they make for the radiative forcing and for the climate response? How important was it? The discussion on p. 9 is confusing. The authors claim that there was 0.07 TgS added, but to what? And they claim that there is a 4-7% annual increase, but of what and where? They spelled Hofmann wrong. And clearly this value is not a long-term amount, and Hofmann et al. measured it for a short period of time and a different period than Sarychev.

A number of recent studies have shown that the background level of the stratosphere aerosol is increasing after 2000, and the Sarychev eruption is one of the volcanic eruptions that have contributed to this increase (e.g., Solomon et al., 2011). This increase of aerosol in the tropical stratosphere can be found using various satellite data.

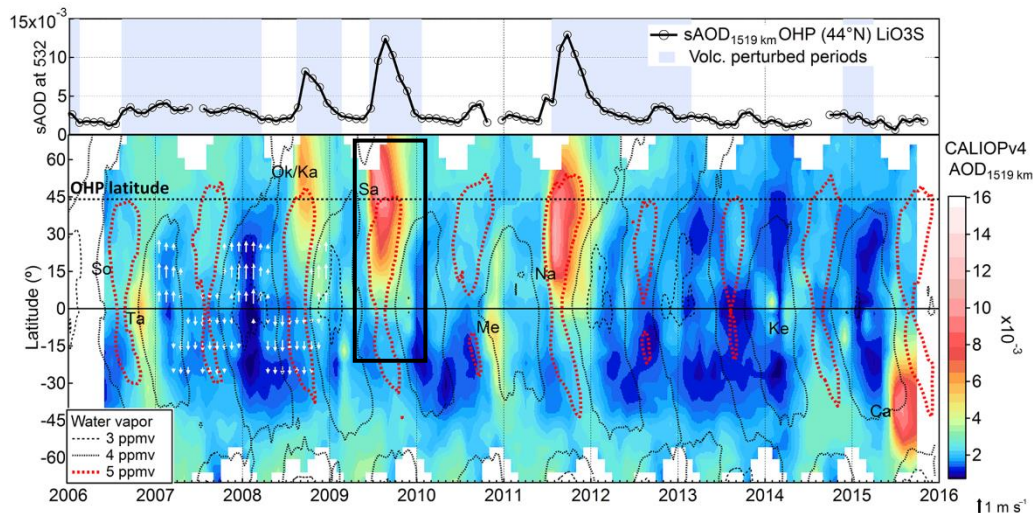


Figure 1. Time series of monthly mean averaged stratospheric aerosol optical depth (AOD) between 15 and 19 km from OHP LiO3S lidar (top) and time-latitude section of zonal-mean AOD from CALIOP in log-scaled color map with indications of VEI 4 eruptions (bottom). Time periods considered as perturbed by volcanism are shaded light blue in the top panel. White arrows (in 2007–2008) represent the mean meridional component of monthly and zonally averaged horizontal wind at 100 hPa from ERA-Interim reanalysis. Dashed and dotted contours depict the zonal-mean water vapor mixing ratio at 100 hPa from Aura MLS.

As shown by the figure from Khaykin et al. (2017), Figure 1, we can see that although the Sarychev peak is located at 48°N, the AOD in the tropical stratosphere was enhanced after its eruption. Just as you mentioned, since the Sarychev eruption happened in summer 2009, one may speculate that the equatorward transport is related to the anticyclonic Rossby wave breaking caused by the Asian summer monsoon (ASM). But one can only assume the ASM helped, but can not answer questions like how did the ASM facilitate the transport? At what vertical range and horizontal location can the ASM help the transport and is there any other factor that can influence the transport? If another high-latitude eruption occurs, can we estimate if the volcanic plume will reach the tropical stratosphere based on information such as the time and location of the eruption and the plume height?

In this study, we show that:

A high-latitude volcanic eruption can significantly influence the tropical stratosphere under favourable meteorological conditions.

The ASM can help to establish transport pathways, but only at specific vertical ranges (360-400 K) and in specific horizontal region (downstream of the ASM anticyclone). The PV-based transport barrier considered in this study marks the boundary of the ASM quite well. It means if the plume is originally outside of the barrier, it may have the chance to be entrained along the circulation and shed to lower latitudes, but if the plume is originally inside of the barrier, it will probably be trapped inside of the ASM.

Also, in this paper, we further established a practical method to simulate the time series of the SO₂ injected by Sarychev eruption, which is also applicable to other volcanic eruptions. Applying this method to other eruption cases, a time and altitude-resolved volcanic SO₂ inventory maybe built up. This part of the work is relatively new, and may be interesting to scientists who want to enrich the SO₂ inventory from volcanisms in their climate model, and scientists who want to compare transport simulations from other Lagrangian trajectory models with ours using the MPTRAC model.

As to the specific questions, the “4%” is roughly calculated by dividing the number of SO₂ parcels end up in the tropical stratosphere (between 30°N and 30°S above the 380 K isentropic surface) by the total number of SO₂ parcels released into the upper troposphere and lower stratosphere. A brief explanation has been added in Section 4.1.

We have stated in our paper that majority of the sulfate aerosol remains at the mid- and high latitudes. However, because the SO₂ mass injected by the Sarychev eruption into the atmosphere is large (1.2 ± 0.2 Tg), the stratospheric aerosol layer in the tropics is significantly enhanced even though only a small fraction “4%” of the sulfate aerosol entered the tropical stratosphere. In our study, we have shown with MIPAS aerosol detections, that at the end of July 2009 and at the beginning of September 2009, the number of MIPAS aerosol detections in the tropical stratosphere is respectively about seven times and 14 times as large as the number before the Sarychev eruption. We have modified Fig. 5 in our paper to make this enhancement clearer. Figure 1 borrowed from Khaykin et al. (2017) can also demonstrate the enhancement of stratospheric aerosol after the Sarychev eruption.

The radiative forcing related to this enhanced aerosol and the climate response are very important to quantify, and they will be part of our future work.

If we assume that 4% of 1.4 Tg of SO₂ released by Sarychev eruption into the upper troposphere and lower stratosphere is entirely converted into gaseous H₂SO₄ and entered the tropical stratosphere in a form of 75%-25% H₂SO₄-H₂O solution, this accounts for an additional 0.07 Tg of sulfate aerosol.

The “4-7% annual increase” in the background stratospheric aerosol layer is not a result from our study. It is a conclusion in the paper of Hofmann et al. (2009). In Hofmann et al. (2009), the authors used long-term lidars observations at Mauna Loa Observatory in Hawaii (19°N) and Boulder in Colorado (40°N) since 1994 and 2000 respectively. Hofmann et al. (2009) find there is an increasing average trend in aerosol backscatter above 20 km after 2000 of about 4–7% per year, which requires 0.015–0.02 TgS per year to maintain (as in Fig. 2).

The Mauna Loa Observatory in Hawaii is located in the tropics, so the stratospheric aerosol data observed there could be a decent long-term record of the tropical stratospheric aerosol. We compare our “0.07 Tg” of sulfate aerosol with this long-term trend to prove the amount of sulfate aerosol added to the tropical stratosphere by the Sarychev eruption is significant comparing with the aerosol background.

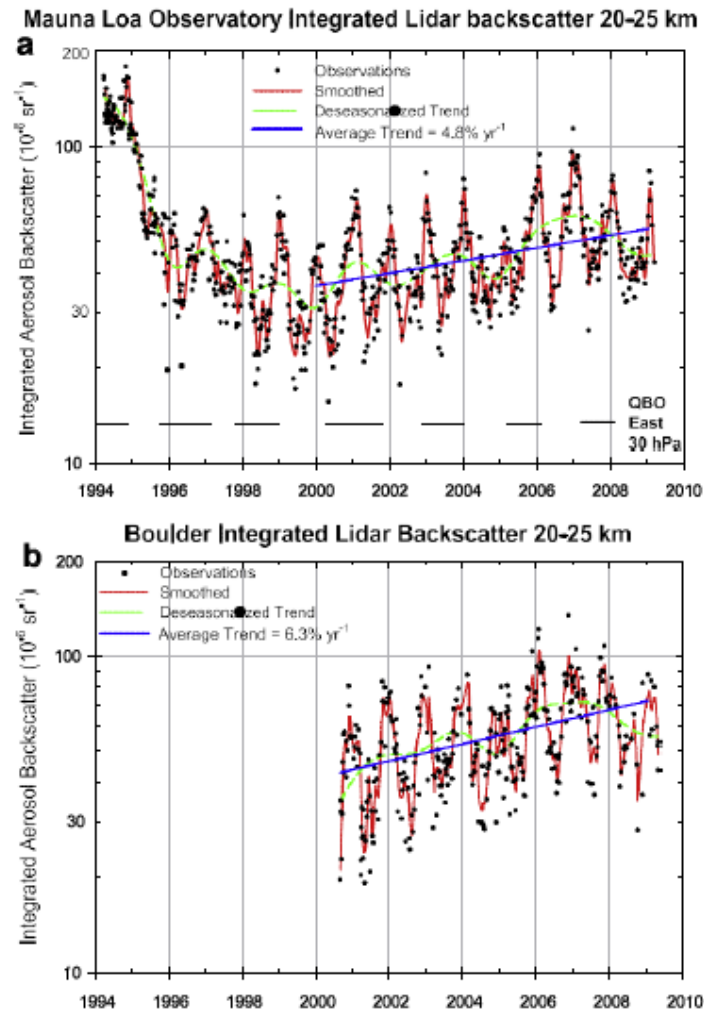


Figure 2. Integrated backscatter for the 20–25 km altitude range at (a) Mauna Loa Observatory and (b) Boulder, Colorado. (Hofmann et al, 2009)

The paper has a large number of errors and confusing statements. And I am not sure the results are new or interesting. I recommend that the paper either be rejected or sent back to the authors for major revision, clearing up all these issues.

In section 4.2 there are many results about the circulation presented, but the authors never say where they got the data and how they did the calculations. What models or reanalyses were used. The technique of using parcels and trajectories is also quite confusing and not clearly explained.

Section 4.2 shows the results we got from forward trajectory simulations carried out with the MPTRAC model. The initialization for each of the parcels is the longitude, latitude, altitude and SO₂ mass. The time period covered is from 12 June 2009 to 16 June 2009, when the explosive eruption occurred, as show in Fig. 2. Our initialization is derived by using a backward trajectory method and AIRS SO₂ observation, and total SO₂ mass estimates from previous studies.

Following Hoffmann at al. (2016), 6-hourly ERA-interim wind fields are used to carry out the trajectory simulations. The model outputs are given every six hours, but only results on selected time are shown in Fig. 3 and Fig. 4 for comparison with satellite observations.

We believe we have used Section 2.3 to introduce the MPTRAC model and also mentioned the ERA-interim data. Section 3 explains how we carried out the simulation.

The authors should use continuous numbering of lines for the entire, and number every one. It is much harder for the reviewer to use page number and line number, and count the numbers and scroll to the top or bottom of the page to find out which line. This annoys reviewers. Make it easier for them!

We changed the line number pattern in our revised version.

p. 3, lines 27-28: Emission rates of what? I don't understand how you can use measurements of upper

tropospheric SO₂ to measure emission rates of SO₂ from a volcanic eruption. You have to know what is happening at the volcanic vent, and sample it more often than once or twice a day. And the units in the figure do not make sense to me. You have to explain this.

Thank you for your suggestion. In fact in this study, the term “SO₂ emission” refers to the SO₂ emitted or injected into the upper troposphere and lower stratosphere during the explosive volcanic eruption. This clarification has been added to the manuscript where the “SO₂ emission” first appears.

In our study, we considered the SO₂ within a radius of 75 km to the location of Sarychev as the SO₂ injected by the volcanic eruption. So the unit of the SO₂ emission $\text{kg m}^{-1} \text{s}^{-1}$ can be simply converted to $\text{kg m}^{-3} \text{s}^{-1}$ by dividing the area. But the SO₂ emission is actually not evenly distributed in this circular area, so we use the exact longitude, latitude, altitude of the SO₂ to initialize the trajectories. So in Fig. 2, we group the SO₂ emission only by time and altitude instead of showing the area-averaged value.

Even though the emission calculation is explained at the top of p. 5, I do not understand. You have fixed the number of parcels at 100,000 in each column. So how can the number be proportional to the SO₂ amount?

100,000 air parcels refer to the total number for all AIRS air columns, but the number of air parcels in each of the air columns is different. The air columns that correspond to larger SO₂ index (associated with larger SO₂ column density) will get more air parcels. For further details, we referred to Hoffmann et al.(2016).

The authors seem to confuse emission and injection. Emission is from the volcanic vent. Injection is where the emissions end up in the atmosphere. The way the paper is written, discussion of emissions and emission rates is very confusing.

In the revised manuscript, we changed the “SO₂ emission rate” into “SO₂ emission time series”. The “SO₂ emission time series” refers to the mass and altitude of the SO₂ emitted or injected into the atmosphere during the volcanic eruption.

There are a number of acronyms that are never defined, like UTLS, TTL, and AIRS. The paper mixes UK and US spelling. Choose one and use it consistently.

Fixed. All of the acronyms defined in the abstract are spelled out again the first time they are used in the body of the paper. Thank you.

The references are not in alphabetical order.

Fixed. Thank you.

I do not understand Fig. 2. How can there be emissions of SO₂ in the stratosphere? And I also do not understand the units used for emission.

The study is not concerned with the emission directly at the volcanic vent.

As we mentioned above, we will clarify that the “SO₂ emission” refers to the SO₂ emitted or injected into the atmosphere during the explosive volcanic eruption.

The “ $\text{kg m}^{-1} \text{s}^{-1}$ ” may not be a reasonable unit for “rate”, so we change the “SO₂ emission rate” in this paper to “SO₂ emission time series”.

The figures have many errors, with missing sources of the data, missing units, and confusing labeling. See the comments on the attached annotated manuscript.

Thank you. Please see the attached manuscript for the replies.

For example, for Fig. 10 since the unit is % for many figures, yet the shading goes from 0 to 0.007, does this mean all the numbers are <<0.01 %. This is such a small number, why is it even given?

In Fig. 8 and Fig. 10, the shading values are derived by counting the number of air parcels at altitude between the height of the 360 and 400 K isentropic surfaces in each bin and then dividing this number by the total number of air parcels during the simulation time period. The size of the bins is 2° in longitude × 1° in latitude. For example, to get the bottom right panel of Fig.8, we first count the total number of the air parcels from 21 to 31 July 2009 (11 days). Since we get the model results four times per day, and the number of air parcels for each model output is 100,000, so the total number $X = 100,000 \times 4 \times 11$. Then we count the number of air parcels between 360 and 400 K isentropic surfaces in each bin. Assuming this number is Y. The “proportion” equals to $Y/X \times 100$.

The values are usually very small because the bin size is small (, so the Y is usually not large), but the denominator is very large. However, small values obviously do not equal to meaningless values.

We find it is a useful way to show the plume evolution with time. Very similar pictures can be found in other

studies, e.g., Fig. 3 in Garny and Randel (2016).

For Fig. 10 and in section 4.2, the data are “above 400 K.” What does this mean? There is no temperature above 400 K in the atmosphere. Is this potential temperature? Is it values of potential temperature above 400 K? Is it altitude above the 400 K potential temperature level? The authors have to be very clear with what they mean.

Thank you for pointing this out. We mean “altitude above the 400 K potential temperature level”

There are multiple English errors.

We have tried to fix the errors in the revision. Once the paper is accepted for final publication, it will undergo language and copy-editing by Copernicus publication.

Please address all of the 101 comments in the attached annotated manuscript.

Please see the replies in the attached manuscript.

References

- Garny, H., and Randel, W. J.: Transport pathways from the Asian monsoon anticyclone to the stratosphere, *Atmos. Chem. Phys.*, 16, 2703-2718, doi: 10.5194/acp-16-2703-2016, 2016.
- Griessbach, S., Hoffmann, L., Spang, R., von Hobe, M., Müller, R., and Riese, M.: Infrared limb emission measurements of aerosol in the troposphere and stratosphere, *Atmos. Meas. Tech.*, 9, 4399-4423, doi:10.5194/amt-9-4399-2016, 2016.
- Haywood, J. M., Jones, A., Clarisse, L., Bourassa, A., Barnes, J., Telford, P., Bellouin, N., Boucher, O., Agnew, P., Clerbaux, C., Coheur, P., Degenstein, D., and Braesicke, P.: Observations of the eruption of the Sarychev volcano and simulations using the HadGEM2 climate model, *J. Geophys. Res. Atmos.*, 115, D21212, doi: 10.1029/2010JD014447, 2010.
- Hoffmann, L., Griessbach, S., and Meyer, C. I.: Volcanic emissions from AIRS observations: detection methods, case study, and statistical analysis, in: *Remote Sensing of Clouds and the Atmosphere XIX and Optics in Atmospheric Propagation and Adaptive Systems XVII*, edited by: Comeron, A., Kassianov, E. I., Schafer, K., Picard, R. H., Stein, K., and Gonglewski, J. D., Proceedings of SPIE, Spie-Int Soc Optical Engineering, Bellingham, doi: 92421410.1117/12.2066326, 2014.
- Hoffmann, L., Rößler, T., Griessbach, S., Heng, Y., and Stein, O.: Lagrangian transport simulations of volcanic sulfur dioxide emissions: Impact of meteorological data products, *J. Geophys. Res. Atmos.*, 121, 4651-4673, doi: 10.1002/2015JD023749, 2016.
- Khaykin, S. M., Godin-Beekmann, S., Keckhut, P., Hauchecorne, A., Jumelet, J., Vernier, J. P., Bourassa, A., Degenstein, D. A., Rieger, L. A., Bingen, C., Vanhellemont, F., Robert, C., DeLand, M., and Bhartia, P. K.: Variability and evolution of the midlatitude stratospheric aerosol budget from 22 years of ground-based lidar and satellite observations, *Atmos. Chem. Phys.*, 17, 1829-1845, doi: 10.5194/acp-17-1829-2017, 2017.
- Ploeger, F., Gottschling, C., Griessbach, S., Grooß, J. U., Guenther, G., Konopka, P., Müller, R., Riese, M., Stroh, F., Tao, M., Ungermann, J., Vogel, B., and von Hobe, M.: A potential vorticity-based determination of the transport barrier in the Asian summer monsoon anticyclone, *Atmos. Chem. Phys.*, 15, 13145-13159, doi: 10.5194/acp-15-13145-2015, 2015.
- Textor, C., H.-F. Graf, M. Herzog, and J. M. Oberhuber, Injection of gases into the stratosphere by explosive volcanic eruptions, *J. Geophys. Res.*, 108(D19), 4606, doi:10.1029/2002JD002987, 2003.



Summary of reply to the comments in the supplement of reviewer #3

Equatorward dispersion of high-latitude volcanic plume and its relation to the Asian summer monsoon: a case study of the Sarychev eruption in 2009

Xue Wu^{1,2}, Sabine Griessbach¹, Lars Hoffmann¹

5 ¹Jülich Supercomputing Centre, Forschungszentrum Jülich, Jülich, Germany

²Key Laboratory of Middle Atmosphere and Global Environment Observation, Institute of Atmospheric Physics, Chinese Academy of Sciences, Beijing, China


Correspondence to: Xue Wu (xu.wu@fz-juelich.de)


Abstract.


10 Tropical volcanic eruptions have been widely studied for their significant contribution to **1** the stratospheric aerosol loading and global climate impacts, but the impact of high-latitude volcanic eruptions on the stratospheric aerosol layer is not clear and the pathway of transporting aerosol from high-latitudes to the tropical stratosphere is not well understood. In this work, we focus on the high-latitude volcano Sarychev (48.1°N, 153.2°E), which erupted **2** during the Asian summer monsoon (ASM) season in 2009, and the influence of ASM
15 on the equatorward dispersion of the volcanic plume. First, the sulfur dioxide (SO₂) emission rate and plume height of the Sarychev eruption are estimated with SO₂ observations of the Atmospheric Infrared Sounder (AIRS) and a backward trajectory approach, using the Lagrangian particle dispersion model Massive-Parallel Trajectory Calculations **3** (MPTRAC). Then, the transport and dispersion of the plume are simulated using the derived emission rate time series. The transport simulations are compared with SO₂ observations from AIRS and
20 validated with aerosol observations from the Michelson Interferometer for Passive Atmospheric Sounding (MIPAS). The simulations show that about **4** % of the emissions were transported to the tropical stratosphere within 50 days after the beginning of the eruption, and the plume dispersed towards the tropical tropopause layer (TTL) through isentropic transport above the subtropical jet. The simulations and MIPAS aerosol data both show that in the **5** vertical range of 360–400 K, the equatorward transport was primarily driven by anticyclonic
25 Rossby wave breaking enhanced by the ASM in boreal summer. The volcanic plume was entrained along the anticyclone flows and reached the TTL as it was transported south-westwards into the deep tropics downstream of the anticyclone. Further, the ASM anticyclone influenced the pathway of aerosols by isolating an ‘aerosol hole’ inside of the ASM, which was surrounded by aerosol-rich air outside. This transport barrier was best indicated using the potential vorticity gradient approach. Long-term MIPAS aerosol detections show that after
30 entering the TTL, the aerosol from the Sarychev eruption remained in the tropical stratosphere for about 10 months and ascended slowly. The ascent speed agreed well with the ascent speed **6** water vapour tape recorder. In contrast, by running a hypothetical **7** simulation for a wintertime eruption, it is confirmed that under winter circulations, the equatorward transport of the plume would be suppressed by the strong subtropical jet and weak wave breaking events. In this **8** hypothetical scenario, **9** high-latitude volcanic eruption would not be able to
35 contribute to the tropical stratospheric aerosol layer.


Summary of Comments on reply to acp-2017-425-RC3-supplement.pdf


Page: 1


 Number: 1 Author: Date: 8/23/2017 10:31:41 PM
[delete]


 Author: Date: 8/23/2017 10:31:41 PM
Fixed. Thank you.


 Number: 2 Author: Date: 8/23/2017 10:31:41 PM
give actual date


 Author: Date: 8/23/2017 10:31:41 PM
Fixed. Thank you.


 Number: 3 Author: Date: 8/23/2017 10:31:41 PM
[delete] Do not define acronyms if you do not use them again.


 Author: Date: 8/23/2017 10:31:41 PM
Fixed. Thank you.


 Number: 4 Author: Date: 8/23/2017 10:31:41 PM
SO₂ gas or aerosols?


 Author: Date: 8/23/2017 10:31:41 PM
Fixed. Thank you.


 Number: 5 Author: Date: 8/23/2017 10:31:41 PM
of what variable?


 Author: Date: 8/23/2017 10:31:41 PM
It refers to the potential temperature levels. It is fixed in the manuscript. Thank you.


 Number: 6 Author: Date: 8/23/2017 10:31:41 PM
of the wate


 Author: Date: 8/23/2017 10:31:41 PM
Fixed. Thank you.


 Number: 7 Author: Date: 8/23/2017 10:31:41 PM
Did you also do a simulation for the actual event to test your model?

 Author: Date: 8/23/2017 10:31:41 PM
Yes. Results shown from Fig. 8 to Fig. 11 are based on the simulations of the real eruption. I have added a sentence in the abstract to avoid the ambiguity. Thanks a lot.

 Number: 8 Author: Date: 8/23/2017 10:31:41 PM
hypothetical

 Author: Date: 8/23/2017 10:31:41 PM
Fixed. Thank you.

 Number: 9 Author: Date: 8/23/2017 10:31:41 PM
a high

 Author: Date: 8/23/2017 10:31:41 PM
Fixed. Thank you.



1 Introduction


The impact of volcanic aerosol on climate has received wide attention over decades. Robock (2000, 2013) ¹ve a comprehensive review on this subject. The major sources of the stratospheric aerosol are volcanic sulfur gases, mainly in form of SO₂, which are oxidized and converted into sulfate aerosol within hours to weeks (von Glasow et al., 2009). The sulfate aerosol is responsible for profound effects on the global climate (McCormick et al., 1995; Robock, 2000). Sulfate aerosol is a strong reflector of visible solar radiation and causes cooling of the troposphere for ²ars; while it is also an effective absorber of ³ar infrared solar radiation and may induce heating of the stratosphere. In contrast, H₂O and CO₂ in the volcanic emissions do not have much measurable impact on the global climate since they are less abundant ⁴an atmospheric H₂O and CO₂ reservoir (Gerlach, 1991; Gerlach, 2011). Volcanic ash usually only causes regional influence on climate for weeks, because of its large particle size, fast sedimentation, and consequently short life time in atmosphere (Niemeier et al., 2009).

The stratospheric aerosol layer enhanced by volcanism not only has a significant impact on the Earth's radiative budget (McCormick et al., 1995; Robock, 2000), it also has an impact on chemical processes in the lower stratosphere (Rodriguez et al., 1991; Solomon et al., 1993), in particular, on ozone depletion (Jäger and Wege, 1990; Tilmes et al., 2008; Solomon et al., 2016). Conventionally ⁵large volcanic eruptions with a volcanic explosivity index (VEI) larger than 4, are thought to play a key role in the stratospheric sulfate aerosol budget. Recently, several studies focused on ⁶hall and moderate-sized volcanic eruptions (VEI ≤ 4) (Kravitz et al., 2011; Solomon et al., 2011; Vernier et al., 2011; Ridley et al., 2014) and considered them as the primary source of the notable increase of stratospheric aerosol since 2000 that slowed down global warming (Solomon et al., 2011; Neely et al., 2013; Haywood et al., 2014). Models neglecting the effects of less intense volcanic eruptions tend to overestimate the tropospheric warming (Santer et al., 2014). The potential climate impact of volcanic emissions also largely depends on the time of year when the eruption takes place, the injection height and the surrounding meteorological conditions (Kravitz et al., 2011). The season influences sulfate formation and the zonal asymmetry of the polar vortex can affect the aerosol's transport. The eruption plume height is fundamental for aerosol microphysics in the atmosphere and the large scale ⁸irculations affect the transport of the plume. ⁷b instead of only using the VEI, it is more sensible to study the atmospheric impacts by including volcanic eruptions based on the amount of stratospheric SO₂ injection together with eruption height (Brühl et al., 2015; Timmreck, 2012). Further information on volcanic SO₂ emissions and plume altitudes ⁹e crucial in climate models when estimating trends of global temperature or ozone depletion.


The majority of studies on global climate impact of volcanic eruptions focuses on tropical eruptions. Extratropical volcanic eruptions are expected to have less impact on the global climate, because the downward flow of the Brewer–Dobson circulation in the stratospheric extra-tropics prevents sulfate aerosol from rising up (Seviour et al., 2012), and sulfate aerosol in the extratropical stratosphere easily subsides back to the troposphere within months (Holton et al., 1995; Kremser et al., 2016). Although some studies show that extratropical volcanic eruptions can also have a significant impact on climate (Highwood and Stevenson, 2003; Oman et al., 2005; Oman et al., 2006; Kravitz and Robock, 2011; Pausata et al., 2015a; Pausata et al., 2015b), the impact is usually found to be limited to the specific hemisphere in which the eruption occurred (Graf and Timmreck, 2001; Kravitz and Robock, 2011; Pausata et al., 2015b).

However, a high-latitude volcanic eruption may also contribute to the tropical stratospheric aerosol loading and even affect the other hemisphere (Schmidt et al., 2010). In this paper, we focus on the eruption of the high-


1 Number: 1 Author: Date: 8/23/2017 10:31:41 PM
gives or gave

 Author: Date: 8/23/2017 10:31:41 PM
Fixed. Thank you.


1 Number: 2 Author: Date: 8/23/2017 10:31:41 PM
How many?

 Author: Date: 8/23/2017 10:31:41 PM
Fixed. Thank you.


1 Number: 3 Author: Date: 8/23/2017 10:31:41 PM
and longwave

 Author: Date: 8/23/2017 10:31:41 PM
Fixed. And a reference is added here.


1 Number: 4 Author: Date: 8/23/2017 10:31:41 PM
than the

 Author: Date: 8/23/2017 10:31:41 PM
Fixed. Thank you.


1 Number: 5 Author: Date: 8/23/2017 10:31:41 PM
Not correct. VEI is an index of explosivity, not of the impact on climate. For example, Mount St. Helens was VEI 5, but has no impact on climate.

 Author: Date: 8/23/2017 10:31:41 PM
Yes. You are right. But we have to admit that, in the past (even nowadays), when people tried to study the climate impacts of explosive volcanic eruptions, they selected eruption cases by using VEI, instead of erupted SO₂ mass. When an increase in the tropical stratospheric aerosol loading since 2000 was found, even without major volcanic eruption, moderate and small volcanic eruption cases defined with smaller VEI got attention.
Also, in the past, most of the researches on the climate impacts of explosive volcanic eruptions were based on tropical eruptions. But some mid-latitude or high-latitude volcanic eruptions can not only increase the aerosol in the northern hemisphere, but also can enhance the tropical aerosol optical depth and influence the global climate similar to a tropical eruption. However, this influence is conditional. It may require a relatively large amount of SO₂ injected and transported to the tropical tropopause layer or higher altitudes and entering the Brewer-Dobson circulation. The time of eruption, the SO₂ injection height and the wind fields are all essential elements that determine the transport efficiency. And these are all studied in this paper.
The St. Hellen eruption in May 1980 you have mentioned could be a very interesting case to compare with the Sarychev case. The St. Hellen eruption did not have impressive global climate impact not only because its relatively small SO₂ emission, about 0.775 Tg according to the data provided by the global volcanism program (<http://volcano.si.edu/volcano.cfm?vn=321050>), but also because of its location and the time of the eruption. St Hellen is a high-latitude volcano and in May 1980, the SO₂ was emitted when the meteorological condition was unfavorable of the equatorward transport of the SO₂. Quite a lot of volcanic eruptions in the tropics with SO₂ injection far less than 0.775 Tg can caused large increase of aerosol optical depth (AOD) in the tropical stratosphere, and subsequently have a great potential to influence the global climate, e.g., Manam (Time: January 2005/Lat: 4.1°S/SO₂ mass: 0.14Tg/SO₂ injection top height: 24km), Tavurvur (Time: October 2006/Lat: 4.3°S/SO₂ mass: 0.3Tg/SO₂ injection top height: 18km), and Kelud (Time: February 2014/Lat: 7.9°S/SO₂ mass: 0.2Tg/SO₂ injection top height: 19km).
Here in the introduction, we decide to give a very brief description about the related research in the past, and explain why we are interested in the Sarychev case. Although the Sarychev eruption in 2009 was a moderate eruption (in term of VEI), but it is a representative of high-latitude eruptions that contribute to the tropical stratospheric aerosol budget.


1 Number: 6 Author: Date: 8/23/2017 10:31:41 PM
No. See previous comment about VEI. It is the amount of SO₂ put into the stratosphere that determines the impact on climate.

 Author: Date: 8/23/2017 10:31:41 PM
Please see reply to the previous comment.

1 Number: 7 Author: Date: 8/23/2017 10:31:41 PM
So why do you even mention VEI above?

 Author: Date: 8/23/2017 10:31:41 PM
Please see the reply to the comments above.

1 Number: 8 Author: Date: 8/23/2017 10:31:41 PM
circulation affects

 Author: Date: 8/23/2017 10:31:41 PM
Fixed. Thank you.

1 Number: 9 Author: Date: 8/23/2017 10:31:41 PM




1 Introduction

The impact of volcanic aerosol on climate has received wide attention over decades. Robock (2000, 2013) give a comprehensive review on this subject. The major sources of the stratospheric aerosol are volcanic sulfur gases, mainly in form of SO₂, which are oxidized and converted into sulfate aerosol within hours to weeks (von Glasow et al., 2009). The sulfate aerosol is responsible for profound effects on the global climate (McCormick et al., 1995; Robock, 2000). Sulfate aerosol is a strong reflector of visible solar radiation and causes cooling of the troposphere for years; while it is also an effective absorber of near infrared solar radiation and may induce heating of the stratosphere. In contrast, H₂O and CO₂ in the volcanic emissions do not have much measurable impact on the global climate since they are less abundant than atmospheric H₂O and CO₂ reservoir (Gerlach, 1991; Gerlach, 2011). Volcanic ash usually only causes regional influence on climate for weeks, because of its large particle size, fast sedimentation, and consequently short life time in atmosphere (Niemeier et al., 2009).

The stratospheric aerosol layer enhanced by volcanism not only has a significant impact on the Earth's radiative budget (McCormick et al., 1995; Robock, 2000), it also has an impact on chemical processes in the lower stratosphere (Rodriguez et al., 1991; Solomon et al., 1993), in particular, on ozone depletion (Jäger and Wege, 1990; Tilmes et al., 2008; Solomon et al., 2016). Conventionally, large volcanic eruptions with a volcanic explosivity index (VEI) larger than 4, are thought to play a key role in the stratospheric sulfate aerosol budget. Recently, several studies focused on small and moderate-sized volcanic eruptions (VEI ≤ 4) (Kravitz et al., 2011; Solomon et al., 2011; Vernier et al., 2011; Ridley et al., 2014) and considered them as the primary source of the notable increase of stratospheric aerosol since 2000 that slowed down global warming (Solomon et al., 2011; Neely et al., 2013; Haywood et al., 2014). Models neglecting the effects of less intense volcanic eruptions tend to overestimate the tropospheric warming (Santer et al., 2014). The potential climate impact of volcanic emissions also largely depends on the time of year when the eruption takes place, the injection height and the surrounding meteorological conditions (Kravitz et al., 2011). The season influences sulfate formation and the zonal asymmetry of the polar vortex can affect the aerosol's transport. The eruption plume height is fundamental for aerosol microphysics in the atmosphere and the large scale circulations affect the transport of the plume. So instead of only using the VEI, it is more sensible to study the atmospheric impacts by including volcanic eruptions based on the amount of stratospheric SO₂ injection together with eruption height (Brühl et al., 2015; Timmreck, 2012). Further information on volcanic SO₂ emissions and plume altitudes are crucial in climate models when estimating trends of global temperature or ozone depletion.

The majority of studies on global climate impact of volcanic eruptions focuses on tropical eruptions. Extratropical volcanic eruptions are expected to have less impact on the global climate, because the downward flow of the Brewer–Dobson circulation in the stratospheric extra-tropics prevents sulfate aerosol from rising up (Seviour et al., 2012), and sulfate aerosol in the extratropical stratosphere easily subsides back to the troposphere within months (Holton et al., 1995; Kremser et al., 2016). Although some studies show that extratropical volcanic eruptions can also have a significant impact on climate (Highwood and Stevenson, 2003; Oman et al., 2005; Oman et al., 2006; Kravitz and Robock, 2011; Pausata et al., 2015a; Pausata et al., 2015b), the impact is usually found to be limited to the specific hemisphere in which the eruption occurred (Graf and Timmreck, 2001; Kravitz and Robock, 2011; Pausata et al., 2015b).

However, a high-latitude volcanic eruption may also contribute to the tropical stratospheric aerosol loading and even affect the other hemisphere (Schmidt et al., 2010). In this paper, we focus on the eruption of the high-

 Author: Date: 8/23/2017 10:31:41 PM
Fixed. Thank you.



latitude volcano, Sarychev in 2009, which is considered as one of the high-latitude eruptions that affect tropical latitudes (von Savigny et al., 2015) and is responsible for the increase in tropical stratospheric aerosol optical depth. In particular, we study the transport pathway of the Sarychev aerosol from the extra-tropical lower stratosphere to the TTL. In order to analyse the transport of the Sarychev plume and the role of the ASM in the dispersion process, in Section 2 we first present the Lagrangian transport model and data used for simulations. In Section 3, we derive the altitude-resolved Sarychev volcanic emission time series using AIRS SO₂ measurements and an inverse modelling approach. The equatorward dispersion of the Sarychev emissions revealed by MIPAS aerosol detections and trajectory simulations and the relation to ASM are shown in Section 4. Results of this study are further discussed in Section 5 and summarized in Section 6.

2 Observations and model

2.1 AIRS

AIRS (Aumann et al., 2003) is an infrared sounder with across-track scanning capabilities aboard the National Aeronautics and Space Administration's (NASA's) Aqua satellite. Aqua was launched in May 2002 and operates in a nearly polar, Sun-synchronous orbit at an altitude of about 710 km with a period of 98 min. The AIRS footprint size is 13.5 km×13.5 km for nadir and 41 km×21.4 km for the outermost scan angles. The along-track distance between two adjacent scans is 18 km. AIRS provides nearly continuous measurement coverage during 14.5 orbits per day and covers the globe almost twice a day. The observations provide good horizontal resolution and make it ideal data for observing the fine filamentary structures of volcanic SO₂ plumes.

In this study, we use an SO₂ index defined by brightness temperature differences (BTDs) based on SO₂ spectral features in the 7.3 μm waveband (Hoffmann et al., 2014) to estimate emission rates and evaluate the Lagrangian transport simulations. The SO₂ index increases with increasing SO₂ column density and it is most sensitive to SO₂ at altitudes from 8 to 13 km. The SO₂ index of Hoffmann et al. (2014) performs better on suppressing background signals than the SO₂ index provided in the NASA operational data products. It is therefore well suited to track low SO₂ concentrations over time. In this work, we applied a detection threshold of 2 K for the SO₂ index to identify volcanic emissions.

AIRS was able to detect the SO₂ cloud from the beginning of the eruption of Sarychev on 12 June 2009 up to five weeks later. Observations during the first five days after the eruption have been used for estimating the emission rates. Observations at a later stage are used for comparison with the Lagrangian transport simulations.

2.2 MIPAS

MIPAS (Fischer et al., 2008) is an infrared limb emission spectrometer aboard European Space Agency's (ESA's) Envisat, which was in operation from July 2002 to April 2012, providing nearly 10 years of measurements. The vertical coverage of its nominal mode was 7–72 km from January 2005 to April 2012. MIPAS has a field of view of about 3 km×30 km (vertically and horizontally) at the tangent point and dimension of the measurement volume along the line of sight is about 300 km. The horizontal distance between two adjacent limb scans is about 500 km. In 2009, the general measurement pattern of MIPAS is to measure eight days in nominal mode followed by one day in middle atmosphere mode and one day in upper atmosphere

T Number: 1 Author: Date: 8/23/2017 10:31:41 PM
affects

S Author: Date: 8/23/2017 10:31:41 PM
Thank you. But the verb is for "eruptions".

T Number: 2 Author: Date: 8/23/2017 10:31:41 PM
If there was such an increase, it was very small. Please explain how large it was, and why you think it was significant.

S Author: Date: 8/23/2017 10:31:41 PM
We agree that the influence of Sarychev eruption was not as significant as some other large volcanic eruptions like Pinatubo, or but it clearly increased the topical stratospheric aerosol, which is impressive for a high-latitude eruption. Some figures in previous studies have shown this aerosol increase using Scanning Imaging Absorption Spectrometer for Atmospheric CHartography (SCIAMACHY), the Optical Spectrograph and InfraRed Imaging System (OSIRIS) and the Cloud-Aerosol Lidar with Orthogonal Polarization (CALIOP) data. We have added two more references here.
We can see that the increase is very notable. There was not a "number" that we can borrow from previous study to show how large the increase was, but later in this paper, we show with the MIPAS data that the increase is significant and lasted for quite a long time.

T Number: 3 Author: Date: 8/23/2017 10:31:41 PM
is

S Author: Date: 8/23/2017 10:31:41 PM
Thank you. But the verb is for "eruptions".

T Number: 4 Author: Date: 8/23/2017 10:31:41 PM
All acronyms have to be defined. What is this?

S Author: Date: 8/23/2017 10:31:41 PM
Fixed. Thank you.

T Number: 5 Author: Date: 8/23/2017 10:31:41 PM
brightness temperature differences between what and what?

S Author: Date: 8/23/2017 10:31:41 PM
We have added an equation in the manuscript to explain.

T Number: 6 Author: Date: 8/23/2017 10:31:41 PM
How can you see emission by looking a the upper troposphere?

S Author: Date: 8/23/2017 10:31:41 PM
the SO₂ emission in this study refers to the SO₂ released or injected into the atmosphere during the process of the explosive eruption. We have add a sentence in the introduction, where the term "emission" first appeared to clarify. Thank you very much for pointing this out.

T Number: 7 Author: Date: 8/23/2017 10:31:41 PM
What is this? The temperature of what? If you are using a non-standard index, you have to describe it and explain how it is calculated, and why you used this criterion.

S Author: Date: 8/23/2017 10:31:41 PM
Thank you for pointing this out. The equation added above may help to understand. This threshold is provided by previous well-established studies and a reference has been added here. For more details see Hoffmann et al. (2014).

T Number: 8 Author: Date: 8/23/2017 10:31:41 PM
Emission of what? Rate of what?

S Author: Date: 8/23/2017 10:31:41 PM
Fixed. Thank you.

T Number: 9 Author: Date: 8/23/2017 10:31:41 PM
emission of SO₂ or of longwave radiation?

S Author: Date: 8/23/2017 10:31:41 PM
Here, the "emission" refers to the radiation emission.



mode. On each day, about 14 orbits with about 90 profiles per orbit are measured. From January 2005 to April 2012, the vertical sampling grid spacing between the tangent altitudes is 1.5 km in the UTLS and 3 km above.

In this study, we use MIPAS altitude-resolved aerosol data (Griessbach et al., 2016). In the first step, we used the aerosol-cloud-index to identify cloud or aerosol contaminated spectra, and in the second step we use a brightness temperature correction method to separate aerosol from ice clouds. The resulting aerosol product may contain any type of aerosol, e.g. volcanic ash, sulfate aerosol, mineral dust as well as non-ice polar stratospheric clouds (PSCs). MIPAS detected Sarychev aerosol starting on 13 June 2009.

2.3 MPTRAC

The Massive-Parallel Trajectory Calculations (MPTRAC) model is a Lagrangian particle dispersion model, which is particularly suited to study volcanic eruption events (Heng et al., 2015; Hoffmann et al., 2016). In the MPTRAC model, trajectories for individual air parcels are calculated based on numerical integration of the kinematic equation of motion and simulations are driven by wind fields from global meteorological reanalyses. Turbulent diffusion is modelled by uncorrelated Gaussian random displacements of the air parcels with zero mean and standard deviations $\sigma_x = \sqrt{D_x \Delta t}$ (horizontally) and $\sigma_z = \sqrt{D_z \Delta t}$ (vertically). D_x and D_z are the horizontal and vertical diffusivities respectively, and Δt is the time step for the trajectory calculations. For the Sarychev simulation, D_x is assigned to be $50 \text{ m}^2 \text{ s}^{-1}$ in the troposphere and D_z is assigned to be $0.1 \text{ m}^2 \text{ s}^{-1}$ in the stratosphere following Stohl et al. (2005). Furthermore, the sub-grid scale wind fluctuations are simulated by a Markov model (Stohl et al., 2005; Hofmann et al., 2016). Loss processes of chemical species, SO_2 in our simulations, are simulated based on an exponential decay of the mass assigned to each air parcel, with a constant half lifetime of seven days.


In this study, the MPTRAC model is driven with the ERA-Interim data (Dee et al., 2011) interpolated on a $1^\circ \times 1^\circ$ horizontal grid on 60 model levels with the vertical range extending from the surface to 0.1 hPa. The ERA-Interim data provided at 0000, 0600, 1200, and 1800 UTC.

3 Simulations and observations of the Sarychev plume


3.1 Reconstruction of the Sarychev SO_2 emission time series

The Sarychev peak with summit at 1496 m, is located at 48.1°N , 153.2°E , and it is one of the most active volcanoes of the Kuril Islands. It erupted most recently in June 2009 (VEI = 4). On 11 June 2009, two weak ash eruptions were first detected (Levin et al., 2010) and during the main explosive phase from 12 to 16 June 2009, ash, water vapour, and an estimated $1.2 \pm 0.2 \text{ Tg}$ of SO_2 were injected into the UTLS, making it one of the largest stratospheric injections in the last 50 years (Haywood et al., 2010). Sulfate aerosol was detected several days after the eruption and the enhancement of the optical depth caused by the Sarychev eruption lasted for months, returning to pre-Sarychev eruption values in the beginning of 2010 (Doeringer et al., 2012; Jégou et al., 2013). As shown in Fig. 1 (top), Sarychev is located at the northern edge of the subtropical jet and to the northeast of the ASM (marked by the black rectangle). In the vertical section (Fig. 1, bottom), the dynamical tropopause, defined by a potential vorticity (PV) value of 2 PV units (PVU), is around 11 km at the location of the Sarychev.


1 Number: 1 Author: Date: 8/23/2017 10:31:41 PM
define. What is this?

 Author: Date: 8/23/2017 10:31:41 PM
Fixed. Thank you.


1 Number: 2 Author: Date: 8/23/2017 10:31:41 PM
What is this?

 Author: Date: 8/23/2017 10:31:41 PM
Explanations add. Thank you.


1 Number: 3 Author: Date: 8/23/2017 10:31:41 PM
a Lagrangian

 Author: Date: 8/23/2017 10:31:41 PM
Fixed. Thank you.


1 Number: 4 Author: Date: 8/23/2017 10:31:41 PM
what about the stratosphere?

 Author: Date: 8/23/2017 10:31:41 PM
Fixed. Thank you.


1 Number: 5 Author: Date: 8/23/2017 10:31:41 PM
what about the troposphere?

 Author: Date: 8/23/2017 10:31:41 PM
Fixed. Thank you.


1 Number: 6 Author: Date: 8/23/2017 10:31:41 PM
are

 Author: Date: 8/23/2017 10:31:41 PM
Fixed. Thank you.

1 Number: 7 Author: Date: 8/23/2017 10:31:41 PM
Use UK or US spelling, but not both. If you use sulfate, then use vapor.

 Author: Date: 8/23/2017 10:31:41 PM
Fixed. Thank you.

1 Number: 8 Author: Date: 8/23/2017 10:31:41 PM
Why, if it went into the UTLS? Isn't UT upper troposphere? How much went into the stratosphere?

 Author: Date: 8/23/2017 10:31:41 PM
Haywood et al., 2010 got the conclusion by comparing the change of stratospheric aerosol optical depth at 550 nm. Please refer to Haywood et al., 2010 (Table 2). The Sarychev eruption in 2009 ranks No.9. But they did not estimate the proportion of SO₂ that went to the stratosphere. Later in this paper the proportion of SO₂ injected into the stratosphere is estimated.



To reconstruct the altitude-resolved SO₂ emission time series, we follow the approach of Hoffmann et al. (2016) and use backward trajectories and AIRS SO₂ measurements. Since AIRS measurements do not provide altitude information, we establish a column of air parcels at each location of an AIRS SO₂ detection. The vertical range of the column is 0–25 km, covering the possible vertical dispersion range of the SO₂ plume in the first few days.

5 The AIRS footprint size varies between 14 and 41 km, so in the horizontal direction we choose an average of 30 km as the full width at half maximum (FWHM) for the Gaussian scatter of the air parcels. In our simulation, a fixed number of 100,000 air parcels is assigned to all air columns and the number of air parcels in each column is 2nearly proportional to 1the SO₂ index. Then backward trajectories were calculated for all air parcels, and trajectories that are at least 2 days but no more than 5 days long and that have passed the volcano domain are

10 recorded as emissions of Sarychev. The volcano domain is defined to be within a radius of 75 km to the location of Sarychev and 0–20 km in the vertical direction, covering all possible injection heights. Sensitivity experiments have been conducted to optimize these pre-assigned parameters to obtain best simulation results. Haywood et al. (2010) estimated that 1.2 Tg of SO₂ were injected into the UTLS on 15 and 16 June 2009 with a 15 % error estimate (± 0.2 Tg). Considering that there were minor emissions before 15 June (Levin et al., 2010;

15 Jégou et al., 2013; Carboni et al., 2016), we allocated a mass of 1.4 Tg to the derived SO₂ emissions. The reconstructed SO₂ emission time series is shown in Fig. 2.

In Fig. 2, black dots denote the thermal tropopause derived from ERA–interim data at the Sarychev. Sarychev released SO₂ almost without interruption in the first five days, but with large variations in height and magnitude. Smaller eruptions began on 12 June followed by continuous eruptions on 13 June, ranging from 7 km to about

20 17 km. Significant SO₂ injections occurred on 14–15 June between 10 and 18 km, followed by minor emissions until 16 June. The majority of SO₂ (58%, ~0.81Tg) was injected directly into the extratropical lower stratosphere, and the largest SO₂ injection occurred between 12 and 17 km. 2these time line of the eruptions is consistent with the observation of the Japanese Meteorological Agency Multifunctional Transport Satellite (MTSAT) (Levin et al., 2010; Rybin et al., 2011) and the Optical Spectrograph and Infrared Imaging System (OSIRIS) measurements, showing that the peak backscatter of aerosols measured 4here between 12 and 16 km (Kravitz et al., 2011).

The derived SO₂ emission rate time series 5e the basis of the simulations of SO₂ plume in the following sections.


3.2 Simulation and validation of the Sarychev plume dispersion

30 A new set of 100,000 air parcels is assigned to the derived SO₂ emission shown in Fig. 2, with 14,000 kg of SO₂ in each of the air 6parcel. The trajectories initialized with this SO₂ emission are calculated with the MPTRAC model from 12 June 2009 (first eruption) to 31 July 2009. The simulated evolution of the SO₂ plume is shown in Fig. 3 (left column) and compared with the AIRS SO₂ measurements (right column). 7ote that only SO₂ column density values larger than 2 Dobson units (DU) are shown. The evolution of simulated plume altitudes is

35 shown in Fig. 4 together with tangent altitudes of the MIPAS aerosol detections. Figure 3 and Fig. 4 show that, as the SO₂ was injected into different altitudes, the SO₂ plume splitted roughly into two branches after the eruption, moving eastwards and westwards, and at the same time, most of the emissions 8oving poleward. From 22 June, the SO₂ plume over Eastern Siberia stretched towards three directions: northeast, south, and south east. The SO₂ in the elongated filament over the Eastern Siberia and North-east China with altitudes below 9 km was


T Number: 1 Author: Date: 8/23/2017 10:31:41 PM

What is this?

 Author: Date: 8/23/2017 10:31:41 PM
Please see section 2.1


T Number: 2 Author: Date: 8/23/2017 10:31:41 PM

How can this be if you fix the number at 100,000?

 Author: Date: 8/23/2017 10:31:41 PM
100,000 air parcels refer to the total number air parcels in all of the air columns, but the number of air parcels in each of the air columns is different. The air columns that correspond to larger SO2 index (showing larger SO2 column density) will get more air parcels.


T Number: 3 Author: Date: 8/23/2017 10:31:41 PM

This

 Author: Date: 8/23/2017 10:31:41 PM
Fixed. Thank you.


T Number: 4 Author: Date: 8/23/2017 10:31:41 PM

was

 Author: Date: 8/23/2017 10:31:41 PM
Fixed. Thank you.


T Number: 5 Author: Date: 8/23/2017 10:31:41 PM

is

 Author: Date: 8/23/2017 10:31:41 PM
Fixed. Thank you.


T Number: 6 Author: Date: 8/23/2017 10:31:41 PM

parcels.

 Author: Date: 8/23/2017 10:31:41 PM
Fixed. Thank you.


T Number: 7 Author: Date: 8/23/2017 10:31:41 PM

[delete] Every sentence should be noted or it should not be in the paper.

 Author: Date: 8/23/2017 10:31:41 PM
Fixed. Thank you.

T Number: 8 Author: Date: 8/23/2017 10:31:41 PM

moved

 Author: Date: 8/23/2017 10:31:41 PM
Fixed. Thank you.



diluted and partly depleted and converted into aerosol afterwards and the other two filaments moved toward east. The SO₂ plume over the Northwest American continent stretched towards east and west, forming a long filament running through Northern Canada. The SO₂ concentration declined exponentially and only a fraction of SO₂ remained near the Bering Strait and Northern Canada till 28 June.

5 In Fig. 3, in order to validate the simulation of plume dispersion, and also to indirectly validate the reconstructed emission rates, we compare the simulations of plume dispersion with AIRS SO₂ measurements. The SO₂ index from AIRS detections was converted into SO₂ column density using the correlation function described in Hoffmann et al. (2014), which was built using radiative transfer calculations. AIRS was able to detect the SO₂ cloud from the beginning of the eruption of Sarychev up to five weeks later (not fully shown in the figure). The
10 SO₂ column density derived from AIRS agrees well with the SO₂ column density derived from the Infrared Atmospheric Sounding Interferometer (IASI) in magnitude, e.g. see Fig. 3 in the study of Haywood et al. (2010) and Fig. 2 in the study of Jégou et al. (2013). Generally, the simulations agree well with the AIRS measurements in position and diffusion and the simulations can provide more information on the SO₂ distribution than the AIRS measurements alone. The differences between the SO₂ clouds, e.g. on 24 June (over the western Pacific)
15 are partly attributed to a mismatch in time of the AIRS SO₂ measurements and the simulation output. In magnitude, the SO₂ column density from AIRS is slightly larger than that from MPTRAC simulations, and the SO₂ maxima are found in different **1**location. This is also found by Hoffmann et al. (2016) for other eruption events and this was attributed to the fact that the inverse modelling approach is optimized to reproduce the spatial extent of the plume but not the absolute emission. Except for **2**discrepancy between the times of the
20 compared data, this remaining difference may also be attributed to the initial setting of the total SO₂ mass, the SO₂ life time and the uncertainties of the **3**CMWF-interim winds.


In Fig. 4, the altitudes of the simulated SO₂ plume are compared with the tangent altitudes of MIPAS aerosol detections to verify the vertical distribution of the SO₂ plume. Aerosol produced by the Sarychev eruption was detected by MIPAS within a few days after the initial eruption. In general, the altitudes of the simulated SO₂
25 plume are comparable to the MIPAS aerosol altitudes. The majority of the air parcels were between 10 and 20 km and moved eastwards. A thin filament over the north Pacific ascended to up to 20 km and moved westward to East Asia by the end of June 2009, which was well verified by the MIPAS detections. **4**Some apparent inconsistencies, e.g., along the west coast of North **5**American on 23 June and over the northeast Pacific on 24 and 25 June. We attributed **6**to the fact that the SO₂ at lower altitudes (below 14 km) had been converted into
30 aerosol more quickly than the SO₂ at higher altitudes (above 16 km). The various vertical distributions of the air parcels were also verified by some overlapping MIPAS detections, e.g., over northwest America. Overall, this comparison demonstrates that the MPTRAC simulation provides a quite accurate representation of the observed horizontal and vertical distribution of the Sarychev **7**O₂ plume.

4 Equatorward dispersion of the Sarychev plume and the role of the ASM


35 4.1 Equatorward dispersion of Sarychev plume

Although the majority of the Sarychev plume was transported towards the north pole, it's found in our simulations that there was clear equatorward dispersion from extratropical stratosphere to the tropical lower stratosphere, as seen in Fig. 5 (top). The plume reached the tropical stratosphere about one week after the


T Number: 1 Author: Date: 8/23/2017 10:31:41 PM
locations.

 Author: Date: 8/23/2017 10:31:41 PM
Fixed. Thank you.


T Number: 2 Author: Date: 8/23/2017 10:31:41 PM
the discrepancy

 Author: Date: 8/23/2017 10:31:41 PM
Fixed. Thank you.


T Number: 3 Author: Date: 8/23/2017 10:31:41 PM
ERA

 Author: Date: 8/23/2017 10:31:41 PM
Fixed. Thank you.


T Number: 4 Author: Date: 8/23/2017 10:31:41 PM
Not a sentence.

 Author: Date: 8/23/2017 10:31:41 PM
Fixed. Thank you.


T Number: 5 Author: Date: 8/23/2017 10:31:41 PM
America

 Author: Date: 8/23/2017 10:31:41 PM
Fixed. Thank you.

T Number: 6 Author: Date: 8/23/2017 10:31:41 PM
them

 Author: Date: 8/23/2017 10:31:41 PM
Fixed. Thank you.

T Number: 7 Author: Date: 8/23/2017 10:31:41 PM
But you are comparing aerosols and not gas.

 Author: Date: 8/23/2017 10:31:41 PM
Thank you for pointing this out. We agree it is not accurate to say Fig. 4 (left panels) shows the SO₂ plume, although in the beginning of the simulation the plume is composed of SO₂.
The model we have used to simulate the evolution of the plume is not able to simulate the oxidation of SO₂. In fact the conversion from SO₂ to sulfate aerosol is happening during the transport process. We assume in the validation of the transport simulations, that the SO₂ is collocated with the sulfate aerosol, assuming that the sedimentation of the small sulfate aerosol particles is negligible for the time scale considered.



eruption, and crossed the Equator by the end of June 2009. Till the end of July 2009, there were nearly 4% of the air parcels that had entered the tropical stratosphere. This trend is further verified by the MIPAS aerosol detections (middle and bottom panels in Fig. 5). As shown by the MIPAS aerosol detections, shortly after the eruption of Sarychev, large quantities of stratospheric aerosol formed from directly injected SO₂. Most of the stratospheric aerosol stayed at Northern Hemisphere mid- and high latitudes. However, there was **1** increasing number of aerosol detections in the tropical stratosphere. The aerosol in the extratropical stratosphere was removed by the end of 2009, while the aerosol that had entered the tropical stratosphere stayed for months. Aerosol optical depths from OSIRIS and scattering ratio from CALIPSO lidar measurements have also shown similar equatorward dispersion of the aerosol after the eruption of Sarychev (Haywood et al., 2010; Solomon et al., 2011).

4.2 The role of the ASM anticyclone

As shown by the evolution of Sarychev plume in section 3.2, active Rossby wave breaking events at mid-latitudes during boreal summer have significantly influenced the plume dispersion. In boreal summer, the ASM is among the most prominent circulation patterns. **2** Figure 6 shows a cross section of the ASM in boreal summer 2009. Generally, the ASM ranged from 360–400 K, marked by the negative PV anomaly of **3** and it was bounded by the subtropical and equatorial jets. The thermal tropopause averaged over 40–120°E was elevated up to about 390 K. The ASM anticyclonic circulation facilitates meridional transport when the subtropical jet weakens and retreats northward (Haynes and Shuckburgh, 2000). Figure 7 depicts the MIPAS aerosol measurements between 40–120°E during June–August 2009. The aerosol detections between 360 and 400 K were collocated with the core of the ASM, extending from the mid-latitude UTLS to the **4** TL. The aerosol that made **5** their way above the subtropical jet core to lower latitudes along the isentropic surfaces cannot be explained by convection but only by large-scale transport associated with the ASM.

Using our trajectory simulations, it is straightforward to see the role of ASM anticyclonic circulation in influencing the pathway of the plume. The distributions of air parcels in the vertical range of 360–400 K (in percentage of total number of air parcels released after the eruption) by **6** 30 June, 10 July, 20 July and 31 July 2009 are shown in Fig. 8. The red contour is the geopotential height of 14,320 m on 150 hPa pressure surface, denoting a commonly used boundary of the ASM anticyclone (Randel and Park, 2006). At latitudes between 15–40°N in summer, the 150 hPa pressure surface is around 370 K. The black contour is the PV-based ASM transport barrier for July 2009 (1.8 PVU) on 370 K isentropic surface as defined by Ploeger et al. (2015).

In the first 19 days (top left panel in Fig. 8), from first eruption on 12 June to 30 June 2009, the plume mostly moved eastward and remained at mid- and high latitudes. After another 10 days (top right panel in Fig. 8), air parcels were entrained into the anticyclonic circulations of the American monsoon and a fraction was shed towards the tropics. The remaining air parcels that entered the ASM circulation were entrained along the flow surrounding the ASM anticyclone and moved south-westward approaching the tropics. In the following 20 days (bottom panels in Fig. 8), some air parcels were dragged along the flow south of the ASM, and some were shed out from the south-eastern flank of the anticyclone and spread over the tropics. The American monsoon plays a similar role as the ASM in transporting air parcels to lower latitudes, but it is much weaker in strength. The ‘aerosol hole’ between 360 and 400 K illustrated the ASM’s role as a transport barrier between the air inside and outside of the anticyclone. In our case, it is better demarcated by the PV-based barrier than the geopotential

T Number: 1 Author: Date: 8/23/2017 10:31:41 PM

Increasing from what? Obviously, if you start at 0, the number increases.

S Author: Date: 8/23/2017 10:31:41 PM

The sentences in this paragraph are rephrased.

T Number: 2 Author: Date: 8/23/2017 10:31:41 PM

Where did these data come from? There are no direct observations of PV.

S Author: Date: 8/23/2017 10:31:41 PM

Fixed in the figure caption. Thank you.

T Number: 3 Author: Date: 8/23/2017 10:31:41 PM

units?

S Author: Date: 8/23/2017 10:31:41 PM

Fixed. Thank you.

T Number: 4 Author: Date: 8/23/2017 10:31:41 PM

What is this? Define all acronyms.

S Author: Date: 8/23/2017 10:31:41 PM

Fixed. Thank you.

T Number: 5 Author: Date: 8/23/2017 10:31:41 PM

its

S Author: Date: 8/23/2017 10:31:41 PM

Fixed. Thank you.

T Number: 6 Author: Date: 8/23/2017 10:31:41 PM

delete

S Author: Date: 8/23/2017 10:31:41 PM

Fixed. Thank you.



height criterion. The northern barrier of the subtropical jet was strong, while the southern barrier was more permeable for meridional transport.

This meridional transport under the influence of the ASM revealed by the simulations shown in Fig. 8 is verified by the MIPAS aerosol detections shown in Fig. 9. Because of the sparse horizontal coverage of MIPAS detections, 1.5-day forward and 1.5-day backward trajectories initialized by MIPAS aerosol detections were calculated to fill gaps in space and time. Compared with MIPAS detections in Fig. 9, the simulations in Fig. 8 could successfully reproduce the maxima, minima and filaments of the aerosol distributions. It is also verified by MIPAS detections that the transport barrier of ASM is better demarcated by the PV-based barrier.

The transport pathway to low latitudes for aerosols above 400 K is shown by simulations in Fig. 10 and MIPAS aerosol detections in Fig. 11. At altitudes above the ASM, trajectories are driven by easterlies and meridional, isentropic winds. In the end of July 2009, air parcels above 400 K were transported to lower latitudes (as far as about 15°N), but could not reach the Equator. This suggests that ASM play the most significant role between 360 and 400 K, which may vary in spatial extent associated with the strength of the ASM.

However, a sensitivity test simulation of the same eruption in winter (January 2009) shows that, in northern hemisphere winter, meridional transport from extra-tropic to the tropics is typically suppressed by the strong winter subtropical jets. Forward trajectories initialized by the Sarychev SO₂ emissions (as shown in Fig. 2), but driven by winter wind fields in January and February 2009 are shown in Fig. 12. Compared with the summer scenario in Fig. 8, wind speeds in winter 2009 between 360 and 400 K were faster, and the trajectories could span the northern hemisphere within 20 days. About 40 days after eruption, air parcels were almost evenly distributed at mid- and high latitudes, but no air parcels did approach the Equator.

4.3 Upward transport of Sarychev aerosol

Simulation results from Figs. 8 to 11 have shown that the ASM anticyclone enhanced the equatorward dispersion of the Sarychev aerosol in the vertical range of 360–400 K, but the ASM did not facilitate the equatorward dispersion above 400K. The increased aerosol in the tropical stratosphere above 400 K (~ 18 km) could only be explained by the upward transport above the TTL. Above the tropopause diabatic heating surface (generally around 360 K), air masses that enter the TTL are considered to be lifted effectively by the radiative heating (Gettelman et al., 2004; Fueglistaler et al., 2009).

In Fig. 13, the upward transport of aerosol in the tropics is clearly demonstrated by the MIPAS aerosol detections at high altitudes between 10°N and 10°S. At 15 km, an enhanced aerosol signal was found from July 2009 and lasted for about 10 months. It returned to pre-Sarychev level at the end of May 2010. At 20 km, enhanced aerosol signal was detected in October 2009, and in another four months, the enhanced aerosol signal was found at 25 km. The overlaid ascent speed of water vapour tape recorder is derived with Aura Microwave Limb Sounder (MLS) measurements from Glanville et al. (2017). The ascent speed of the Sarychev aerosol agrees well with the ascent speed of the water vapour tape recorder before and after the data gap at the end of 2009 and beginning of 2010, which can be explained since the Sarychev aerosol is mainly in form of H₂SO₄-H₂O solution. This gap in the MIPAS aerosol data is caused by semi-annual temperature variations at higher altitudes (Griessbach et al., 2016).

1 Number: 1 Author: Date: 8/23/2017 10:31:41 PM

Explain in detail what this means and how you did the calculations.

5 Author: Date: 8/23/2017 10:31:41 PM

The trajectories are initialized with MIPAS aerosol detections on each day from 12 June 2009 to 31 July 2009. These detections are traced both forward and backward for 1.5 days with the MPTRAC model, so the length of each of the trajectories would be 3 days/72 hours. The model output interval are 6 hours, so this calculation produces aerosol data 12 times as many as the original MIPAS detections. A brief explanation is added in the manuscript.

1 Number: 2 Author: Date: 8/23/2017 10:31:41 PM

above in temperature or altitude?

5 Author: Date: 8/23/2017 10:31:41 PM

Fixed. Thank you.

1 Number: 3 Author: Date: 8/23/2017 10:31:41 PM

Until the end

5 Author: Date: 8/23/2017 10:31:41 PM

Fixed. Thank you.

1 Number: 4 Author: Date: 8/23/2017 10:31:41 PM

the zero

5 Author: Date: 8/23/2017 10:31:41 PM

Fixed. Thank you.

1 Number: 5 Author: Date: 8/23/2017 10:31:41 PM

delete

5 Author: Date: 8/23/2017 10:31:41 PM

Fixed. Thank you.




5 Discussion


The results of our study in **1** above sections suggest that the ASM anticyclone plays a key role in transporting the Sarychev aerosol **2** extra-tropical lower stratosphere into the TTL. In various studies, this quasi-isentropic transport from extra-tropics to the TTL is referred as in-mixing process (e.g., Konopka et al., 2009). Horizontal in-mixing of tracer species has been observed (e.g. Folkins et al., 1999) or modelled (e.g. Konopka et al., 2010), and has been used to explain the seasonal and annual cycle of tracer species (Abalos et al., 2013; Ploeger et al., 2013). The role of in-mixing is prominent when there are large gradients in these tracers between the tropics and the extra-tropics. The study of Abalos et al. (2013) shows that the main contribution to in-mixing originates in the northern hemisphere and is related to the Asian monsoon, and this in-mixing process takes place in the TTL close to the tropopause. These extra-tropics to tropics transport events are also considered to be driven by anticyclonic Rossby wave breaking (Homeyer and Bowman, 2013). The net equatorward transport peaks downstream of large anticyclones in the potential temperature range between 370 and 390 K (Homeyer and Bowman, 2013). Above the TTL, in-mixing rapidly decreases with height and becomes very weak at altitudes of the tropical pipe (Ploeger et al., 2013). These findings agree well with our study, which shows that the ASM anticyclonic circulation enhanced the equatorward transport between 360 and 400 K, but not above 400 K.


The pathway of the Sarychev plume approaching the deep tropics is modulated by the transport barrier at the boundary of the ASM anticyclone as well. The 'aerosol hole' shown in Figs. 8 and 9 that ranges from 360 to 400 K and collocates with the core of ASM, only appears during the ASM season. Conventionally, the geopotential height of 14,320 m on 150 hPa is used to define the boundary of the ASM anticyclone, but from the perspective of transport, the PV-based barrier defined by Ploeger et al. (2015) can better represent the boundary.


Our results also show that the meteorological background conditions during a volcanic eruptions have a significant impact on the transport of the volcanic aerosol. For instance, the Puyehue-Cordón Caulle emissions reached the lower stratosphere and were rapidly transported eastward by the jet stream (Klüser et al, 2013; Hoffmann et al., 2016), while the Nabro emissions were captured by the ASM circulation in UTLS region (Fairlie et al., 2014; Heng et al., 2016). In this study, the transport of the equatorward dispersion of Sarychev aerosol is driven by the ASM anticyclone. Aerosol entering TTL via ASM further entered the ascending branch of the Brewer–Dobson circulation. This enabled the Sarychev aerosol to remain in the stratosphere for months and further spread over both hemispheres. In this way, the Sarychev eruption may not only influence the northern hemisphere, but could also have potential impact on the global chemical composition and radiative budget similar to a tropical volcanic eruption. Although only a fraction of the SO₂ emission (~4% out of 1.4 Tg) was transported to the tropical stratosphere by the end of July 2009, if the SO₂ is entirely converted into gaseous H₂SO₄ and condensed into a 75%-25% H₂SO₄-H₂O solution, **3** the total aerosol mass loading added by Sarychev eruption would be about 0.07 Tg of sulfur, which is about three times larger than the 0.01–0.02 Tg of sulfur per year required to explain the average aerosol increase of 4–7 % per year after 2002 **4** (ofman et al., 2009).


Moreover **5** shore aerosols were transported to or ascended to the tropical stratosphere after July 2009. Although the relative change of the aerosol concentration, the SO₂ and sulfate aerosol transported to the tropics and further to the southern hemisphere will not only perturb the radiative balance but also have a substantial effect on microphysical processes, such as coagulation and growth of **6** cloud condensation nuclei (Manktelow et al., 2009; Schmidt et al., 2010).


 Number: 1 Author: Date: 8/23/2017 10:31:41 PM
the above


 Author: Date: 8/23/2017 10:31:41 PM
Fixed. Thank you.


 Number: 2 Author: Date: 8/23/2017 10:31:41 PM
from the


 Author: Date: 8/23/2017 10:31:41 PM
Fixed. Thank you.


 Number: 3 Author: Date: 8/23/2017 10:31:41 PM
Added to what?


 Author: Date: 8/23/2017 10:31:41 PM
Fixed. Thank you.


 Number: 4 Author: Date: 8/23/2017 10:31:41 PM
Hofmann

 Author: Date: 8/23/2017 10:31:41 PM
Fixed. Thank you.

 Number: 5 Author: Date: 8/23/2017 10:31:41 PM
more than what? More in time or space?

 Author: Date: 8/23/2017 10:31:41 PM
Fixed. Thank you.

 Number: 6 Author: Date: 8/23/2017 10:31:41 PM
Wrong! CCN are important in the troposphere, but not in the stratosphere.

 Author: Date: 8/23/2017 10:31:41 PM
Here we have deleted several sentences that are not very closely related to our results.

We believe with no doubt that CCN is very important in the troposphere. Here, we did not argue exclusively about the importance of CCN in the stratosphere. Stratospheric aerosols can also sediment into the troposphere, modify the aerosol composition and thus might for example impact cirrus clouds.

And in fact, CCN also plays a very important role in the stratosphere. Although the stratosphere is much cleaner and dryer than the troposphere, there is a long history of observing the stratospheric clouds. Needless to say, stratospheric clouds have an unignorable effect on the global climate. A significant amount of particulate matter in the stratosphere can act as CCN, e.g. the debris from meteoritic ablation, aluminium oxide spherules from space shuttle launches, and most importantly, the sulfate aerosol. For example, the sulfate aerosols in supercooled liquid state or ice particle state provide an essential condition for the formation of stratospheric clouds. The permanent stratospheric sulfate aerosol layer between about 12 and 30 km will be significantly enhanced after explosive volcanic eruptions.

Reference: Hamill, P., and Toon, O. B.: Polar stratospheric clouds and the ozone hole, *Phys. Today*, 44, 34-42, doi: 10.1063/1.881277, 1991.

Tabazadeh, A., Turco, R. P., Drdla, K., Jacobson, M. Z., and Toon, O. B.: A study of type I polar stratospheric cloud formation, *Geophys. Res. Lett.*, 21, 1619-1622, doi: 10.1029/94GL01368, 1994.



Since the potential climate impact of high-latitude volcanic emissions largely depends on their plume height and the meteorological background conditions, it is essential to initialize ¹the simulations with realistic time- and altitude-resolved SO₂ emission rate. The backward trajectory approach used in this study to reconstruct the emission time series proves to be an efficient way to produce realistic SO₂ emission rate time series.

5 6 Summary

In this study, we analysed the equatorward transport pathway of volcanic aerosol from the high-latitude volcanic eruption of the Sarychev in 2009. The analysis was based on MIPAS aerosol detections, AIRS SO₂ measurements and trajectory simulations.


First, the time- and altitude-resolved SO₂ emission rate was derived using backward trajectories initialized with
10 AIRS SO₂ measurements. Second, the dispersion of Sarychev plume from the beginning of the eruption (12 June 2009) to 31 July 2009 was simulated based on the derived SO₂ emissions rate. The horizontal distribution of the plume and its altitudes were validated with AIRS SO₂ measurements and MIPAS aerosol measurements respectively. The comparisons showed that there was good agreement between the simulations and observations.
15 The results presented in this study suggest that in boreal summer, the transport and dispersion of volcanic emissions were greatly influenced by the dominating ASM circulation, which facilitates the meridional transport of aerosols from the extra-tropical UTLS to the TTL by entraining air along the anticyclonic flows and shedding the air to the deep tropics downstream of the anticyclonic circulation. Meanwhile, the ASM anticyclone effectively isolates the air inside of the ASM from aerosol-rich air outside the anticyclone. The transport barrier at the boundary of the ASM is better denoted by the barrier defined by the PV gradient approach. However, the
20 ASM only influenced the plume dispersion significantly in the vertical range of 360–400 K. The ASM anticyclone did not have notable impact on the equatorward dispersion above 400 K, where the Sarychev aerosol was confined in the northern hemisphere.


The simulations show that until the end of July 2009, about 4% of the emission had entered the tropical stratosphere. Increased ²number of aerosol was detected by MIPAS in the tropical stratosphere afterwards. After
25 entering the TTL, the aerosol experienced large-scale ascent in the Brewer–Dobson circulation. The ascent speed agrees well with the ascent speed of the water vapour tape recorder. Aerosol signal in the tropics was enhanced within one month of the eruption, and returned to pre-Sarychev level after about 10 months.


The Sarychev eruption had the chance to contribute to the stratospheric aerosol loading in the tropics because it
30 occurred in boreal summer when the equatorward transport was enhanced by the ASM anticyclone. If the eruption happened in winter, the volcanic aerosol would be confined to the latitudes of strong subtropical jets.


7 Code and data availability

AIRS data are distributed by the NASA Goddard Earth Sciences Data Information and Services Center (AIRS Science Team and Chahine, 2007). Envisat MIPAS Level-1B data are distributed by the European Space Agency. The ERA–Interim reanalysis data were obtained from the European Centre for Medium-Range
35 Weather Forecasts. The code of the Massive-Parallel Trajectory Calculations (MPTRAC) model is available under the terms and conditions of the GNU General Public License, Version 3 from the repository at <https://github.com/slcs-jsc/mptrac> (last access: 12 April 2017).

 Number: 1 Author: Date: 8/23/2017 10:31:41 PM
What simulations?

 Author: Date: 8/23/2017 10:31:41 PM
"to initialize the simulations" is changed into "to conduct Lagrangian transport simulations".

 Number: 2 Author: Date: 8/23/2017 10:31:41 PM
wrong English

 Author: Date: 8/23/2017 10:31:41 PM
The sentences here are rephrased.



8 Competing interests

The authors declare that they have no conflict of interest.

- Acknowledgements.* This work was supported by National Natural Science Foundation of China under grant No. 41605023 and International Postdoctoral Exchange Fellowship Program 2015 under grant No. 20151006. The PV gradient based transport barrier data is provided by Dr. Felix Ploeger from Institute of Energy and Climate Research: Stratosphere (IEK-7), Forschungszentrum Jülich GmbH.
- 5

This page contains no comments




References


- Abalos, M., Ploeger, F., Konopka, P., Randel, W., and Serrano, E.: Ozone seasonality above the tropical tropopause: reconciling the Eulerian and Lagrangian perspectives of transport processes, *Atmos. Chem. Phys.*, 13, 10787-10794, doi:10.5194/acp-13-10787-2013, 2013.
- 5 Aumann, H. H., Chahine, M. T., Gautier, C., Goldberg, M. D., Kalnay, E., McMillin, L. M., Revercomb, H., Rosenkranz, P. W., Smith, W. L., Staelin, D. H., Strow, L. L., and Susskind, J.: AIRS/AMSU/HSB on the Aqua mission: design, science objectives, data products, and processing systems, *IEEE Trans. Geosci. Remote Sens.*, 41, 253-264, doi: 10.1109/TGRS.2002.808356, 2003.
- 10 Brühl, C., Lelieveld, J., Tost, H., Höpfner, M., and Glatthor, N.: Stratospheric sulfur and its implications for radiative forcing simulated by the chemistry climate model EMAC, *Journal of Geophysical Research: Atmospheres*, 120, 2103-2118, doi: 10.1002/2014JD022430, 2015.
- Butchart, N., Scaife, A. A., Bourqui, M., de Grandpre, J., Hare, S. H. E., Kettleborough, J., Langematz, U., Manzini, E., Sassi, F., Shibata, K., Shindell, D., and Sigmond, M.: Simulations of anthropogenic change in the strength of the Brewer-Dobson circulation, *Climate Dynam.*, 27, 727-741, 10.1007/s00382-006-0162-4, 2006.
- 15 Carboni, E., Grainger, R. G., Mather, T. A., Pyle, D. M., Thomas, G. E., Siddans, R., Smith, A. J. A., Dudhia, A., Koukouli, M. E., and Balis, D.: The vertical distribution of volcanic SO₂ plume measured by IASI, *Atmos. Chem. Phys.*, 16, 4343-4367, doi: 10.5194/acp-16-4343-2016, 2016.
- 20 Dee, D. P., Uppala, S. M., Simmons, A. J., Berrisford, P., Poli, P., Kobayashi, S., Andrae, U., Balmaseda, M. A., Balsamo, G., Bauer, P., Bechtold, P., Beljaars, A. C. M., van de Berg, L., Bidlot, J., Bormann, N., Delsol, C., Dragani, R., Fuentes, M., Geer, A. J., Haimberger, L., Healy, S. B., Hersbach, H., Hólm, E. V., Isaksen, I., Kållberg, P., Köhler, M., Matricardi, M., McNally, A. P., Monge-Sanz, B. M., Morcrette, J. J., Park, B. K., Peubey, C., de Rosnay, P., Tavolato, C., Thépaut, J. N., and Vitart, F.: The ERA-Interim reanalysis: configuration and performance of the data assimilation system, *Q. J. R. Meteorol. Soc.*, 137, 553-597, doi: 10.1002/qj.828, 2011.
- 25 Doeringer, D., Eldering, A., Boone, C. D., González Abad, G., and Bernath, P. F.: Observation of sulfate aerosols and SO₂ from the Sarychev volcanic eruption using data from the Atmospheric Chemistry Experiment (ACE), *J. Geophys. Res. Atmos.*, 117, D03203, doi: 10.1029/2011JD016556, 2012.
- 30 Fadnavis, S., Semeniuk, K., Pozzoli, L., Schultz, M. G., Ghude, S. D., Das, S., and Kakatkar, R.: Transport of aerosols into the UTLS and their impact on the Asian monsoon region as seen in a global model simulation, *Atmos. Chem. Phys.*, 13, 8771-8786, doi: 10.5194/acp-13-8771-2013, 2013.
- Fairlie, T. D., Vernier, J. P., Natarajan, M., and Bedka, K. M.: Dispersion of the Nabro volcanic plume and its relation to the Asian summer monsoon, *Atmos. Chem. Phys.*, 14, 7045-7057, doi: 10.5194/acp-14-7045-2014, 2014.
- 35 Fischer, H., Birk, M., Blom, C., Carli, B., Carlotti, M., von Clarmann, T., Delbouille, L., Dudhia, A., Ehret, D., Endemann, M., Flaud, J. M., Gessner, R., Kleinert, A., Koopman, R., Langen, J., López-Puertas, M., Mosner, P., Nett, H., Oelhaf, H., Perron, G., Remedios, J., Ridolfi, M., Stiller, G., and Zander, R.: MIPAS: an instrument for atmospheric and climate research, *Atmos. Chem. Phys.*, 8, 2151-2188, doi: 10.5194/acp-8-2151-2008, 2008.
- 40 Folkins, I., Loewenstein, M., Podolske, J., Oltmans, S. J., and Proffitt, M.: A barrier to vertical mixing at 14 km in the tropics: Evidence from ozonesondes and aircraft measurements, *J. Geophys. Res. Atmos.*, 104, 22095-22102, doi: 10.1029/1999JD900404, 1999.
- Fueglistaler, S., Dessler, A. E., Dunkerton, T. J., Folkins, I., Fu, Q., and Mote, P. W.: Tropical Tropopause Layer, *Rev. Geophys.*, 47, 31, doi: 10.1029/2008rg000267, 2009.
- 45 Gerlach, T.: Volcanic versus anthropogenic carbon dioxide, *Eos, Trans. Am. Geophys. Union*, 92, 201-202, doi: 10.1029/2011EO240001, 2011.
- Gerlach, T. M.: Present-day CO₂ emissions from volcanoes, *Eos, Trans. Am. Geophys. Union*, 72, 249-255, doi: 10.1029/90EO10192, 1991.
- 50 Gettelman, A., Forster, P. M. d. F., Fujiwara, M., Fu, Q., Vömel, H., Gohar, L. K., Johanson, C., and Ammerman, M.: Radiation balance of the tropical tropopause layer, *J. Geophys. Res. Atmos.*, 109, D07103, doi: 10.1029/2003JD004190, 2004.
- Glanville, A. A., and Birner, T.: Role of vertical and horizontal mixing in the tape recorder signal near the tropical tropopause, *Atmos. Chem. Phys.*, 17, 4337-4353, doi: 10.5194/acp-17-4337-2017, 2017.
- 55 Griessbach, S., Hoffmann, L., Spang, R., von Hobe, M., Müller, R., and Riese, M.: Infrared limb emission measurements of aerosol in the troposphere and stratosphere, *Atmos. Meas. Tech.*, 9, 4399-4423, doi:10.5194/amt-9-4399-2016, 2016.
- Haynes, P., and Shuckburgh, E.: Effective diffusivity as a diagnostic of atmospheric transport: 2. Troposphere and lower stratosphere, *J. Geophys. Res. Atmos.*, 105, 22795-22810, doi: 10.1029/2000JD900092, 2000.

This page contains no comments



- Haywood, J. M., Jones, A., Clarisse, L., Bourassa, A., Barnes, J., Telford, P., Bellouin, N., Boucher, O., Agnew, P., Clerbaux, C., Coheur, P., Degenstein, D., and Braesicke, P.: Observations of the eruption of the Sarychev volcano and simulations using the HadGEM2 climate model, *J. Geophys. Res. Atmos.*, 115, D21212, doi: 10.1029/2010JD014447, 2010.
- 5 Haywood, J. M., Jones, A., and Jones, G. S.: The impact of volcanic eruptions in the period 2000–2013 on global mean temperature trends evaluated in the HadGEM2-ES climate model, *Atmos. Sci. Lett.*, 15, 92–96, doi: 10.1002/asl2.471, 2014.
- Heng, Y., Hoffmann, L., Griessbach, S., Rößler, T., and Stein, O.: Inverse transport modeling of volcanic sulfur dioxide emissions using large-scale simulations, *Geosci. Model Dev.*, 9, 1627–1645, doi:10.5194/gmd-9-1627-2016, 2016.
- 10 Hoffmann, L., Griessbach, S., and Meyer, C. I.: Volcanic emissions from AIRS observations: detection methods, case study, and statistical analysis, in: *Remote Sensing of Clouds and the Atmosphere XIX and Optics in Atmospheric Propagation and Adaptive Systems XVII*, edited by: Comeron, A., Kassianov, E. I., Schafer, K., Picard, R. H., Stein, K., and Gonglewski, J. D., Proceedings of SPIE, Spie-Int Soc Optical Engineering, Bellingham, doi: 92421410.1117/12.2066326, 2014.
- 15 Hoffmann, L., Rößler, T., Griessbach, S., Heng, Y., and Stein, O.: Lagrangian transport simulations of volcanic sulfur dioxide emissions: Impact of meteorological data products, *J. Geophys. Res. Atmos.*, 121, 4651–4673, doi: 10.1002/2015JD023749, 2016.
- Hofmann, D., Barnes, J., O'Neill, M., Trudeau, M., and Neely, R.: Increase in background stratospheric aerosol observed with lidar at Mauna Loa Observatory and Boulder, Colorado, *Geophys. Res. Lett.*, 36, L15808, doi: 10.1029/2009GL039008, 2009.
- Jégou, F., Berthet, G., Brogniez, C., Renard, J. B., François, P., Haywood, J. M., Jones, A., Bourgeois, Q., Lurton, T., Auriol, F., Godin-Beekmann, S., Guimbaud, C., Krysztofiak, G., Gaubicher, B., Chartier, M., Clarisse, L., Clerbaux, C., Balois, J. Y., Verwaerde, C., and Dageron, D.: Stratospheric aerosols from the Sarychev volcano eruption in the 2009 Arctic summer, *Atmos. Chem. Phys.*, 13, 6533–6552, doi: 10.5194/acp-13-6533-2013, 2013.
- 1 Remser, S., Thomason, L. W., von Hobe, M., Hermann, M., Deshler, T., Timmreck, C., Toohey, M., Stenke, A., Schwarz, J. P., Weigel, R., Fueglistaler, S., Prata, F. J., Vernier, J.-P., Schlager, H., Barnes, J. E., Antuña-Marrero, J.-C., Fairlie, D., Palm, M., Mahieu, E., Notholt, J., Rex, M., Bingen, C., Vanhellemont, F., Bourassa, A., Plane, J. M. C., Klocke, D., Carn, S. A., Clarisse, L., Trickl, T., Neely, R., James, A. D., Rieger, L., Wilson, J. C., and Meland, B.: Stratospheric aerosol – Observations, processes, and impact on climate, *Rev. Geophys.*, 54, 278–335, doi: 10.1002/2015RG000511, 2016.
- Konopka, P., Groß, J.-U., Plöger, F., and Müller, R.: Annual cycle of horizontal in-mixing into the lower tropical stratosphere, *J. Geophys. Res. Atmos.*, 114, D19111, doi: 10.1029/2009JD011955, 2009.
- 35 Konopka, P., Groß, J. U., Günther, G., Ploeger, F., Pommrich, R., Müller, R., and Livesey, N.: Annual cycle of ozone at and above the tropical tropopause: observations versus simulations with the Chemical Lagrangian Model of the Stratosphere (CLaMS), *Atmos. Chem. Phys.*, 10, 121–132, doi: 10.5194/acp-10-121-2010, 2010.
- Kravitz, B., and Robock, A.: Climate effects of high-latitude volcanic eruptions: Role of the time of year, *J. Geophys. Res.*, 116, D01105, doi: 10.1029/2010JD014448, 2011.
- 40 Kravitz, B., Robock, A., Bourassa, A., Deshler, T., Wu, D., Mattis, I., Finger, F., Hoffmann, A., Ritter, C., Bitar, L., Duck, T. J., and Barnes, J. E.: Simulation and observations of stratospheric aerosols from the 2009 Sarychev volcanic eruption, *J. Geophys. Res. Atmos.*, 116, D18211, doi: 10.1029/2010JD015501, 2011.
- Klüser, L., Erbertseder, T., and Meyer-Arneck, J.: Observation of volcanic ash from Puyehue–Cordón Caulle with IASI, *Atmos. Meas. Tech.*, 6, 35–46, doi:10.5194/amt-6-35-2013, 2013.
- 45 Levin, B. W., Rybin, A. V., Vasilenko, N. F., Prytkov, A. S., Chibisova, M. V., Kogan, M. G., Steblov, G. M., and Frolov, D. I.: Monitoring of the eruption of the Sarychev Peak Volcano in Matua Island in 2009 (central Kurile islands), *Dokl. Earth Sci.*, 435, 1507–1510, doi: 10.1134/s1028334x10110218, 2010.
- Manktelow, P. T., Carslaw, K. S., Mann, G. W., and Spracklen, D. V.: Variable CCN formation potential of regional sulfur emissions, *Atmos. Chem. Phys.*, 9, 3253–3259, doi: 10.5194/acp-9-3253-2009, 2009.
- 50 Neely, R. R., Toon, O. B., Solomon, S., Vernier, J. P., Alvarez, C., English, J. M., Rosenlof, K. H., Mills, M. J., Bardeen, C. G., Daniel, J. S., and Thayer, J. P.: Recent anthropogenic increases in SO₂ from Asia have minimal impact on stratospheric aerosol, *Geophys. Res. Lett.*, 40, 999–1004, doi: 10.1002/grl.50263, 2013.
- Niemeier, U., Timmreck, C., Graf, H. F., Kinne, S., Rast, S., and Self, S.: Initial fate of fine ash and sulfur from large volcanic eruptions, *Atmos. Chem. Phys.*, 9, 9043–9057, doi: 10.5194/acp-9-9043-2009, 2009.
- 55 Oman, L., Robock, A., Stenchikov, G. L., and Thordarson, T.: High-latitude eruptions cast shadow over the African monsoon and the flow of the Nile, *Geophys. Res. Lett.*, 33, L18711, doi: 10.1029/2006GL027665, 2006.
- Pausata, F. S. R., Chafik, L., Caballero, R., and Battisti, D. S.: Impacts of high-latitude volcanic eruptions on ENSO and AMOC, *Proc. Natl. Acad. Sci. U.S.A.*, 112, 13784–13788, doi: 10.1073/pnas.1509153112, 2015.
- 60

 Number: 1 Author: Date: 8/23/2017 10:31:41 PM
Needs to be alphabetical order.

 Author: Date: 8/23/2017 10:31:41 PM
Fixed. Thank you.



- Ploeger, F., Gottschling, C., Griessbach, S., Groß, J. U., Guenther, G., Konopka, P., Müller, R., Riese, M., Stroh, F., Tao, M., Ungermaier, J., Vogel, B., and von Hobe, M.: A potential vorticity-based determination of the transport barrier in the Asian summer monsoon anticyclone, *Atmos. Chem. Phys.*, 15, 13145-13159, doi: 10.5194/acp-15-13145-2015, 2015.
- 5 Ploeger, F., Günther, G., Konopka, P., Fueglistaler, S., Müller, R., Hoppe, C., Kunz, A., Spang, R., Groß, J. U., and Riese, M.: Horizontal water vapor transport in the lower stratosphere from subtropics to high latitudes during boreal summer, *J. Geophys. Res. Atmos.*, 118, 8111-8127, doi: 10.1002/jgrd.50636, 2013.
- Randel, W. J., and Park, M.: Deep convective influence on the Asian summer monsoon anticyclone and associated tracer variability observed with Atmospheric Infrared Sounder (AIRS), *J. Geophys. Res. Atmos.*, 111, D12314, doi: 10.1029/2005JD006490, 2006.
- 10 Ridley, D. A., Solomon, S., Barnes, J. E., Burlakov, V. D., Deshler, T., Dolgii, S. I., Herber, A. B., Nagai, T., Neely, R. R., Nevzorov, A. V., Ritter, C., Sakai, T., Santer, B. D., Sato, M., Schmidt, A., Uchino, O., and Vernier, J. P.: Total volcanic stratospheric aerosol optical depths and implications for global climate change, *Geophys. Res. Lett.*, 41, 7763-7769, doi: 10.1002/2014GL061541, 2014.
- 15 Robock, A.: Volcanic eruptions and climate, *Rev. Geophys.*, 38, 191-219, doi: 10.1029/1998RG000054, 2000.
- Robock, A.: The Latest on Volcanic Eruptions and Climate, *Eos, Trans. Am. Geophys. Union*, 94, 305-306, doi: 10.1002/2013EO350001, 2013.
- Rodriguez, J. M., Ko, M. K. W., and Sze, N. D.: Role of the heterogeneous conversion of N₂O₅ on sulfate aerosols in global ozone losses, *Nature*, 352, 134-137, doi: 10.1038/352134a0, 1991.
- 20 Rybin, A., Chibisova, M., Webley, P., Steensen, T., Izbekov, P., Neal, C., and Realmuto, V.: Satellite and ground observations of the June 2009 eruption of Sarychev Peak volcano, Matua Island, Central Kuriles, *Bull. Volcanol.*, 73, 1377-1392, doi: 10.1007/s00445-011-0481-0, 2011.
- Santer, B. D., Bonfils, C., Painter, J. F., Zelinka, M. D., Mears, C., Solomon, S., Schmidt, G. A., Fyfe, J. C., Cole, J. N. S., Nazarenko, L., Taylor, K. E., and Wentz, F. J.: Volcanic contribution to decadal changes in tropospheric temperature, *Nature Geosci.*, 7, 185-189, doi: 10.1038/ngeo2098, 2014.
- 25 Schmidt, A., Carslaw, K. S., Mann, G. W., Wilson, M., Breider, T. J., Pickering, S. J., and Thordarson, T.: The impact of the 1783–1784 AD Laki eruption on global aerosol formation processes and cloud condensation nuclei, *Atmos. Chem. Phys.*, 10, 6025-6041, doi: 10.5194/acp-10-6025-2010, 2010.
- Seviour, W. J. M., Butchart, N., Hardiman, S. C.: The Brewer–Dobson circulation inferred from ERA-Interim, *Q. J. R. Meteorol. Soc.*, 138, 878–888, doi: 10.1002/qj.966, 2012.
- 30 Solomon, S., Daniel, J. S., Neely, R. R., Vernier, J.-P., Dutton, E. G., and Thomason, L. W.: The Persistently Variable “Background” Stratospheric Aerosol Layer and Global Climate Change, *Science*, 333, 866-870, doi: 10.1126/science.1206027, 2011.
- Solomon, S., Ivy, D. J., Kinnison, D., Mills, M. J., Neely R. R., Schmidt, A.: Emergence of healing in the Antarctic ozone layer, *Science*, doi: http://dx.doi.org/10.1126/science.aae0061, 2016.
- 35 Solomon, S., Sanders, R. W., Garcia, R. R., and Keys, J. G.: Increased chlorine dioxide over Antarctica caused by volcanic aerosols from Mount-Pinatubo, *Nature*, 363, 245-248, doi: 10.1038/363245a0, 1993.
- Stohl, A., Forster, C., Frank, A., Seibert, P., and Wotawa, G.: Technical note: The Lagrangian particle dispersion model FLEXPART version 6.2, *Atmos. Chem. Phys.*, 5, 2461-2474, doi:10.5194/acp-5-2461-2005, 2005.
- 40 Tilmes, S., Müller, R., and Salawitch, R.: The sensitivity of polar ozone depletion to proposed geoengineering schemes, *Science*, 320, 1201-1204, doi: 10.1126/science.1153966, 2008.
- Timmreck, C.: Modeling the climatic effects of large explosive volcanic eruptions, *WIREs Clim. Change*, 3, 545-564, doi: 10.1002/wcc.192, 2012.
- 45 Vernier, J. P., Thomason, L. W., Pommereau, J. P., Bourassa, A., Pelon, J., Garnier, A., Hauchecorne, A., Blanot, L., Trepte, C., Degenstein, D., and Vargas, F.: Major influence of tropical volcanic eruptions on the stratospheric aerosol layer during the last decade, *Geophys. Res. Lett.*, 38, L12807, doi: 10.1029/2011GL047563, 2011.
- von Glasow, R., Bobrowski, N., and Kern, C.: The effects of volcanic eruptions on atmospheric chemistry, *Chem. Geol.*, 263, 131–142, doi: http://dx.doi.org/10.1016/j.chemgeo.2008.08.020, 2009.
- 50 von Savigny, C., Ernst, F., Rozanov, A., Hommel, R., Eichmann, K. U., Rozanov, V., Burrows, J. P., and Thomason, L. W.: Improved stratospheric aerosol extinction profiles from SCIAMACHY: validation and sample results, *Atmos. Meas. Tech.*, 8, 5223-5235, doi: 10.5194/amt-8-5223-2015, 2015.

This page contains no comments

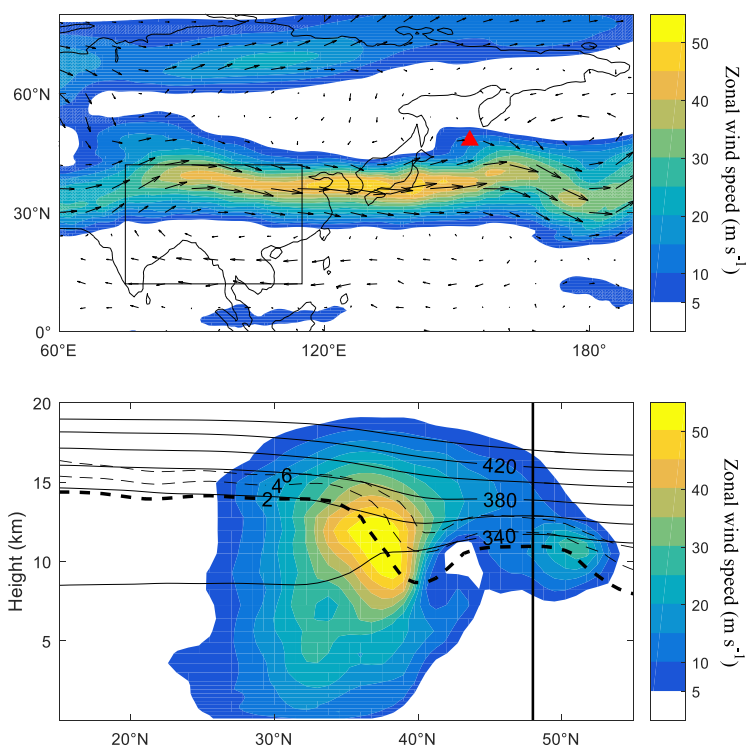


Figure 1: **1**pp: zonal wind (shaded) and **2**nd vectors on the 370 K isentropic surface at 0 UTC on 12 June 2009. The location of the Sarychev peak is denoted with a red triangle. The black rectangle **3** indicates the area of **4** developing ASM anticyclone. **5**ptom: vertical section of zonal wind (shaded) and contours of potential temperature from 340 K to 440 K (black solid lines) and potential vorticity from 2 PVU to 6 PVU (black dashed lines) along 153°E. The vertical black line denotes the latitude (48.1°N) of the Sarychev peak.

T Number: 1 Author: Date: 8/23/2017 10:31:41 PM
What is the source for these data?

S Author: Date: 8/23/2017 10:31:41 PM
Data source is added in the figure caption. Thank you.

T Number: 2 Author: Date: 8/23/2017 10:31:41 PM
what is the scale for the length of the vectors?

S Author: Date: 8/23/2017 10:31:41 PM
The scale is added in the top panel. Thank you.

T Number: 3 Author: Date: 8/23/2017 10:31:41 PM
indicates

S Author: Date: 8/23/2017 10:31:41 PM
Fixed. Thank you.

T Number: 4 Author: Date: 8/23/2017 10:31:41 PM
the developing

S Author: Date: 8/23/2017 10:31:41 PM
Fixed. Thank you.

T Number: 5 Author: Date: 8/23/2017 10:31:41 PM
What is the source of the data? Why that latitude? Is this the same time as the top panel?

S Author: Date: 8/23/2017 10:31:41 PM
Data source is added in the figure caption.
The location of the volcano Sarychev peak is 48°N, 153°E, so a vertical line may help readers to know where the volcano is.
The top panel shows the wind fields from a horizontal view, and the location of the volcano is marked with a red triangle.

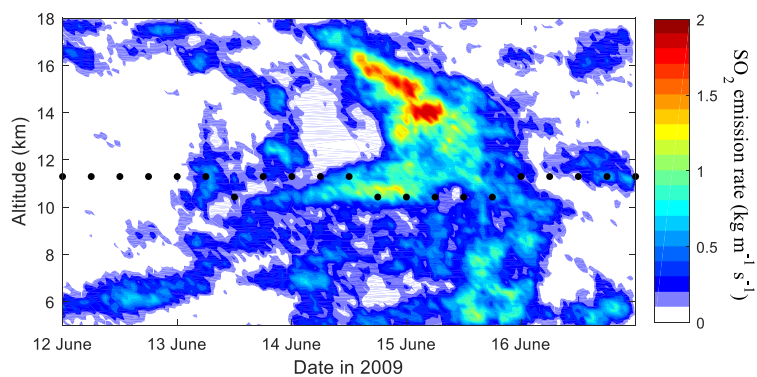



Figure 2: Sarychev SO₂ **mission** time series derived with AIRS measurements using a backward trajectory approach. The emission data is binned every 1 hour and 0.2 km. Black dots denote the height of the thermal tropopause.

Number: 1 Author: Date: 8/23/2017 10:31:41 PM

The units do not seem right.

And how can there be emissions in the stratosphere? Emissions come from the volcano.

 Author: Date: 8/23/2017 10:31:41 PM

We consider emissions into a vertical column over the volcano, so the unit " $\text{kg m}^{-1} \text{s}^{-1}$ " is a reasonable unit. For details please see the point-to-point reply.

The injection height of SO_2 by explosive volcanic eruptions can up to more than 10 km, and it is not rare to find SO_2 in the stratosphere directly injected by volcanism.

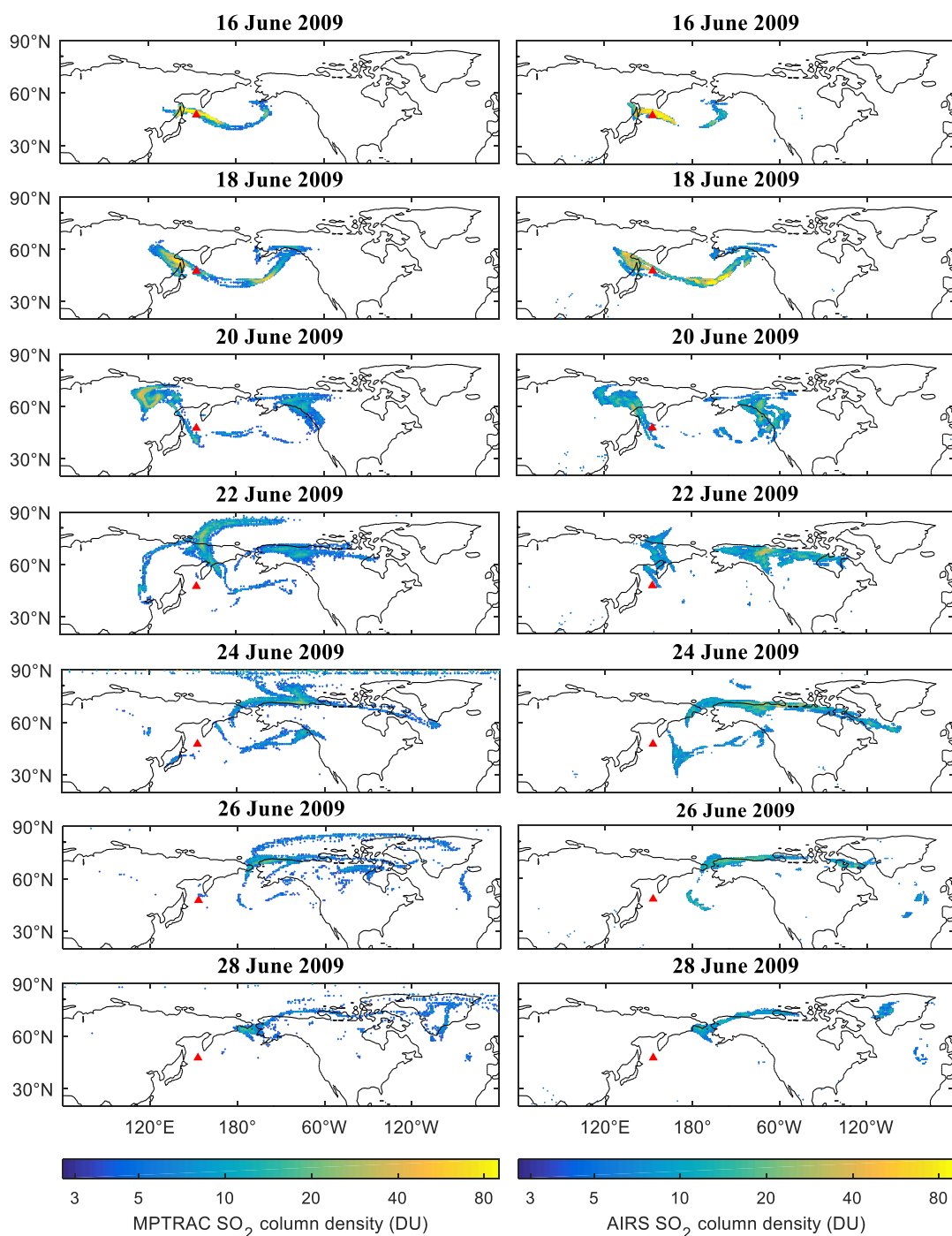


Figure 3: The evolution of SO₂ column density from MPTRAC (left, in Dobson units) and SO₂ column density from AIRS (right) for the period 16–28 June 2009. The MPTRAC SO₂ column density are shown for 0 UTC on selected days and AIRS data are collected within ± 6 hours. Only values larger than 2 DU are shown. The red triangle denotes the location of the Sarychev peak.

Number: 1 Author: Date: 8/23/2017 10:31:41 PM

DU are not units of density. This is the column burden.

Author: Date: 8/23/2017 10:31:41 PM

We believe Dobson units are often used to describe column densities of SO₂. We did not mean the "density of SO₂ gas" in the caption of Fig. 3, or anywhere else in this paper.

Number: 2 Author: Date: 8/23/2017 10:31:41 PM

Explain what MPTRAC is and how the data were generated. Is this a model? Was it initialized only once at the time of the eruption, or again each day? From what observations?

Author: Date: 8/23/2017 10:31:41 PM

Yes, MPTRAC is a model. We have introduced the model in Section 2.3.

The forward trajectories are initialized with air parcels. The essential information for each of the parcels is the longitude, latitude, altitude and SO₂ mass. The time period when we have this necessary information is from 12 June 2009 to 16 June 2009, when the explosive eruption occurred, as shown in Fig. 2. This initial information is derived by using a backward trajectory method and the AIRS SO₂ observation, and SO₂ mass from previous studies.

The forward trajectories are initialized once, and 6-hourly ERA-interim wind fields are used to carry on the trajectories simulations. The model outputs are given every six hours, but only results on selected time are shown in Fig. 3 and Fig. 4 for comparison with satellite observations. Although the simulation was only initialized once, but the simulation results agree well with observations.

Please see section 2.3 and section 3 for introduction of the MPTRAC model and how we carry out the simulation.

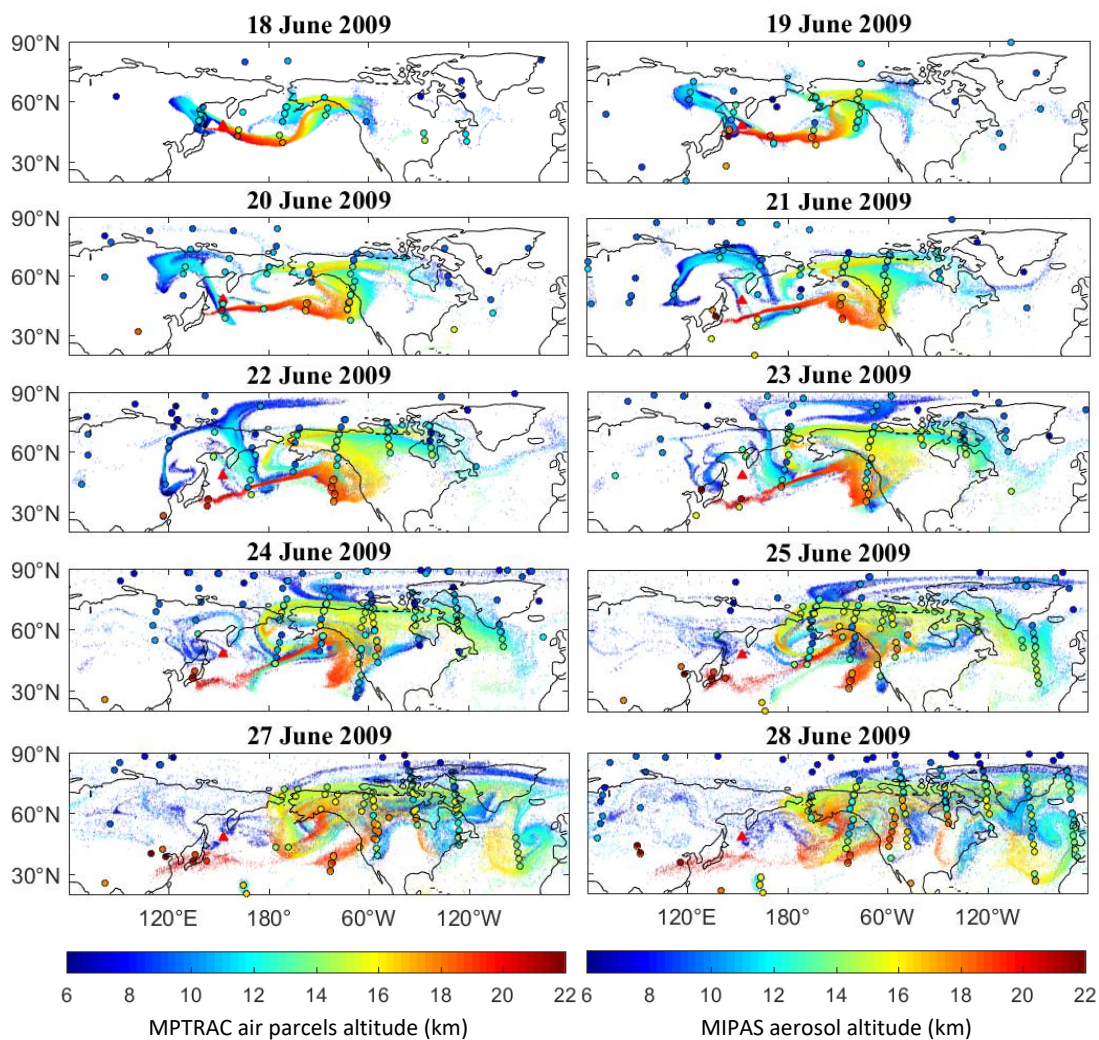




Figure 4: The evolution of SO₂ air parcel altitudes from MPTRAC (shown for 0 UTC on selected days) and MIPAS aerosol detections within ± 6 hours, denoted with color-filled circle markers. The altitudes of all air parcels, regardless of their SO₂ values, are shown. The red triangle denotes the location of the Sarychev peak.

 Number: 1 Author: Date: 8/23/2017 10:31:41 PM
So what is the shading in the MIPAS panels, if the data are only shown in the circles?

 Author: Date: 8/23/2017 10:31:41 PM
MIPAS data is shown with circles and filled with color.

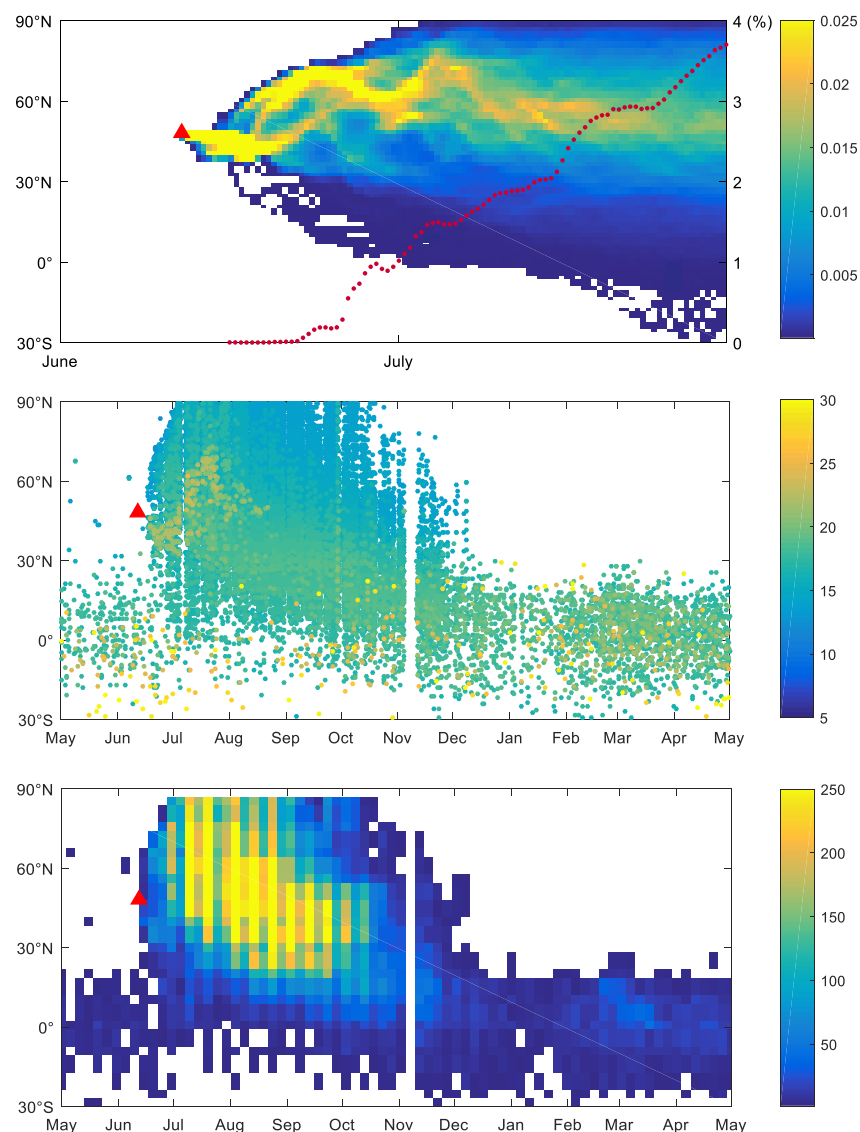


Figure 5: Top: **1** percentage (%) of air parcels **2** above 380 K from MPTRAC simulation binned every 12 hours and 2° in latitude. Red dots denote the percentage of air parcels between 30°N and 30°S. Middle: MIPAS aerosol altitudes (km) above 380K from May 2009 to April 2010. Bottom: number of MIPAS aerosol detections. Detections are binned every 5 days and 5° in latitude. The red triangle denotes the time and latitude of the first Sarychev eruption.

T Number: 1 Author: Date: 8/23/2017 10:31:41 PM

Is the shading really %? Does this mean that at every latitude, the value is << 1%?

S Author: Date: 8/23/2017 10:31:41 PM

Yes, in the top panel of Fig. 5, the shading values are the time-latitude distribution of air parcels above the height of 380K in percentage of total number of air parcels. The values are derived by counting the number of air parcels at altitude above the height of the 380 K isentropic surface in each bin and then dividing this number by the total number of air parcels during the simulation time period. The size of the bins is 12 hours \times 2° in latitude.

The model outputs are given every 6 hours (4 times per day), and the time period of simulation is from 12 June 2009 to 31 July 2009 (50 days). So the total number of the outputs is $4 \times 50 = 200$. The number of air parcels is assigned to 100,000. So the total number of air parcels during the simulation period is $200 \times 100,000$.

The shading values are very small because the denominator is large. We apologize for making it so confusing.

In the revised Fig. 5, we decide to change the way of calculation. The "total number of air parcels in each bin" replaces the originally used "total number of air parcels during the simulation time period" as the denominator. The total number of air parcels in each bin is $2 \times 100,000$. In this way, the shading values will not depend on the simulation time period or the bin size. Instead of showing the relative distribution of the air parcels, the revised figure could give the specific percentage at a given latitude and time.

T Number: 2 Author: Date: 8/23/2017 10:31:41 PM

Potential temperature above 380 K or altitude about theta = 380K?

S Author: Date: 8/23/2017 10:31:41 PM

It is the altitude where the potential temperature equals to 380 K. We have change it into "above the 380 K isentropic surface" to avoid the ambiguity.

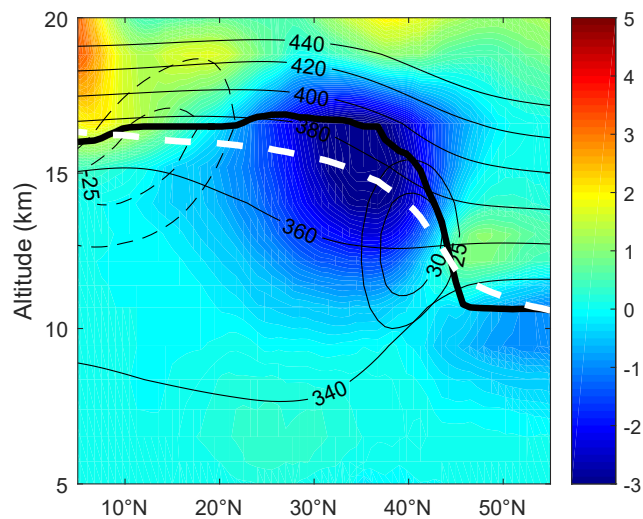







Figure 6: Zonal mean zonal wind anomaly (shaded) in the Asian monsoon anticyclone (40–120°E) with respect to the zonal mean, averaged over 2009 summer (June–August). Zonal wind (black, solid/dashed positive/negative) is averaged between 40 and 120°E. The first thermal tropopause zonally averaged over 0–360°E is shown as dashed white line, averaged over 40 to 120°E as thick black line.


 Number: 1 Author: Date: 8/23/2017 10:31:41 PM
What is the source of the data?

 Author: Date: 8/23/2017 10:31:41 PM
Data source added. Thank you.

 Number: 2 Author: Date: 8/23/2017 10:31:41 PM
units?

 Author: Date: 8/23/2017 10:31:41 PM
Fixed. Thank you.

 Number: 3 Author: Date: 8/23/2017 10:31:41 PM
what does this mean?

 Author: Date: 8/23/2017 10:31:41 PM
Fixed. Thank you.

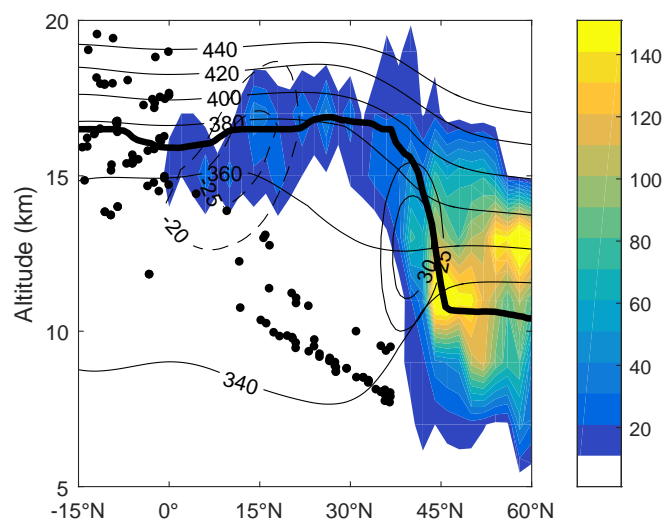




Figure 7: Number of MIPAS aerosol detections between 40°E and 120°E during June-August 2009 (binned every 2 km in altitude and 2° in latitude). Sparse detections (number of detections in each bin is smaller than 10) are shown with black dots. The tropopause, potential temperature, and zonal wind are **1**me as shown in Fig. 6.

 Number: 1 Author: Date: 8/23/2017 10:31:41 PM
the same

 Author: Date: 8/23/2017 10:31:41 PM
Fixed. Thank you.

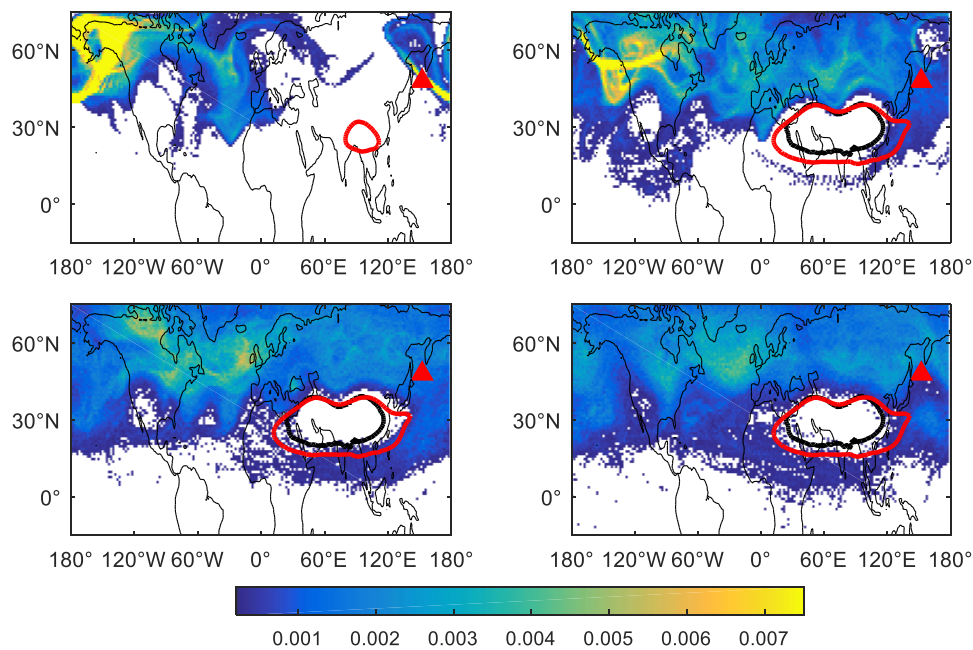


Figure 8: **1**percentage (%) of air parcels by 30 June (top left), 10 July (top right), 20 July (bottom left) and 31 July 2009 (bottom right) between 360 and 400 K from **2**PTRAC simulations. Results are binned every 2° in longitude and 1° in latitude. The **3**320 geopotential height (m) **4**150 hPa is marked in red and the PV-based barrier **5**370 K is marked in black. The red triangle denotes the location of the **6**Gurychev.

T Number: 1 Author: Date: 8/23/2017 10:31:41 PM
So all the values are << 0.01%?

S Author: Date: 8/23/2017 10:31:41 PM

In Fig. 8, the shading values are derived by counting the number of air parcels at altitude between the height of the 360 and 400 K isentropic surfaces in each bin and then dividing this number by the total number of air parcels during the simulation time period. The size of the bins is 2° in longitude × 1° in latitude.

Similar to the top panel of Fig. 5, the values are very small because the bin size is small but the denominator is large. The shading values in Fig. 10 and Fig. 12 are also generated with the same method. We find it is a useful way to show the plume evolution with time. Very similar pictures can be found in other studies, e.g., Fig. 3 in Garny and Randel (2016).

Reference: Garny, H., and Randel, W. J.: Transport pathways from the Asian monsoon anticyclone to the stratosphere, Atmos. Chem. Phys., 16, 2703-2718, 10.5194/acp-16-2703-2016, 2016.

T Number: 2 Author: Date: 8/23/2017 10:31:41 PM
How carried out? What was the initialization procedure?

S Author: Date: 8/23/2017 10:31:41 PM

Please refer to section 2.3 and section 3.

T Number: 3 Author: Date: 8/23/2017 10:31:41 PM
14,320 m geopotential height

S Author: Date: 8/23/2017 10:31:41 PM

Fixed. Thank you.

T Number: 4 Author: Date: 8/23/2017 10:31:41 PM
of

S Author: Date: 8/23/2017 10:31:41 PM

"on 150 hPa" is changed into "on the 150 hPa pressure surface"

T Number: 5 Author: Date: 8/23/2017 10:31:41 PM
at

S Author: Date: 8/23/2017 10:31:41 PM

"on 370 K" is changed into "on the 370 K isentropic surface".

T Number: 6 Author: Date: 8/23/2017 10:31:41 PM
Sarychev volcano.

S Author: Date: 8/23/2017 10:31:41 PM

Fixed. Thank you.

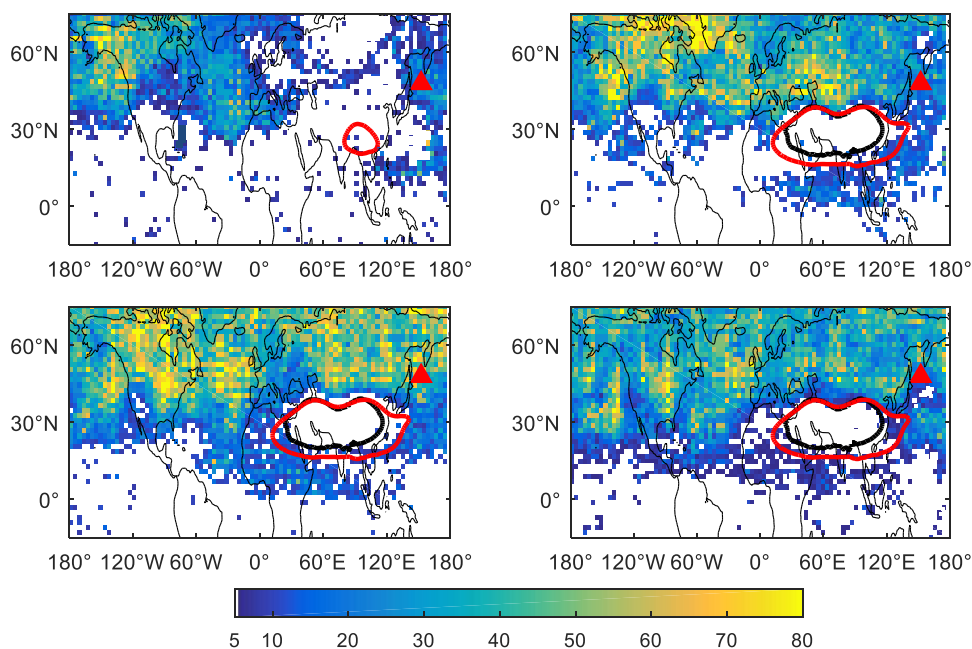







Figure 9: Number of MIPAS aerosol ¹ detections and aerosol data generated with 1.5-day forward and 1.5-day backward trajectory calculation, ² 30 June (top ³st), 10 July (top right), 20 July (bottom left) and 31 July (bottom right) between 360 and 400 K. Results are binned every 4° in longitude and 2° in latitude. The ⁴ 320 geopotential height ⁵ on 150 hPa is marked in red and the PV-based barrier on 370 K is marked in black. Red triangle denotes the location of Sarychev.


 Number: 1 Author: Date: 8/23/2017 10:31:41 PM
What does this mean? What are detections? What are data?


 Author: Date: 8/23/2017 10:31:41 PM
Fixed. Thank you.


 Number: 2 Author: Date: 8/23/2017 10:31:41 PM
on [what year?]


 Author: Date: 8/23/2017 10:31:41 PM
Fixed. Thank you.


 Number: 3 Author: Date: 8/23/2017 10:31:41 PM
left),

 Author: Date: 8/23/2017 10:31:41 PM
Fixed. Thank you.

 Number: 4 Author: Date: 8/23/2017 10:31:41 PM
14,320 m

 Author: Date: 8/23/2017 10:31:41 PM
Fixed. Thank you.

 Number: 5 Author: Date: 8/23/2017 10:31:41 PM
[delete]

 Author: Date: 8/23/2017 10:31:41 PM
Fixed. Thank you.

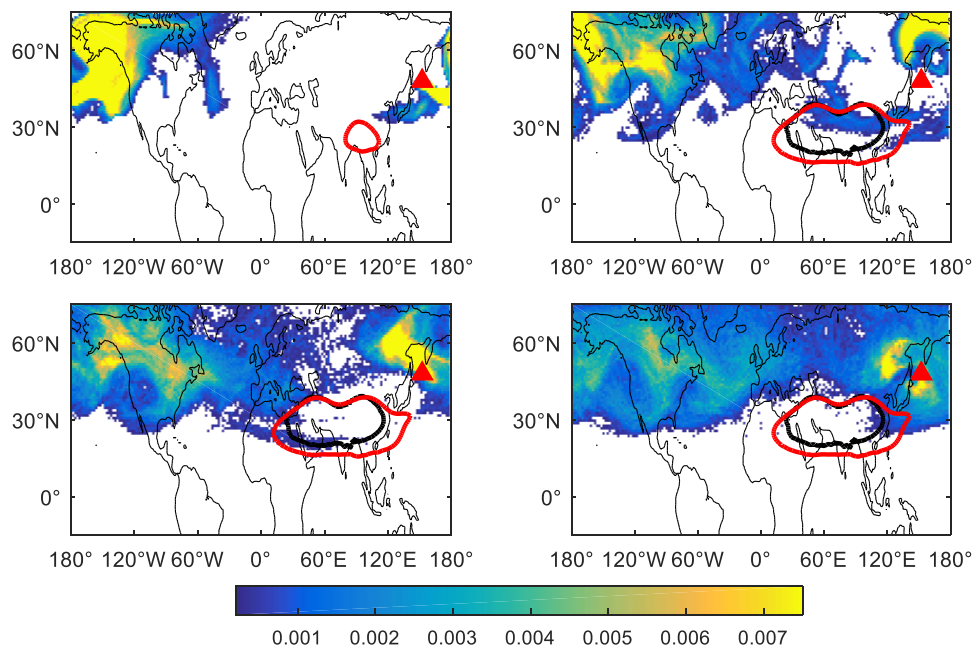


Figure 10: Same as Fig. 8 but for percentage (%) of total air parcels above 400 K.

This page contains no comments

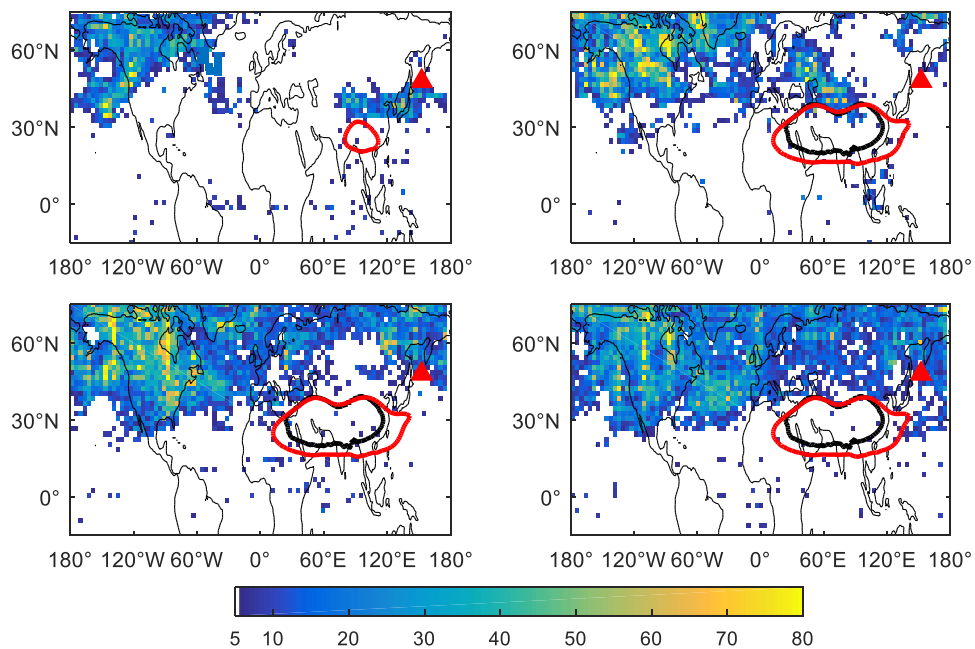


Figure 11: Same as Fig. 9, but for number of detections above 400 K.

This page contains no comments

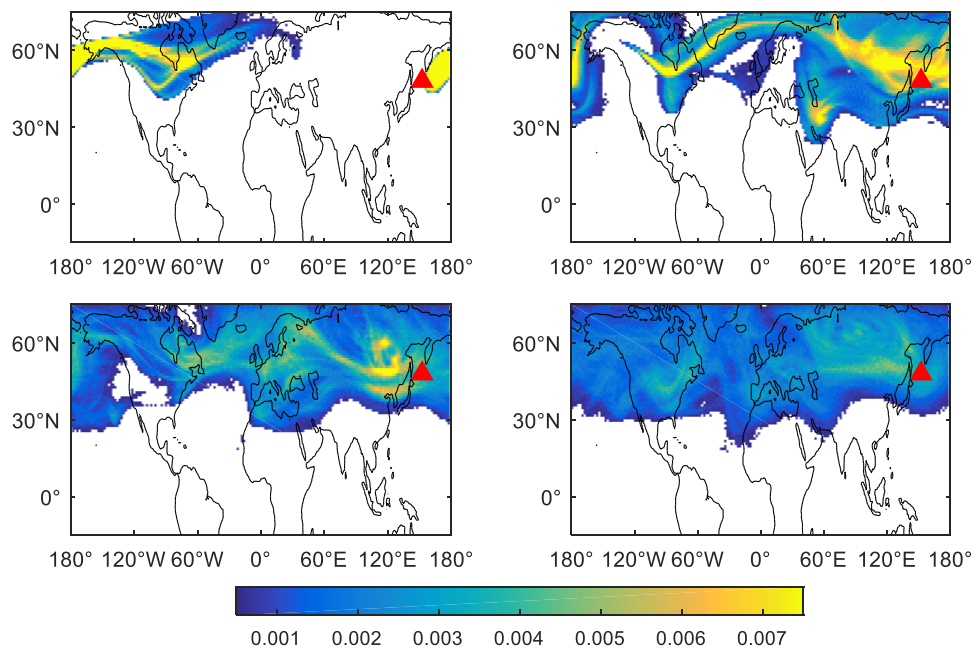




Figure 12: Percentage (%) of air parcels for the wintertime sensitivity study, 10 January (top left), 20 January (top right), 31 January (bottom left) and 10 February 2009 (bottom right) from an MPTRAC simulation for a hypothetical eruption of the Sarychev between 360 and 400 K. Results are binned every 2° in longitude and 1° in latitude. Red triangle denotes the location of Sarychev.

 Number: 1 Author: Date: 8/23/2017 10:31:41 PM
???

 Author: Date: 8/23/2017 10:31:41 PM
Fixed. Thank you.

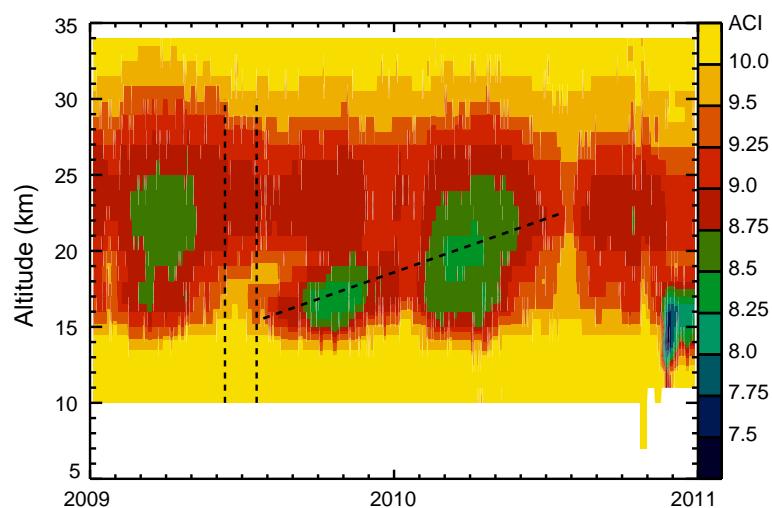


Figure 13: 9-day running median of **1** aerosol-cloud-index (ACI) between **2** 20°N and 10°S from 2009 to 2010. **3** ascent speed of the water vapour tape recorder (solid line) is derived from Glanville et al., 2016 using MLS observations. Black dashed lines indicate the **4** eruption date and 20 July when the simulations show first substantial transport to 10°N–10°S.

T Number: 1 Author: Date: 8/23/2017 10:31:41 PM
what are the units?

S Author: Date: 8/23/2017 10:31:41 PM
Explanation added in the manuscript. Please refer to section 2.2

T Number: 2 Author: Date: 8/23/2017 10:31:41 PM
for all longitudes?

S Author: Date: 8/23/2017 10:31:41 PM
Fixed. Thank you.

T Number: 3 Author: Date: 8/23/2017 10:31:41 PM
What is the speed? What are the units? Why is the black line where it is?

S Author: Date: 8/23/2017 10:31:41 PM
Water vapor above the tropical tropopause layer is considered as a passive tracer. Concentrations of water vapor in the tropical tropopause layer or the tropical lower stratosphere are influenced by the annual cycle in tropical tropopause temperature and this signal is moved upward by the upward branch of the Brewer-Dobson circulation (BDC), creating the so-called tape recorder. So the speed of the water vapor tape recorder is used to investigate the speed of BDC upwelling in the tropics. The tape recorder signal emerges from time-height plots of zonally mean water vapor in the tropical lower stratosphere. The unit for the speed of the water vapor tape recorder is (vertical distance)/time. The commonly used vertical coordinates are pressure levels (hPa) or altitude (km). In Glanville et al. (2017), the tape recorder is derived first by obtaining correlation coefficients between daily data at consecutive altitude levels. The data at the higher altitude levels are then shifted in 1-day increments up to 14 months to find the largest correlation coefficient. A strong correlation between the data at the lower level and the shifted data at the higher level is assumed to follow the tape recorder. More details in the calculation of the tape recorder are described in e.g., Minschwaner et al. (2016). Usually, the base of the BDC upwelling in the tropics, or upward branch of the BDC is located around 70 hPa, so in Fig. 13, we show the slope from the altitude around 70 hPa. And we adjust the horizontal location of the black solid line to the time when our simulations show first substantial aerosol transport to 10°N–10°S. A brief explanation has been added in Section 4.3.
Reference: Minschwaner, K., Su, H., and Jiang, J. H.: The upward branch of the Brewer-Dobson circulation quantified by tropical stratospheric water vapor and carbon monoxide measurements from the Aura Microwave Limb Sounder, *J. Geophys. Res.*, 121, 2790–2804, doi: 10.1002/2015JD023961, 2016.

T Number: 4 Author: Date: 8/23/2017 10:31:41 PM
what is it?

S Author: Date: 8/23/2017 10:31:41 PM
Rephrased. Thank you.

Equatorward dispersion of a high-latitude volcanic plume and its relation to the Asian summer monsoon: a case study of the Sarychev eruption in 2009

Xue Wu^{1,2}, Sabine Griessbach¹, Lars Hoffmann¹

5 ¹Jülich Supercomputing Centre, Forschungszentrum Jülich, Jülich, Germany

²Key Laboratory of Middle Atmosphere and Global Environment Observation, Institute of Atmospheric Physics, Chinese Academy of Sciences, Beijing, China

Correspondence to: Xue Wu (xu.wu@fz-juelich.de)

Abstract.

10 Tropical volcanic eruptions have been widely studied for their significant contribution to ~~the~~ stratospheric aerosol loading and global climate impacts, but the impact of high-latitude volcanic eruptions on the stratospheric aerosol layer is not clear and the pathway of transporting aerosol from high-latitudes to the tropical stratosphere is not well understood. In this work, we focus on the high-latitude volcano Sarychev (48.1°N, 153.2°E), which erupted ~~in June 2009 during the Asian summer monsoon (ASM) season in 2009~~, and the influence of ~~the Asian summer monsoon (ASM)~~ on the equatorward dispersion of the volcanic plume. First, the sulfur dioxide (SO₂) emission ~~time series~~ and plume height of the Sarychev eruption are estimated with SO₂ observations of the Atmospheric Infrared Sounder (AIRS) and a backward trajectory approach, using the Lagrangian particle dispersion model Massive-Parallel Trajectory Calculations (~~MPTRAC~~). Then, the transport and dispersion of the plume are simulated using the derived SO₂ emission rate time series. The transport simulations are compared with SO₂ observations from AIRS and validated with aerosol observations from the Michelson Interferometer for Passive Atmospheric Sounding (MIPAS). The simulations show that about 4% of the sulfur emissions were transported to the tropical stratosphere within 50 days after the beginning of the eruption, and the plume dispersed towards the tropical tropopause layer (TTL) through isentropic transport above the subtropical jet. The MPTRAC simulations and MIPAS aerosol data both show that between the potential temperature levels of 360 and 400 K in the vertical range of 360–400 K, the equatorward transport was primarily driven by anticyclonic Rossby wave breaking enhanced by the ASM in boreal summer. The volcanic plume was entrained along the anticyclone flows and reached the TTL as it was transported south-westwards into the deep tropics downstream of the anticyclone. Further, the ASM anticyclone influenced the pathway of aerosols by isolating an ‘aerosol hole’ inside of the ASM, which was surrounded by aerosol-rich air outside.

25 between the potential temperature levels of 360 and 400 K in the vertical range of 360–400 K, the equatorward transport was primarily driven by anticyclonic Rossby wave breaking enhanced by the ASM in boreal summer. The volcanic plume was entrained along the anticyclone flows and reached the TTL as it was transported south-westwards into the deep tropics downstream of the anticyclone. Further, the ASM anticyclone influenced the pathway of aerosols by isolating an ‘aerosol hole’ inside of the ASM, which was surrounded by aerosol-rich air outside.

30 This transport barrier was best indicated using the potential vorticity gradient approach. Long-term MIPAS aerosol detections show that after entering the TTL, the aerosol from the Sarychev eruption remained in the tropical stratosphere for about 10 months and ascended slowly. The ascent speed agreed well with the ascent speed of ~~the water vapour~~ vapor tape recorder. Furthermore, a hypothetical MPTRAC simulation for a wintertime eruption was carried out. In contrast, by running a hypothetical simulation for a wintertime eruption, it is shown confirmed that under winter circulations, the equatorward transport of the plume would be suppressed by the strong subtropical jet and weak wave breaking events. In this hypothetical scenario, a high-latitude volcanic eruption would not be able to contribute to the tropical stratospheric aerosol layer.

1 Introduction

The impact of volcanic aerosol on climate has received wide attention over decades. Robock (2000, 2013) ~~gave~~ gave a comprehensive review on this subject. The major sources of the stratospheric aerosol are volcanic sulfur gases, mainly in form of [sulfur dioxide \(SO₂\)](#)SO₂, which are oxidized and converted into sulfate aerosol within hours to weeks (von Glasow et al., 2009). The sulfate aerosol is responsible for profound effects on the global climate (McCormick et al., 1995; Robock, 2000). Sulfate aerosol is a strong reflector of visible solar radiation and causes cooling of the troposphere ~~for years~~; while it is also an effective absorber of near infrared solar radiation. [Larger particles seen after an eruption can also absorb infrared radiation \(Stenchikov et al., 1998\)](#), so ~~they~~ they may induce heating of the stratosphere. In contrast, H₂O and CO₂ in the volcanic emissions do not have much measurable impact on the global climate since they are less abundant than [the](#) atmospheric H₂O and CO₂ reservoir (Gerlach, 1991; Gerlach, 2011). Volcanic ash usually only causes regional influence on climate for weeks, because of its large particle size, fast sedimentation, and consequently short life time in atmosphere (Niemeier et al., 2009).

The stratospheric aerosol layer enhanced by volcanism not only has a significant impact on the Earth's radiative budget (McCormick et al., 1995; Robock, 2000), it also has an impact on chemical processes in the lower stratosphere (Rodriguez et al., 1991; Solomon et al., 1993), in particular, on ozone depletion (Jäger and Wege, 1990; Tilmes et al., 2008; Solomon et al., 2016). Conventionally, large volcanic eruptions with a volcanic explosivity index (VEI) larger than 4, are thought to play a key role in the stratospheric sulfate aerosol budget. Recently, several studies focused on small and moderate-sized volcanic eruptions (VEI ≤ 4) (Kravitz et al., 2011; Solomon et al., 2011; Vernier et al., 2011; Ridley et al., 2014) and considered them as the primary source of the notable increase of stratospheric aerosol since 2000 that slowed down global warming (Solomon et al., 2011; Neely et al., 2013; Haywood et al., 2014). Models neglecting the effects of less intense volcanic eruptions tend to overestimate the tropospheric warming (Santer et al., 2014). The potential climate impact of volcanic emissions also largely depends on the time of year when the eruption takes place, the injection height and the surrounding meteorological conditions (Kravitz et al., 2011). The [atmospheric conditions in different seasons](#) influences sulfate formation and the zonal asymmetry of the polar vortex can affect the aerosol's transport. The eruption plume height is fundamental for aerosol microphysics in the atmosphere and the ~~large-large-scale~~ [circulation affects](#)~~circulations affect~~ the transport of the plume. So instead of only using the VEI, it is more sensible to study the atmospheric impacts by including volcanic eruptions based on the amount of stratospheric SO₂ injection together with eruption height (Brühl et al., 2015; Timmreck, 2012). Further information on volcanic SO₂ emissions and plume altitudes ~~is are~~ crucial in climate models when estimating trends of global temperature or ozone depletion.

The majority of studies on global climate impact of volcanic eruptions focuses on tropical eruptions. Extratropical volcanic eruptions are expected to have less impact on the global climate, because the downward flow of the Brewer–Dobson circulation ([BDC](#)) in the stratospheric extra-tropics prevents sulfate aerosol from rising up (Seviour et al., 2012), and sulfate aerosol in the extratropical stratosphere easily subsides back to the troposphere within months (Holton et al., 1995; Kremser et al., 2016). Although some studies show that extratropical volcanic eruptions can also have a significant impact on climate (Highwood and Stevenson, 2003; Oman et al., 2005; Oman et al., 2006; Kravitz and Robock, 2011; Pausata et al., 2015a; Pausata et al., 2015b),

the impact is usually found to be limited to the specific hemisphere in which the eruption occurred (Graf and Timmreck, 2001; Kravitz and Robock, 2011; Pausata et al., 2015b).

However, a high-latitude volcanic eruption may also contribute to the tropical stratospheric aerosol loading and even affect the other hemisphere (Schmidt et al., 2010). [In this paper, we focus on a moderate volcanic eruption, the Sarychev eruption in 2009 \(VEI = 4\),](#) which is considered as one of the high-latitude eruptions that affect tropical latitudes (von Savigny et al., 2015) and ~~are which is~~ responsible for the increase in tropical stratospheric aerosol optical depth ([Khaykin et al., 2017; Rieger et al., 2015](#)). In particular, we study the transport pathway of the Sarychev [SO₂ emission and](#) aerosol from the extra-tropical lower stratosphere to the [tropical tropopause layer \(TTL\)](#)~~TTL~~. [In this study, the term “SO₂ emission” refers to the SO₂ released or injected into the atmosphere during the explosive eruption of Sarychev. The “tropical stratosphere” refers to the region between 30°N and 30°S above the 380 K isentropic surface.](#) In order to ~~analyse~~[analyze](#) the transport of the Sarychev plume and [to assess](#) the role of the [Asian summer monsoon \(ASM\)](#) in the dispersion process, in Section 2 we first present the Lagrangian transport model and data used for simulations. In Section 3, we derive the altitude-resolved Sarychev ~~volcanic~~[SO₂ emission](#) time series using [Atmospheric Infrared Sounder \(AIRS\)](#)~~AIRS~~ SO₂ measurements and an inverse modelling approach. The equatorward dispersion of the Sarychev [SO₂ emissions](#) revealed by [Michelson Interferometer for Passive Atmospheric Sounding \(MIPAS\)](#)~~MIPAS~~ aerosol detections and trajectory simulations and the relation to [the ASM](#) are shown in Section 4. Results of this study are further discussed in Section 5 and summarized in Section 6.

2 Observations and model

2.1 AIRS

AIRS (Aumann et al., 2003) is an infrared sounder with across-track scanning capabilities aboard the National Aeronautics and Space Administration's (NASA's) Aqua satellite. Aqua was launched in May 2002 and operates in a nearly polar, Sun-synchronous orbit at an altitude of about 710 km with a period of 98 min. The AIRS footprint size is 13.5 km × 13.5 km for nadir and 41 km × 21.4 km for the outermost scan angles. The along-track distance between two adjacent scans is 18 km. AIRS provides nearly continuous measurement coverage during 14.5 orbits per day and covers the globe almost twice a day. The observations provide good horizontal resolution and make it ideal data for observing the fine filamentary structures of volcanic SO₂ plumes.

In this study, we use ~~an the~~ [SO₂ index \(SI, unit: K\) defined in Hoffmann et al. \(2014\) to estimate the SO₂ emission time series and evaluate the Lagrangian transport simulations. The SI is defined as the](#) brightness temperature differences ~~based on SO₂ spectral features~~ in the 7.3 μm waveband ~~(Hoffmann et al., 2014) to estimate emission rates and evaluate the Lagrangian transport simulations.~~

$$SI = BT(\nu_{1407.2 \text{ cm}^{-1}}) - BT(\nu_{1371.5 \text{ cm}^{-1}}), \quad (1)$$

where $BT(\nu)$ is the brightness temperature measured at wavenumber ν . The ~~SO₂ index~~ [SI](#) increases with increasing SO₂ column density and it is most sensitive to SO₂ at altitudes from 8 to 13 km. The ~~SI SO₂ index~~ of Hoffmann et al. (2014) [is more sensitive and](#) performs better on suppressing background [interfering](#) signals than the ~~SI SO₂ index~~ provided in the ~~AIRS~~[NASA](#) operational data products. It is therefore well suited to track low SO₂ concentrations over time. A detection threshold of 2 K [is suitable in this study to](#) identify [the Sarychev SO₂ emissions.](#) [More details on the SI can be found in Hoffmann et al. \(2014; 2016\) and Heng et al. \(2016\).](#)

115 AIRS was able to detect the SO₂ cloud from the beginning of the eruption of Sarychev on 12 June 2009 up to five weeks later. Observations during the first five days after the eruption have been used for estimating the [SO₂ emission time series rates](#). Observations at a later stage are used for comparison with the Lagrangian transport simulations.

2.2 MIPAS

120 MIPAS (Fischer et al., 2008) is an infrared limb emission spectrometer aboard European Space Agency's (ESA's) Envisat, which was in operation from July 2002 to April 2012, providing nearly 10 years of measurements. The vertical coverage of its nominal mode was 7–72 km from January 2005 to April 2012. MIPAS has a field of view of about 3 km×30 km (vertically and horizontally) at the tangent point and ~~dimension—the extent~~ of the measurement volume along the line of sight is about 300 km. The horizontal distance between two adjacent limb scans is about 500 km. In 2009, the general measurement pattern of MIPAS is to measure eight days in nominal mode followed by one day in middle atmosphere mode and one day in upper atmosphere mode. On each day, about 14 orbits with about 90 profiles per orbit are measured. From January 2005 to April 2012, the vertical sampling grid spacing between the tangent altitudes is 1.5 km in the [upper troposphere and lower stratosphere \(UTLS\)](#) and 3 km at altitudes above.

130 In this study, we use MIPAS altitude-resolved aerosol data [retrieved by Griessbach et al. \(2016\) to compare with model results and analyze the transport of volcanic plume. In the first step, the aerosol-cloud-index \(ACI\) is defined to identify cloud or aerosol contaminated spectra. The ACI is defined as the maximum value of both the cloud index \(CI\) and aerosol index \(AI\).](#)

$$ACI = \max(CI; AI), \quad (2)$$

135 [The CI is the standard method to detect clouds and aerosol with MIPAS \(Spang et al., 2001\), which is defined as the ratio between the mean radiances around the 792 cm⁻¹, covering a band with strong CO₂ emissions and the atmospheric window region around 833 cm⁻¹:](#)

$$CI = \frac{\bar{I}_1([788.25, 796.25 \text{ cm}^{-1}])}{\bar{I}_2([832.31, 834.37 \text{ cm}^{-1}])}, \quad (3)$$

where \bar{I}_1 and \bar{I}_2 are the mean radiance of each window.

140 [The AI is defined as the ratio between the mean radiances around the 792 cm⁻¹ CO₂ band and the atmospheric window region between 960 and 961 cm⁻¹:](#)

$$AI = \frac{\bar{I}_1([788.25, 796.25 \text{ cm}^{-1}])}{\bar{I}_3([960.00, 961.00 \text{ cm}^{-1}])}, \quad (4)$$

where \bar{I}_1 and \bar{I}_3 are the mean radiance of each window.

[An ACI threshold value of 7 will be applicable to MIPAS measurements for the detection of aerosol in the UTLS.](#)

145 In the second step, a brightness temperature correction method is used to separate aerosol from ice clouds. The resulting aerosol product may contain any type of aerosol, e.g. volcanic ash, sulfate aerosol, mineral dust as well as non-ice polar stratospheric clouds (PSCs). [MIPAS aerosol measurements for three strong volcanic eruptions in 2011 characterized by large SO₂ \(Grínsvörn, Nabro\) or volcanic ash emissions \(Puyehue–Cordón Caulle\) were compared with horizontal high-resolution AIRS SO₂ and ash index, which had verified the viability of this aerosol detection method to identify volcanic aerosol \(Griessbach et al., 2016\).](#)

150 | [There is a very regular aerosol detection gap every six months around January and July. This gap is caused by semi-annual changes in the AI, and subsequently in the ACI \(Griessbach et al., 2016\). At \$960 \text{ cm}^{-1}\$, an impact of \$\text{CO}_2\$ hot bands \(at around 50 km\) is the most likely explanation for the detection artefact. MIPAS detected Sarychev aerosol since 13 June 2009.](#)

2.3 MPTRAC

155 | The Massive-Parallel Trajectory Calculations (MPTRAC) model is [a](#) Lagrangian particle dispersion model, which is particularly suited to study volcanic eruption events (Heng et al., 2015; Hoffmann et al., 2016). In the MPTRAC model, trajectories for individual air parcels are calculated based on numerical integration of the kinematic equation of motion and simulations are driven by wind fields from global meteorological reanalyses.

160 | [In this study, the MPTRAC model is driven with the ERA-Interim data \(Dee et al., 2011\) interpolated on a \$1^\circ \times 1^\circ\$ horizontal grid on 60 model levels with the vertical range extending from the surface to 0.1 hPa. The ERA-Interim data are provided at 00, 06, 12, and 18 UTC. Outputs of the model simulations are given at the same time interval.](#)

Turbulent diffusion is modelled by uncorrelated Gaussian random displacements of the air parcels with zero mean and standard deviations $\sigma_x = \sqrt{D_x \Delta t}$ (horizontally) and $\sigma_z = \sqrt{D_z \Delta t}$ (vertically). D_x and D_z are the horizontal and vertical diffusivities respectively, and Δt is the time step for the trajectory calculations. For the Sarychev simulation, D_x and D_z is assigned to be [50 \$\text{m}^2 \text{ s}^{-1}\$ and 0 \$\text{m}^2 \text{ s}^{-1}\$ in the troposphere and 0 \$\text{m}^2 \text{ s}^{-1}\$ and 0.1 \$\text{m}^2 \text{ s}^{-1}\$ in the stratosphere.](#) Furthermore, the sub-grid scale wind fluctuations are simulated by a Markov model (Stohl et al., 2005; Hoffmann et al., 2016). Loss processes of chemical species, SO_2 in our simulations, are simulated based on an exponential decay of the [SO₂](#) mass assigned to each air parcel, with a constant half

170 | lifetime of seven days.

3 Simulations and observations of the Sarychev plume

3.1 Reconstruction of the Sarychev SO_2 emission time series

The Sarychev peak with summit at 1496 m, is located at 48.1°N , 153.2°E , and it is one of the most active volcanoes of the Kuril Islands. It erupted most recently in June 2009 (VEI = 4). On 11 June 2009, two weak ash eruptions were first detected (Levin et al., 2010) and during the main explosive phase from 12 to 16 June 2009, ash, water ~~vapour~~[vapor](#), and an estimated $1.2 \pm 0.2 \text{ Tg}$ of SO_2 were injected into the UTLS, making it one of the 10 largest stratospheric injections in the last 50 years (Haywood et al., 2010). Sulfate aerosol was detected several days after the eruption and the enhancement of the optical depth caused by the Sarychev eruption lasted for months, returning to pre-Sarychev eruption values in the beginning of 2010 (Doeringer et al., 2012; Jégou et al., 2013). As shown in Fig. 1 (top), Sarychev is located at the northern edge of the subtropical jet and to the northeast of the ASM (marked by the black rectangle). In the vertical section (Fig. 1, bottom), the dynamical tropopause, defined by a potential vorticity (PV) value of 2 PV units ($\text{PVU} = 10^{-6} \text{ Km}^2 \text{ s}^{-1} \text{ kg}^{-1}$), is around 11 km at the location of the Sarychev.

To reconstruct the altitude-resolved SO_2 emission time series, we follow the approach of Hoffmann et al. (2016) and use backward trajectories and AIRS SO_2 measurements. Since AIRS measurements do not provide altitude information, we establish a column of air parcels at each location of an AIRS SO_2 detection. The vertical range

185 |

of the column is 0–25 km, covering the possible vertical dispersion range of the SO₂ plume in the first few days. The AIRS footprint size varies between 14 and 41 km, so in the horizontal direction we choose an average of 30 km as the full width at half maximum (FWHM) for the Gaussian scatter of the air parcels. In our simulation, a fixed number of 100,000 air parcels is assigned to all air columns and the number of air parcels in each column is linearly proportional to the SO₂ index. Then backward trajectories were calculated for all air parcels, and trajectories that are at least 2 days but no more than 5 days long and that have passed the volcano domain are recorded as emissions of Sarychev. The volcano domain is defined to be within a radius of 75 km to the location of Sarychev and 0–20 km in the vertical direction, covering all possible injection heights. Sensitivity experiments have been conducted to optimize these pre-assigned parameters to obtain best simulation results. Haywood et al. (2010) estimated that 1.2 Tg of SO₂ were injected into the UTLS on 15 and 16 June 2009 with a 15 % error estimate (± 0.2 Tg). Considering that there were minor emissions before 15 June (Levin et al., 2010; Jégou et al., 2013; Carboni et al., 2016), we allocated a mass of 1.4 Tg to the derived SO₂ emissions. The reconstructed SO₂ emission time series is shown in Fig. 2.

In Fig. 2, black dots denote the thermal tropopause derived from ERA–interim data at the Sarychev. Sarychev released SO₂ almost without interruption in the first five days, but with large variations in height and magnitude. Smaller eruptions began on 12 June followed by continuous eruptions on 13 June, ranging from 7 km to about 17 km. Significant SO₂ injections occurred on 14–15 June between 10 and 18 km, followed by minor emissions until 16 June. The majority of SO₂ (58%, ~ 0.81 Tg) was injected directly into the extratropical lower stratosphere, and the largest SO₂ injection occurred between 12 and 17 km. ~~This~~These time line of the eruptions is consistent with the observation of the Japanese Meteorological Agency Multifunctional Transport Satellite (MTSAT) (Levin et al., 2010; Rybin et al., 2011) and the Optical Spectrograph and Infrared Imaging System (OSIRIS) measurements, showing that the peak backscatter of aerosols ~~was measured were~~ between 12 and 16 km (Kravitz et al., 2011).

The derived SO₂ emission ~~rate~~–time series are the basis of the simulations of SO₂ plume in the following sections.

3.2 Simulation and validation of the Sarychev plume dispersion

A new set of 100,000 air parcels is assigned to the derived SO₂ emission shown in Fig. 2, with 14,000 kg of SO₂ in each of the air parcels. The trajectories initialized with this SO₂ emission are calculated with the MPTRAC model from 12 June 2009 (first eruption) to 31 July 2009. The simulated evolution of the SO₂ plume is shown in Fig. 3 (left column) and compared with the AIRS SO₂ measurements (right column). ~~Note that only~~Only SO₂ column density values larger than 2 Dobson units (DU) are shown. The evolution of simulated plume altitudes is shown in Fig. 4 together with tangent altitudes of the MIPAS aerosol detections. The simulation outputs are given every six hours, but only results at selected time and dates are shown. Figure 3 and Fig. 4 show that, as the SO₂ was injected into different altitudes, the SO₂ plume ~~splits~~splitted roughly into two branches after the eruption, moving eastwards and westwards, and at the same time, most of the emissions ~~moved~~moving poleward. From 22 June, the SO₂ plume over Eastern Siberia stretched towards three directions: northeast, south, and south east. The SO₂ in the elongated filament over the Eastern Siberia and North-east China with altitudes below 9 km was diluted and partly depleted and converted into aerosol afterwards and the other two filaments moved toward east. The SO₂ plume over the Northwest American continent stretched towards east and west, forming a long filament

running through Northern Canada. The SO₂ concentration declined exponentially and only a fraction of SO₂ remained near the Bering Strait and Northern Canada till 28 June.

In Fig. 3, in order to validate the simulation of plume dispersion, and also to indirectly validate the reconstructed emission [time series rates](#), we compare the simulations of plume dispersion with AIRS SO₂ measurements. The SO₂ index from AIRS detections was converted into SO₂ column density using the correlation function described in Hoffmann et al. (2014), which was built using radiative transfer calculations. AIRS was able to detect the SO₂ cloud from the beginning of the eruption of Sarychev up to five weeks later (not fully shown in the figure). The SO₂ column density derived from AIRS agrees well with the SO₂ column density derived from the Infrared Atmospheric Sounding Interferometer (IASI) in magnitude, e.g. see Fig. 3 in the study of Haywood et al. (2010) and Fig. 2 in the study of Jégou et al. (2013). Generally, the simulations agree well with the AIRS measurements in position and diffusion and the simulations can provide more information on the SO₂ distribution than the AIRS measurements alone. The differences between the SO₂ clouds, e.g. on 24 June (over the western Pacific) are partly attributed to a mismatch in time of the AIRS SO₂ measurements and the simulation output. In magnitude, the SO₂ column density from AIRS is slightly larger than that from MPTRAC simulations, and the SO₂ maxima are found in different [locations location](#). This is also found by Hoffmann et al. (2016) for other eruption events and this was attributed to the fact that the inverse modelling approach is optimized to reproduce the spatial extent of the plume but not the absolute emission. Except for [the](#) discrepancy between the times of the compared data, this remaining difference may also be attributed to the initial setting of the total SO₂ mass, the SO₂ life time and the uncertainties of the [ECMWF ERA](#)-interim winds.

In Fig. 4, the altitudes of the simulated [volcanic SO₂](#) plume are compared with the tangent altitudes of MIPAS aerosol detections to verify the vertical distribution of the [air parcels from the model SO₂ plume](#). [In the beginning of the simulation, the volcanic plume was composed of SO₂ but the SO₂ was converted to sulfate aerosol during the transport process. Here we assume that the SO₂ remains collocated with the sulfate aerosol and the sedimentation of the small sulfate aerosol particles is negligible for the time scale considered.](#) Aerosol produced [from the SO₂ emissions](#) as detected by MIPAS within a few days after the initial eruption. In general, the altitudes of the SO₂ [air parcels from the MPTAC model](#) are comparable to the MIPAS aerosol altitudes. The majority of the air parcels were between 10 and 20 km and moved eastwards. A thin filament over the north Pacific ascended to up to 20 km and moved westward to East Asia by the end of June 2009, which was well verified by the MIPAS detections. Some inconsistencies [appeared](#), e.g., along the west coast of North [America American](#) on 23 June and over the northeast Pacific on 24 and 25 June. We attributed [them](#) to the fact that the SO₂ at lower altitudes (below 14 km) had been converted into aerosol more quickly than the SO₂ at higher altitudes (above 16 km). The various vertical distributions of the air parcels were also verified by some overlapping MIPAS detections, e.g., over northwest America. Overall, this comparison demonstrates that the MPTRAC simulation provides a quite accurate representation of the observed horizontal and vertical distribution of the Sarychev SO₂ [and aerosol](#) plume.

4 Equatorward dispersion of the Sarychev plume and the role of the ASM

4.1 Equatorward dispersion of Sarychev plume

Although the majority of the Sarychev plume was transported towards the north pole, ~~it's-it is~~ found in our simulations that there was clear equatorward dispersion from ~~the~~ extratropical stratosphere to the tropical lower stratosphere, as seen in Fig. 5 (top). The top panel of Fig. 5 shows the time and latitude distribution of the air parcels above the height of the 380 K isentropic surface in percentage of the total number of air parcels in each bin. The bin size used here is 12 hours \times 2° in latitude. The plume reached the tropical stratosphere about one week after the eruption, and crossed the Equator by the end of June 2009. The red dots in the top panel of Fig. 5 denote the air parcels between 30°N and 30°S above the 380 K isentropic surface in proportion of the total air parcels released in the forward trajectory simulation. ~~Until~~ the end of July 2009, there were nearly 4% of the air parcels that had entered the tropical stratosphere. This trend is further verified by the MIPAS aerosol detections ~~as shown in the middle and bottom panels of Fig. 5.~~ (middle and bottom panels in Fig. 5). As shown by the MIPAS aerosol detections, The middle panel of Fig. 5 demonstrates the aerosol above the 380 K isentropic surface. The altitudes of aerosol above the 400 K isentropic surface are denoted with diamond markers and a different color scheme. The bottom panel of Fig. 5 shows that shortly after the eruption of Sarychev, large quantities of stratospheric aerosol formed from directly injected SO₂. On 31 July 2009, the end of the MPTRAC trajectory simulation, the MIPAS aerosol detections between 30°N and 30°S above the 380 K isentropic surface were increased by about six times compared with the number before the Sarychev eruption. And the increase of tropical stratospheric aerosol continued until the beginning of September 2009. Aerosol detections between 30°N and 30°S above the 400 K isentropic surface also increased but the peak appeared around end of September 2009, later than the peak of the aerosol above the 380 K isentropic surface. The aerosol in the extratropical stratosphere was removed by the end of 2009, while the aerosol that had entered the tropical stratosphere stayed for months. Aerosol optical depths from OSIRIS and scattering ratio from CALIPSO lidar measurements have also shown similar equatorward dispersion of the aerosol after the eruption of Sarychev (Haywood et al., 2010; Solomon et al., 2011).

4.2 The role of the ASM anticyclone

As shown by the evolution of Sarychev plume in section 3.2, active Rossby wave breaking events at mid-latitudes during boreal summer have significantly influenced the plume dispersion. In boreal summer, the ASM is among the most prominent circulation patterns. Figure 6 shows a cross section of the ASM in boreal summer 2009. Generally, the ASM anticyclone ranged from 360–400 K, marked by the negative PV anomaly of -3 PVU and it was bounded by the subtropical and equatorial jets. The thermal tropopause averaged over 40–120°E was elevated up to about 390 K. The ASM anticyclonic circulation facilitates meridional transport when the subtropical jet weakens and retreats northward (Haynes and Shuckburgh, 2000). Figure 7 depicts the MIPAS aerosol measurements between 40–120°E during June–August 2009. The aerosol detections between 360 and 400 K to the south of 40°N were collocated with the core of the ASM, extending from the mid-latitude UTLS to the TTL. The aerosol that made ~~their-its~~ way above the subtropical jet core to lower latitudes along the isentropic surfaces cannot be explained by convection but only by large-scale transport associated with the ASM. Using our trajectory simulations, it is straightforward to see the role of ASM anticyclonic circulation in influencing the pathway of the plume. The distributions of air parcels in the vertical range of 360–400 K (in

300 percentage of total number of air parcels released after the eruption) ~~by-on~~ 30 June, 10 July, 20 July and 31 July
2009 are shown in Fig. 8. The red contour is the geopotential height of 14,320 m on ~~the~~ 150 hPa pressure
surface, denoting a commonly used boundary of the ASM anticyclone (Randel and Park, 2006). At latitudes
between 15–40°N in summer, the 150 hPa pressure surface is around 370 K. The black contour is the PV-based
ASM transport barrier for July 2009 (1.8 PVU) on 370 K isentropic surface as defined by Ploeger et al. (2015).
305 In the first 19 days (top left panel in Fig. 8), from first eruption on 12 June to 30 June 2009, the plume mostly
moved eastward and remained at mid- and high latitudes. After another 10 days (top right panel in Fig. 8), air
parcels were entrained into the anticyclonic circulations of the American monsoon and a fraction was shed
towards the tropics. The remaining air parcels that entered the ASM circulation were entrained along the flow
surrounding the ASM anticyclone and moved south-westward approaching the tropics. In the following 20 days
310 (bottom panels in Fig. 8), some air parcels were dragged along the flow south of the ASM, and some were shed
out from the south-eastern flank of the anticyclone and spread over the tropics. The American monsoon plays a
similar role as the ASM in transporting air parcels to lower latitudes, but it is much weaker in strength. The
'aerosol hole' between 360 and 400 K illustrated the ASM's role as a transport barrier between the air inside and
outside of the anticyclone. In our case, it is better demarcated by the PV-based barrier than the geopotential
315 height criterion. The northern barrier of the subtropical jet was strong, while the southern barrier was more
permeable for meridional transport.

This meridional transport under the influence of the ASM revealed by the simulations shown in Fig. 8 is verified
by the MIPAS aerosol detections shown in Fig. 9. Because of the sparse horizontal coverage of MIPAS
detections, 1.5-day forward and 1.5-day backward trajectories initialized by MIPAS aerosol detections were
320 calculated to fill gaps in space and time. [The trajectories are initialized with MIPAS aerosol detections from 12
June 2009 to 31 July 2009. These detections are traced both forward and backward for 1.5 days with the
MPTRAC model and the model output is provided every six hours. So this calculation produces 12 times as
many aerosol data points as the original MIPAS detections.](#) Compared with MIPAS detections in Fig. 9, the
simulations in Fig. 8 could successfully reproduce the maxima, minima and filaments of the aerosol
325 distributions. It is also verified by MIPAS detections that the transport barrier of ASM is better demarcated by
the PV-based barrier.

The transport pathway to low latitudes for aerosols above 400 K is shown by simulations in Fig. 10 and MIPAS
aerosol detections in Fig. 11. At altitudes above the ASM, trajectories are driven by easterlies and meridional,
isentropic winds. ~~Fit~~ [Until the](#) end of July 2009, air parcels above [the](#) 400 K [isentropic surface](#) were transported
330 to lower latitudes (as far as about 15°N), but could not reach the Equator. This suggests that ASM play the most
significant role between 360 and 400 K, which may vary in spatial extent associated with the strength of the
ASM.

However, a sensitivity test simulation of the same eruption in winter (January 2009) shows that, in northern
hemisphere winter, meridional transport from extra-tropic to the tropics is typically suppressed by the strong
335 winter subtropical jets. Forward trajectories initialized by the Sarychev SO₂ emissions (as shown in Fig. 2), but
driven by winter wind fields in January and February 2009 are shown in Fig. 12. Compared with the summer
scenario in Fig. 8, wind speeds in winter 2009 between 360 and 400 K were faster, and the trajectories could
span the northern hemisphere within 20 days. About 40 days after eruption, air parcels were almost evenly
distributed at mid- and high latitudes, but no air parcels did approach the Equator.

340 4.3 Upward transport of Sarychev aerosol

Simulation results from Figs. 8 to 11 have shown that the ASM anticyclone enhanced the equatorward dispersion of the Sarychev aerosol in the vertical range of 360–400 K, but the ASM did not facilitate the equatorward dispersion above 400K. The increased aerosol in the tropical stratosphere above 400 K (~ 18 km) [as seen in the middle and bottom panels of Fig. 5](#) could only be explained by the upward transport above the
345 TTL. Above [the](#) zero diabatic heating surface (generally around [the](#) 360 K [isentropic surface](#)), air masses that enter the TTL are considered to be lifted effectively by [the](#) radiative heating (Gettelman et al., 2004; Fueglistaler et al., 2009).

In Fig. 13, the upward transport of aerosol in the tropics is clearly demonstrated by the MIPAS aerosol detections at high altitudes between 10°N and 10°S. At 15 km, an enhanced aerosol signal was found from July
350 2009 and lasted for about 10 months. It returned to pre-Sarychev level at the end of May 2010. At 20 km, enhanced aerosol signal was detected in October 2009, and in another four months, the enhanced aerosol signal was found at 25 km. ~~The overlaid ascent speed of water vapour tape recorder is derived with Aura Microwave Limb Sounder (MLS) measurements from Glanville et al. (2017). The overlaid speed of the tropical (10°N–10°S) tape recorder signal, namely the slope of water vapor isolines in a time–height plot, is about 10 hPa per month. It is a measure of the effective upward speed of the BDC and it is shown from the altitude of the base of the upward BDC in the tropics (~70 hPa). The aerosol transported to the TTL is moved upward by the BDC.~~ The ascent speed of the Sarychev aerosol agrees well with the ascent speed of the water ~~vapour~~vapor tape recorder before and after the data gap at the end of 2009 and beginning of 2010.

5 Discussion

360 The results of our study in [the](#) above sections suggest that the ASM anticyclone plays a key role in transporting the Sarychev aerosol from [the](#) extra-tropical lower stratosphere into the TTL. In various studies, this quasi-isentropic transport from extra-tropics to the TTL is referred as in-mixing process (e.g., Konopka et al., 2009). Horizontal in-mixing of tracer species has been observed (e.g. Folkins et al., 1999) or modelled (e.g. Konopka et al., 2010), and has been used to explain the seasonal and annual cycle of tracer species (Abalos et al., 2013; Ploeger et al., 2013). The role of in-mixing is prominent when there are large gradients in these tracers between
365 the tropics and the extra-tropics. The study of Abalos et al. (2013) shows that the main contribution to in-mixing originates in the northern hemisphere and is related to the Asian monsoon, and this in-mixing process takes place in the TTL close to the tropopause. These extra-tropics to tropics transport events are also considered to be driven by anticyclonic Rossby wave breaking (Homeyer and Bowman, 2013). The net equatorward transport peaks downstream of large anticyclones in the potential temperature range between 370 and 390 K (Homeyer and Bowman, 2013). Above the TTL, in-mixing rapidly decreases with height and becomes very weak at altitudes of the tropical pipe (Ploeger et al., 2013). These findings agree well with our study, which shows that the ASM anticyclonic circulation enhanced the equatorward transport between 360 and 400 K, but not above 400 K.

375 The pathway of the Sarychev plume approaching the deep tropics is modulated by the transport barrier at the boundary of the ASM anticyclone as well. The ‘aerosol hole’ shown in Figs. 8 and 9 that ranges from 360 to 400 K and collocates with the core of ASM [anticyclone](#), only appears during the ASM season. Conventionally, the

geopotential height of 14,320 m on the 150 hPa pressure level is used to define the boundary of the ASM anticyclone, but from the perspective of transport, the PV-based barrier defined by Ploeger et al. (2015) can better represent the boundary.

Our results show that the meteorological background conditions ~~during a volcanic eruptions~~during a volcanic eruption have a significant impact on the transport of the volcanic aerosol. For instance, the Puyehue-Cordón Caulle emissions reached the lower stratosphere and were rapidly transported eastward by the jet stream (Klüser et al, 2013; Hoffmann et al., 2016), while the Nabro emissions were captured by the ASM circulation in UTLS region (Fairlie et al., 2014; Heng et al., 2016). In this study, the transport of the equatorward dispersion of Sarychev aerosol is driven by the ASM anticyclone. Aerosol entering the TTL via the ASM anticyclone further entered the ascending branch of the ~~Brewer–Dobson circulation~~BDC. This enabled the Sarychev aerosol to remain in the stratosphere for months and further spread over both hemispheres. In this way, the Sarychev eruption may not only influence the northern hemisphere, but could also have potential impact on the global chemical composition and radiative budget similar to a tropical volcanic eruption.

Based on our model simulation, 4% of the air parcels that we released as the SO₂ injected into the atmosphere by the Sarychev eruption has been transported in between 30°N and 30°S above the 380K isentropic surface. This result could be affected by many possible mechanisms of ~~the~~ aerosol loss, like the interaction of sulfate aerosol and clouds, and coagulation in the volcanic plume or with other particles. Larger particle size may result in quicker sedimentation rates, especially at higher altitudes where the mean free path between air molecules far exceeds the particle size and particles fall more rapidly than they would otherwise. The scavenging efficiency of SO₂ could be increased if it is incorporated into growing ice particles (Textor et al., 2003). Also, SO₂ is slightly soluble in liquid water and it may have a small chance to be washed out during the transport process. But as revealed in our study, the efficient pathway of the transport is approximately between the 360 and 400 K isentropic surfaces, where the atmosphere is relatively dryer, cooler and cleaner than the lower troposphere. So our model result can be considered as a representative value. Although only a fraction of the SO₂ (~4% out of 1.2±0.2 Tg) was transported to the tropical stratosphere by the end of July 2009, if the SO₂ is entirely converted into gaseous H₂SO₄ and condensed into a 75%-25% H₂SO₄-H₂O solution, the total aerosol mass loading added to the tropical stratosphere by Sarychev eruption would be about 0.06±0.01 Tg ~~0.07 Tg~~ of sulfate aerosol, which is several times larger than the 0.015–0.02 Tg per year required to explain the background aerosol increase of 4–7 % per year after 2002 as found by Hofmann et al. (2009) at the Mauna Loa Observatory in Hawaii (19.5°N). (Hofman et al., 2009). Moreover, comparing with the time period from 12 June 2009 to 31 July 2009, larger amounts of ~~more~~ aerosols were transported to or ascended to the tropical stratosphere after July 2009. Although the relative change of the aerosol concentration, the SO₂ and sulfate aerosol transported to the tropics and further to the southern hemisphere will not only perturb the radiative balance but also have a substantial effect on microphysical processes, such as coagulation and growth of cloud condensation nuclei (Manktelow et al., 2009; Schmidt et al., 2010).

Since the potential climate impact of high-latitude volcanic emissions largely depends on their plume height and the meteorological background conditions, it is essential to conduct Lagrangian transport simulations ~~initialize the simulations~~ with realistic time- and altitude-resolved SO₂ emission time series ~~rate~~. The backward trajectory approach used in this study to reconstruct the emission time series proves to be an efficient way to produce realistic SO₂ emission ~~rate~~ time series.

6 Summary

In this study, we ~~analyse~~analyze the equatorward transport pathway of volcanic aerosol from the high-latitude volcanic eruption of the Sarychev in 2009. The analysis was based on MIPAS aerosol detections, AIRS SO₂ measurements and trajectory simulations.

First, the time- and altitude-resolved SO₂ emissions ~~s-rate~~ ~~were~~was derived using backward trajectories initialized with AIRS SO₂ measurements. Second, the dispersion of Sarychev plume from the beginning of the eruption (12 June 2009) to 31 July 2009 was simulated based on the derived SO₂ emission time series-rate. The horizontal distribution of the plume and its altitudes were validated with AIRS SO₂ measurements and MIPAS aerosol measurements respectively. The comparisons showed that there was good agreement between the simulations and observations.

The results presented in this study suggest that in boreal summer, the transport and dispersion of volcanic emissions were greatly influenced by the dominating ASM circulation, which facilitates the meridional transport of aerosols from the extra-tropical UTLS to the TTL by entraining air along the anticyclonic flows and shedding the air to the deep tropics downstream of the anticyclonic circulation. Meanwhile, the ASM anticyclone effectively isolates the air inside of the ASM from aerosol-rich air outside the anticyclone. The transport barrier at the boundary of the ASM is better denoted by the barrier defined by the PV gradient approach. However, the ASM only influenced the plume dispersion significantly in the vertical range of 360–400 K. The ASM anticyclone did not have notable impact on the equatorward dispersion above 400 K, where the Sarychev aerosol was confined in the northern hemisphere.

The simulations show that until the end of July 2009, ~~0.06±0.01 Tg of sulfate aerosol~~~~4% of the emission~~ had entered the tropical stratosphere. After July 2009, the amount of aerosol in the tropical stratosphere kept increasing until the beginning of September 2009.~~Increased number of aerosol was detected by MIPAS in the tropical stratosphere afterwards.~~ After entering the TTL, the aerosol experienced large-scale ascent in the ~~Brewer–Dobson circulation~~BDC. The ascent speed agrees well with the ascent speed of the water ~~vapour~~vapor tape recorder. Aerosol signal in the tropics was enhanced within one month of the eruption, and returned to pre-Sarychev level after about 10 months.

The Sarychev eruption had the chance to contribute to the stratospheric aerosol loading in the tropics because it occurred in boreal summer when the equatorward transport was enhanced by the ASM anticyclone. If the eruption happened in winter, the volcanic aerosol would be confined to the latitudes of strong subtropical jets.

7 Code and data availability

AIRS data are distributed by the NASA Goddard Earth Sciences Data Information and Services Center (AIRS Science Team and Chahine, 2007). The SO₂ index data used in this study are available for download at <https://datapub.fz-juelich.de/slcs/airs/volcanoes/> (last access: 21 Aug 2017). Envisat MIPAS Level-1B data are distributed by the European Space Agency. The ERA–Interim reanalysis data were obtained from the European Centre for Medium-Range Weather Forecasts. The code of the Massive-Parallel Trajectory Calculations (MPTRAC) model is available under the terms and conditions of the GNU General Public License, Version 3 from the repository at <https://github.com/slcs-jsc/mptrac> (last access: 12 April 2017).

455 **8 Competing interests**

The authors declare that they have no conflict of interest.

Acknowledgements. This work was supported by National Natural Science Foundation of China under grant No. 41605023 and International Postdoctoral Exchange Fellowship Program 2015 under grant No. 20151006. The

460 PV gradient based transport barrier data is provided by Dr. Felix Ploeger, ~~from Institute of Energy and Climate Research: Stratosphere (IEK-7), Forschungszentrum Jülich GmbH.~~

References

- Abalos, M., Ploeger, F., Konopka, P., Randel, W., and Serrano, E.: Ozone seasonality above the tropical tropopause: reconciling the Eulerian and Lagrangian perspectives of transport processes, *Atmos. Chem. Phys.*, 13, 10787-10794, doi:10.5194/acp-13-10787-2013, 2013.
- Aumann, H. H., Chahine, M. T., Gautier, C., Goldberg, M. D., Kalnay, E., McMillin, L. M., Revercomb, H., Rosenkranz, P. W., Smith, W. L., Staelin, D. H., Strow, L. L., and Susskind, J.: AIRS/AMSU/HSB on the Aqua mission: design, science objectives, data products, and processing systems, *IEEE Trans. Geosci. Remote Sens.*, 41, 253-264, doi: 10.1109/TGRS.2002.808356, 2003.
- Brühl, C., Lelieveld, J., Tost, H., Höpfner, M., and Glatthor, N.: Stratospheric sulfur and its implications for radiative forcing simulated by the chemistry climate model EMAC, *Journal of Geophysical Research: Atmospheres*, 120, 2103-2118, doi: 10.1002/2014JD022430, 2015.
- Butchart, N., Scaife, A. A., Bourqui, M., de Grandpre, J., Hare, S. H. E., Kettleborough, J., Langematz, U., Manzini, E., Sassi, F., Shibata, K., Shindell, D., and Sigmond, M.: Simulations of anthropogenic change in the strength of the Brewer-Dobson circulation, *Climate Dynam.*, 27, 727-741, 10.1007/s00382-006-0162-4, 2006.
- Carboni, E., Grainger, R. G., Mather, T. A., Pyle, D. M., Thomas, G. E., Siddans, R., Smith, A. J. A., Dudhia, A., Koukouli, M. E., and Balis, D.: The vertical distribution of volcanic SO₂ plume measured by IASI, *Atmos. Chem. Phys.*, 16, 4343-4367, doi: 10.5194/acp-16-4343-2016, 2016.
- Dee, D. P., Uppala, S. M., Simmons, A. J., Berrisford, P., Poli, P., Kobayashi, S., Andrae, U., Balmaseda, M. A., Balsamo, G., Bauer, P., Bechtold, P., Beljaars, A. C. M., van de Berg, L., Bidlot, J., Bormann, N., Delsol, C., Dragani, R., Fuentes, M., Geer, A. J., Haimberger, L., Healy, S. B., Hersbach, H., Hód, E. V., Isaksen, L., Kållberg, P., Köhler, M., Matricardi, M., McNally, A. P., Monge-Sanz, B. M., Morcrette, J. J., Park, B. K., Peubey, C., de Rosnay, P., Tavolato, C., Thépaut, J. N., and Vitart, F.: The ERA-Interim reanalysis: configuration and performance of the data assimilation system, *Q. J. R. Meteorol. Soc.*, 137, 553-597, doi: 10.1002/qj.828, 2011.
- Doeringer, D., Eldering, A., Boone, C. D., González Abad, G., and Bernath, P. F.: Observation of sulfate aerosols and SO₂ from the Sarychev volcanic eruption using data from the Atmospheric Chemistry Experiment (ACE), *J. Geophys. Res. Atmos.*, 117, D03203, doi: 10.1029/2011JD016556, 2012.
- Fadnavis, S., Semeniuk, K., Pozzoli, L., Schultz, M. G., Ghude, S. D., Das, S., and Kakatkar, R.: Transport of aerosols into the UTLS and their impact on the Asian monsoon region as seen in a global model simulation, *Atmos. Chem. Phys.*, 13, 8771-8786, doi: 10.5194/acp-13-8771-2013, 2013.
- Fairlie, T. D., Vernier, J. P., Natarajan, M., and Bedka, K. M.: Dispersion of the Nabro volcanic plume and its relation to the Asian summer monsoon, *Atmos. Chem. Phys.*, 14, 7045-7057, doi: 10.5194/acp-14-7045-2014, 2014.
- Fischer, H., Birk, M., Blom, C., Carli, B., Carlotti, M., von Clarmann, T., Delbouille, L., Dudhia, A., Ehhalt, D., Endemann, M., Flaud, J. M., Gessner, R., Kleinert, A., Koopman, R., Langen, J., López-Puertas, M., Mosner, P., Nett, H., Oelhaf, H., Perron, G., Remedios, J., Ridolfi, M., Stiller, G., and Zander, R.: MIPAS: an instrument for atmospheric and climate research, *Atmos. Chem. Phys.*, 8, 2151-2188, doi: 10.5194/acp-8-2151-2008, 2008.
- Folkens, I., Loewenstein, M., Podolske, J., Oltmans, S. J., and Proffitt, M.: A barrier to vertical mixing at 14 km in the tropics: Evidence from ozonesondes and aircraft measurements, *J. Geophys. Res. Atmos.*, 104, 22095-22102, doi: 10.1029/1999JD900404, 1999.
- Fueglistaler, S., Dessler, A. E., Dunkerton, T. J., Folkens, I., Fu, Q., and Mote, P. W.: Tropical Tropopause Layer, *Rev. Geophys.*, 47, 31, doi: 10.1029/2008rg000267, 2009.
- Gerlach, T.: Volcanic versus anthropogenic carbon dioxide, *Eos, Trans. Am. Geophys. Union*, 92, 201-202, doi: 10.1029/2011EO240001, 2011.
- Gerlach, T. M.: Present-day CO₂ emissions from volcanos, *Eos, Trans. Am. Geophys. Union*, 72, 249-255, doi: 10.1029/90EO10192, 1991.
- Gottelman, A., Forster, P. M. d. F., Fujiwara, M., Fu, Q., Vömel, H., Gohar, L. K., Johanson, C., and Ammerman, M.: Radiation balance of the tropical tropopause layer, *J. Geophys. Res. Atmos.*, 109, D07103, doi: 10.1029/2003JD004190, 2004.
- Glanville, A. A., and Birner, T.: Role of vertical and horizontal mixing in the tape recorder signal near the tropical tropopause, *Atmos. Chem. Phys.*, 17, 4337-4353, doi: 10.5194/acp-17-4337-2017, 2017.
- Griessbach, S., Hoffmann, L., Spang, R., von Hobe, M., Müller, R., and Riese, M.: Infrared limb emission measurements of aerosol in the troposphere and stratosphere, *Atmos. Meas. Tech.*, 9, 4399-4423, doi:10.5194/amt-9-4399-2016, 2016.
- Haynes, P., and Shuckburgh, E.: Effective diffusivity as a diagnostic of atmospheric transport: 2. Troposphere and lower stratosphere, *J. Geophys. Res. Atmos.*, 105, 22795-22810, doi: 10.1029/2000JD900092, 2000.

- Haywood, J. M., Jones, A., Clarisse, L., Bourassa, A., Barnes, J., Telford, P., Bellouin, N., Boucher, O., Agnew, P., Clerbaux, C., Coheur, P., Degenstein, D., and Braesicke, P.: Observations of the eruption of the Sarychev volcano and simulations using the HadGEM2 climate model, *J. Geophys. Res. Atmos.*, 115, D21212, doi: 10.1029/2010JD014447, 2010.
- 525 Haywood, J. M., Jones, A., and Jones, G. S.: The impact of volcanic eruptions in the period 2000–2013 on global mean temperature trends evaluated in the HadGEM2-ES climate model, *Atmos. Sci. Lett.*, 15, 92-96, doi: 10.1002/asl2.471, 2014.
- Heng, Y., Hoffmann, L., Griessbach, S., Rößler, T., and Stein, O.: Inverse transport modeling of volcanic sulfur dioxide emissions using large-scale simulations, *Geosci. Model Dev.*, 9, 1627-1645, doi:10.5194/gmd-9-1627-2016, 2016.
- 530 Hoffmann, L., Griessbach, S., and Meyer, C. I.: Volcanic emissions from AIRS observations: detection methods, case study, and statistical analysis, in: *Remote Sensing of Clouds and the Atmosphere XIX and Optics in Atmospheric Propagation and Adaptive Systems XVII*, edited by: Comerón, A., Kassianov, E. I., Schafer, K., Picard, R. H., Stein, K., and Gonglewski, J. D., *Proceedings of SPIE, Spie-Int Soc Optical Engineering*, Bellingham, doi: 92421410.1117/12.2066326, 2014.
- 535 Hoffmann, L., Rößler, T., Griessbach, S., Heng, Y., and Stein, O.: Lagrangian transport simulations of volcanic sulfur dioxide emissions: Impact of meteorological data products, *J. Geophys. Res. Atmos.*, 121, 4651-4673, doi: 10.1002/2015JD023749, 2016.
- Hofmann, D., Barnes, J., O'Neill, M., Trudeau, M., and Neely, R.: Increase in background stratospheric aerosol observed with lidar at Mauna Loa Observatory and Boulder, Colorado, *Geophys. Res. Lett.*, 36, L15808, doi: 10.1029/2009GL039008, 2009.
- 540 Jégou, F., Berthet, G., Brogniez, C., Renard, J. B., François, P., Haywood, J. M., Jones, A., Bourgeois, Q., Lurton, T., Auriol, F., Godin-Beekmann, S., Guimbaud, C., Krysztofiak, G., Gaubicher, B., Chartier, M., Clarisse, L., Clerbaux, C., Balois, J. Y., Verwaerde, C., and Daugeron, D.: Stratospheric aerosols from the Sarychev volcano eruption in the 2009 Arctic summer, *Atmos. Chem. Phys.*, 13, 6533-6552, doi: 10.5194/acp-13-6533-2013, 2013.
- 545 [Khaykin, S. M., Godin-Beekmann, S., Keckhut, P., Hauchecorne, A., Jumelet, J., Vernier, J. P., Bourassa, A., Degenstein, D. A., Rieger, L. A., Bingen, C., Vanhellemont, F., Robert, C., DeLand, M., and Bhartia, P. K.: Variability and evolution of the midlatitude stratospheric aerosol budget from 22 years of ground-based lidar and satellite observations, *Atmos. Chem. Phys.*, 17, 1829-1845, doi: 10.5194/acp-17-1829-2017, 2017.](#)
- 550 [Klüber, L., Erbertseder, T., and Meyer-Arnek, J.: Observation of volcanic ash from Puyehue–Cordón Caulle with IASI, *Atmos. Meas. Tech.*, 6, 35-46, doi:10.5194/amt-6-35-2013, 2013.](#)
- [Konopka, P., Grooß J.-U., Plöger, F., and Müller, R.: Annual cycle of horizontal in-mixing into the lower tropical stratosphere, *J. Geophys. Res. Atmos.*, 114, D19111, doi: 10.1029/2009JD011955, 2009.](#)
- 555 [Konopka, P., Grooß J. U., Günther, G., Ploeger, F., Pommrich, R., Müller, R., and Livesey, N.: Annual cycle of ozone at and above the tropical tropopause: observations versus simulations with the Chemical Lagrangian Model of the Stratosphere \(CLaMS\), *Atmos. Chem. Phys.*, 10, 121-132, doi: 10.5194/acp-10-121-2010, 2010.](#)
- [Kravitz, B., and Robock, A.: Climate effects of high-latitude volcanic eruptions: Role of the time of year, *J. Geophys. Res.*, 116, D01105, doi: 10.1029/2010JD014448, 2011.](#)
- 560 [Kravitz, B., Robock, A., Bourassa, A., Deshler, T., Wu, D., Mattis, I., Finger, F., Hoffmann, A., Ritter, C., Bitar, L., Duck, T. J., and Barnes, J. E.: Simulation and observations of stratospheric aerosols from the 2009 Sarychev volcanic eruption, *J. Geophys. Res. Atmos.*, 116, D18211, doi: 10.1029/2010JD015501, 2011.](#)
- 565 [Kremser, S., Thomason, L. W., von Hobe, M., Hermann, M., Deshler, T., Timmreck, C., Toohey, M., Stenke, A., Schwarz, J. P., Weigel, R., Fueglistaler, S., Prata, F. J., Vernier, J.-P., Schlager, H., Barnes, J. E., Antuña-Marrero, J.-C., Fairlie, D., Palm, M., Mahieu, E., Notholt, J., Rex, M., Bingen, C., Vanhellemont, F., Bourassa, A., Plane, J. M. C., Klocke, D., Carn, S. A., Clarisse, L., Trickl, T., Neely, R., James, A. D., Rieger, L., Wilson, J. C., and Meland, B.: Stratospheric aerosol – Observations, processes, and impact on climate, *Rev. Geophys.*, 54, 278–335, doi: 10.1002/2015RG000511, 2016.](#)
- 570 Levin, B. W., Rybin, A. V., Vasilenko, N. F., Prytkov, A. S., Chibisova, M. V., Kogan, M. G., Steblov, G. M., and Frolov, D. I.: Monitoring of the eruption of the Sarychev Peak Volcano in Matua Island in 2009 (central Kurile islands), *Dokl. Earth Sci.*, 435, 1507-1510, doi: 10.1134/s1028334x10110218, 2010.
- [Manktelow, P. T., Carslaw, K. S., Mann, G. W., and Spracklen, D. V.: Variable CCN formation potential of regional sulfur emissions, *Atmos. Chem. Phys.*, 9, 3253–3259, doi: 10.5194/acp-9-3253-2009, 2009.](#)
- 575 Neely, R. R., Toon, O. B., Solomon, S., Vernier, J. P., Alvarez, C., English, J. M., Rosenlof, K. H., Mills, M. J., Bardeen, C. G., Daniel, J. S., and Thayer, J. P.: Recent anthropogenic increases in SO₂ from Asia have minimal impact on stratospheric aerosol, *Geophys. Res. Lett.*, 40, 999-1004, doi: 10.1002/grl.50263, 2013.
- Niemeier, U., Timmreck, C., Graf, H. F., Kinne, S., Rast, S., and Self, S.: Initial fate of fine ash and sulfur from large volcanic eruptions, *Atmos. Chem. Phys.*, 9, 9043-9057, doi: 10.5194/acp-9-9043-2009, 2009.

- 580 Oman, L., Robock, A., Stenchikov, G. L., and Thordarson, T.: High-latitude eruptions cast shadow over the African monsoon and the flow of the Nile, *Geophys. Res. Lett.*, 33, L18711, doi: 10.1029/2006GL027665, 2006.
- Pausata, F. S. R., Chafik, L., Caballero, R., and Battisti, D. S.: Impacts of high-latitude volcanic eruptions on ENSO and AMOC, *Proc. Natl. Acad. Sci. U.S.A.*, 112, 13784-13788, doi: 10.1073/pnas.1509153112, 2015.
- 585 Ploeger, F., Gottschling, C., Griessbach, S., Grooß J. U., Guenther, G., Konopka, P., Müller, R., Riese, M., Stroh, F., Tao, M., Ungermann, J., Vogel, B., and von Hobe, M.: A potential vorticity-based determination of the transport barrier in the Asian summer monsoon anticyclone, *Atmos. Chem. Phys.*, 15, 13145-13159, doi: 10.5194/acp-15-13145-2015, 2015.
- Ploeger, F., Günther, G., Konopka, P., Fueglistaler, S., Müller, R., Hoppe, C., Kunz, A., Spang, R., Grooß J. U., and Riese, M.: Horizontal water vapor transport in the lower stratosphere from subtropics to high latitudes during boreal summer, *J. Geophys. Res. Atmos.*, 118, 8111-8127, doi: 10.1002/jgrd.50636, 2013.
- Randel, W. J., and Park, M.: Deep convective influence on the Asian summer monsoon anticyclone and associated tracer variability observed with Atmospheric Infrared Sounder (AIRS), *J. Geophys. Res. Atmos.*, 111, D12314, doi: 10.1029/2005JD006490, 2006.
- 595 Ridley, D. A., Solomon, S., Barnes, J. E., Burlakov, V. D., Deshler, T., Dolgii, S. I., Herber, A. B., Nagai, T., Neely, R. R., Nevzorov, A. V., Ritter, C., Sakai, T., Santer, B. D., Sato, M., Schmidt, A., Uchino, O., and Vernier, J. P.: Total volcanic stratospheric aerosol optical depths and implications for global climate change, *Geophys. Res. Lett.*, 41, 7763-7769, doi: 10.1002/2014GL061541, 2014.
- 600 [Rieger, L. A., Bourassa, A. E., and Degenstein, D. A.: Merging the OSIRIS and SAGE II stratospheric aerosol records, *Journal of Geophysical Research: Atmospheres*, 120, 8890-8904, doi: 10.1002/2015JD023133, 2015.](#)
- Robock, A.: Volcanic eruptions and climate, *Rev. Geophys.*, 38, 191-219, 10.1029/1998RG000054, 2000.
- Robock, A.: The Latest on Volcanic Eruptions and Climate, *Eos, Trans. Am. Geophys. Union*, 94, 305-306, doi: 10.1002/2013EO350001, 2013.
- 605 Rodriguez, J. M., Ko, M. K. W., and Sze, N. D.: Role of the heterogeneous conversion of N₂O₅ on sulfate aerosols in global ozone losses, *Nature*, 352, 134-137, doi: 10.1038/352134a0, 1991.
- Rybin, A., Chibisova, M., Webley, P., Steensen, T., Izbekov, P., Neal, C., and Realmuto, V.: Satellite and ground observations of the June 2009 eruption of Sarychev Peak volcano, Matua Island, Central Kuriles, *Bull. Volcanol.*, 73, 1377-1392, doi: 10.1007/s00445-011-0481-0, 2011.
- 610 Santer, B. D., Bonfils, C., Painter, J. F., Zelinka, M. D., Mears, C., Solomon, S., Schmidt, G. A., Fyfe, J. C., Cole, J. N. S., Nazarenko, L., Taylor, K. E., and Wentz, F. J.: Volcanic contribution to decadal changes in tropospheric temperature, *Nature Geosci.*, 7, 185-189, doi: 10.1038/ngeo2098, 2014.
- Schmidt, A., Carslaw, K. S., Mann, G. W., Wilson, M., Breider, T. J., Pickering, S. J., and Thordarson, T.: The impact of the 1783–1784 AD Laki eruption on global aerosol formation processes and cloud condensation nuclei, *Atmos. Chem. Phys.*, 10, 6025-6041, doi: 10.5194/acp-10-6025-2010, 2010.
- 615 Seviour, W. J. M., Butchart, N., Hardiman, S. C.: The Brewer–Dobson circulation inferred from ERA-Interim. *Q. J. R. Meteorol. Soc.*, 138: 878–888. doi:10.1002/qj.966, 2012.
- Solomon, S., Daniel, J. S., Neely, R. R., Vernier, J.-P., Dutton, E. G., and Thomason, L. W.: The Persistently Variable “Background” Stratospheric Aerosol Layer and Global Climate Change, *Science*, 333, 866-870, doi: 10.1126/science.1206027, 2011.
- 620 Solomon, S., Ivy, D. J., Kinnison, D., Mills, M. J., Neely R. R., Schmidt, A.: Emergence of healing in the Antarctic ozone layer. *Science*, doi: http://dx.doi.org/10.1126/science.aae0061, 2016.
- Solomon, S., Sanders, R. W., Garcia, R. R., and Keys, J. G.: Increased chlorine dioxide over Antarctica caused by volcanic aerosols from Mount-Pinatubo, *Nature*, 363, 245-248, doi: 10.1038/363245a0, 1993.
- 625 [Spang, R., Riese, M., and Offermann, D.: CRISTA-2 observations of the south polar vortex in winter 1997: A new dataset for polar process studies, *Geophys. Res. Lett.*, 28, 3159–3162, doi: 10.1029/2000GL012374, 2001.](#)
- [Stenchikov, G. L., Kirchner, I., Robock, A., Graf, H.-F., Antuña, J. C., Grainger, R. G., Lambert, A., and Thomason, L.: Radiative forcing from the 1991 Mount Pinatubo volcanic eruption, *Journal of Geophysical Research: Atmospheres*, 103, 13837-13857, doi: 10.1029/98JD00693, 1998.](#)
- 630 Stohl, A., Forster, C., Frank, A., Seibert, P., and Wotawa, G.: Technical note: The Lagrangian particle dispersion model FLEXPART version 6.2, *Atmos. Chem. Phys.*, 5, 2461-2474, doi:10.5194/acp-5-2461-2005, 2005.
- [Textor, C., H.-F. Graf, M. Herzog, and J. M. Oberhuber, Injection of gases into the stratosphere by explosive volcanic eruptions, *J. Geophys. Res.*, 108\(D19\), 4606, doi:10.1029/2002JD002987, 2003.](#)
- 635 Tilmes, S., Muller, R., and Salawitch, R.: The sensitivity of polar ozone depletion to proposed geoengineering schemes, *Science*, 320, 1201-1204, doi: 10.1126/science.1153966, 2008.
- Timmreck, C.: Modeling the climatic effects of large explosive volcanic eruptions, *WIREs Clim. Change*, 3, 545-564, doi: 10.1002/wcc.192, 2012.

- 640 Vernier, J. P., Thomason, L. W., Pommereau, J. P., Bourassa, A., Pelon, J., Garnier, A., Hauchecorne, A.,
Blanot, L., Trepte, C., Degenstein, D., and Vargas, F.: Major influence of tropical volcanic eruptions on the
stratospheric aerosol layer during the last decade, *Geophys. Res. Lett.*, 38, L12807, doi:
10.1029/2011GL047563, 2011.
- von Glasow, R., Bobrowski, N., and Kern, C.: The effects of volcanic eruptions on atmospheric chemistry,
645 *Chem. Geol.*, 263, 131–142, doi: <http://dx.doi.org/10.1016/j.chemgeo.2008.08.020>, 2009.
- von Savigny, C., Ernst, F., Rozanov, A., Hommel, R., Eichmann, K. U., Rozanov, V., Burrows, J. P., and
Thomason, L. W.: Improved stratospheric aerosol extinction profiles from SCIAMACHY: validation and
sample results, *Atmos. Meas. Tech.*, 8, 5223-5235, doi: 10.5194/amt-8-5223-2015, 2015.

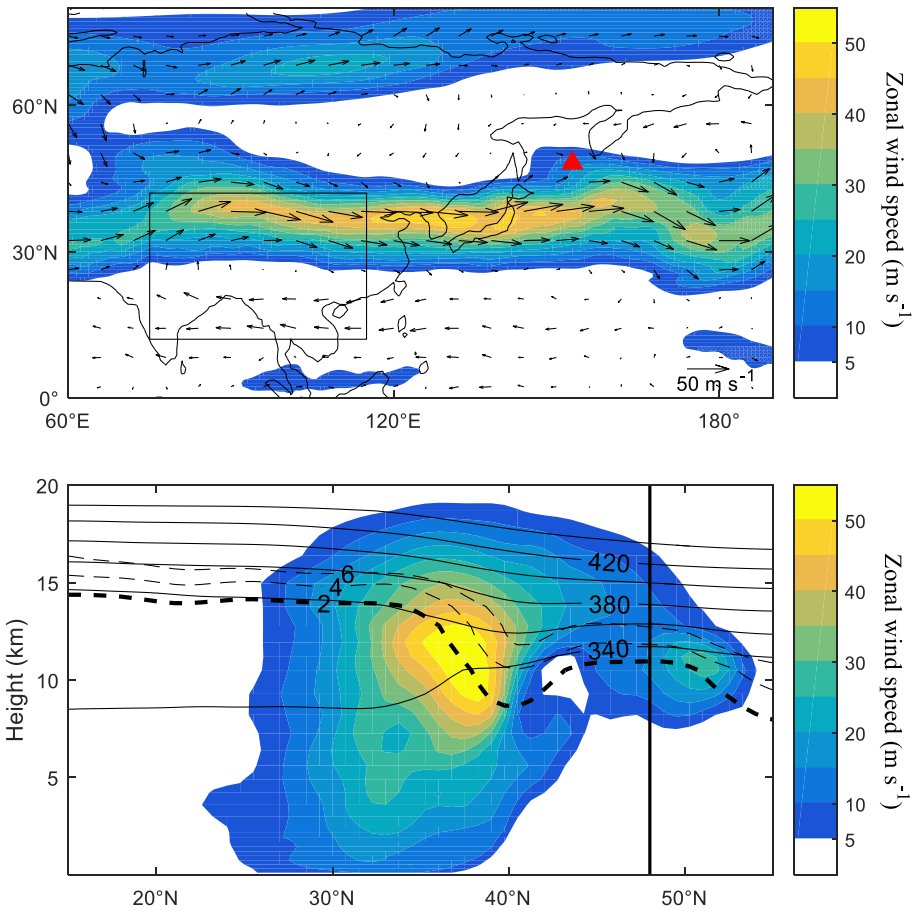


Figure 1: Meteorological conditions at the time of the Sarychev eruption (based on ERA-Interim reanalysis). Top: zonal wind (shaded) and wind vectors on the 370 K isentropic surface at 0 UTC on 12 June 2009. The location of the Sarychev peak is denoted with a red triangle. The black rectangle indicates the area of the developing ASM anticyclone. Bottom: vertical section of zonal wind (shaded) and contours of potential temperature from 340 K to 440 K (black solid lines) and potential vorticity from 2 PVU to 6 PVU (black dashed lines) along 153°E. The vertical black line denotes the latitude (48.1°N) of the Sarychev peak.

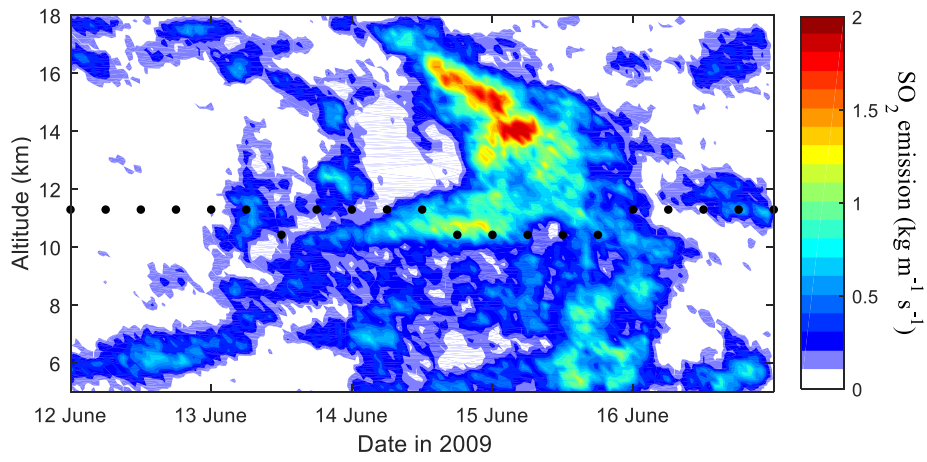


Figure 2: Sarychev SO₂ emission time series derived with AIRS measurements using a backward trajectory approach (see text for details). The emission data is binned every 1 hour and 0.2 km. Black dots denote the height of the thermal tropopause.

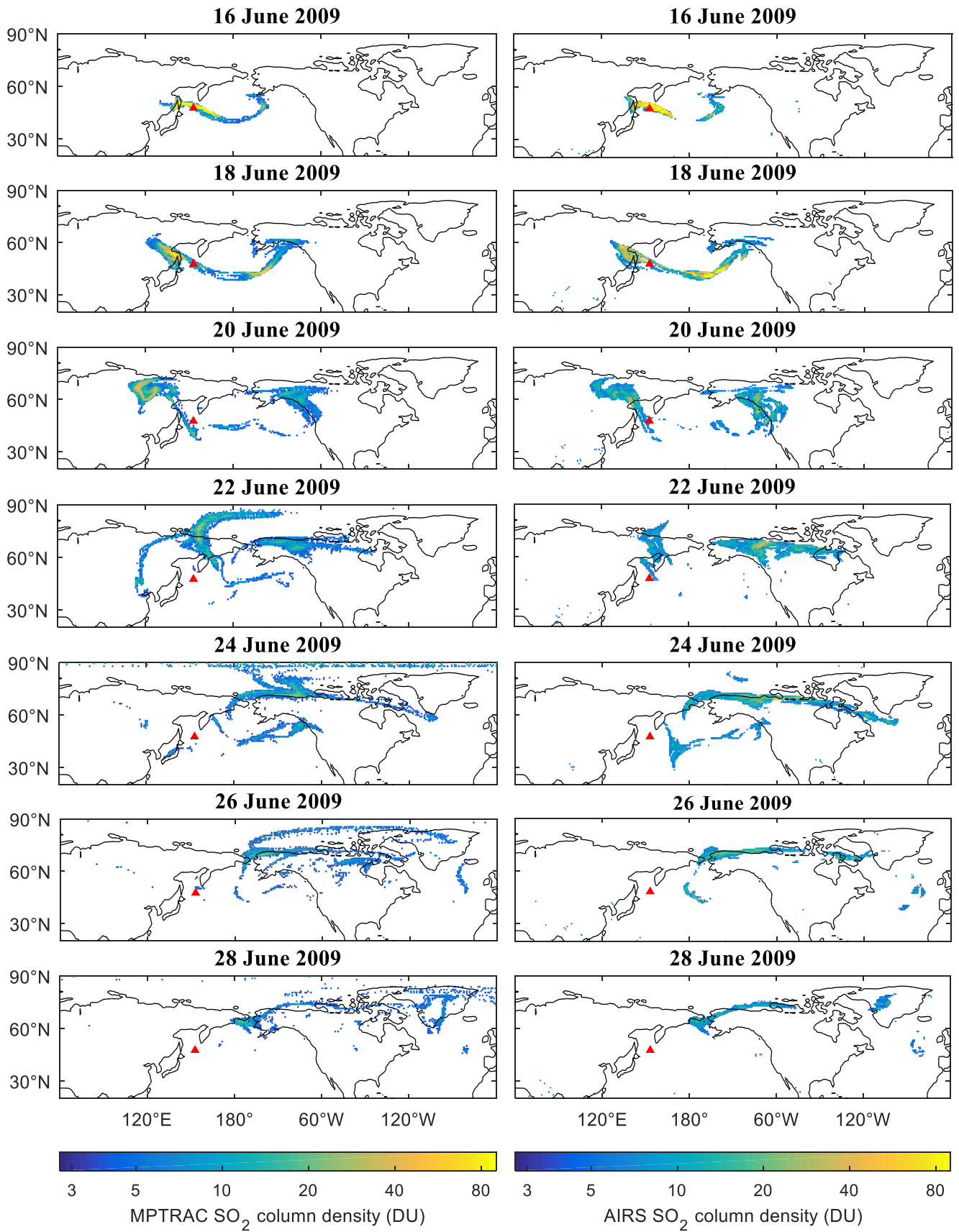


Figure 3: The evolution of SO₂ column density from MPTRAC simulations (left) and AIRS observations (right) for the period 16–28 June 2009. The MPTRAC SO₂ column densities are shown for 0 UTC on selected days and AIRS data are collected within ± 6 hours. Only values larger than 2 DU are shown. The red triangle denotes the location of the Sarychev peak.

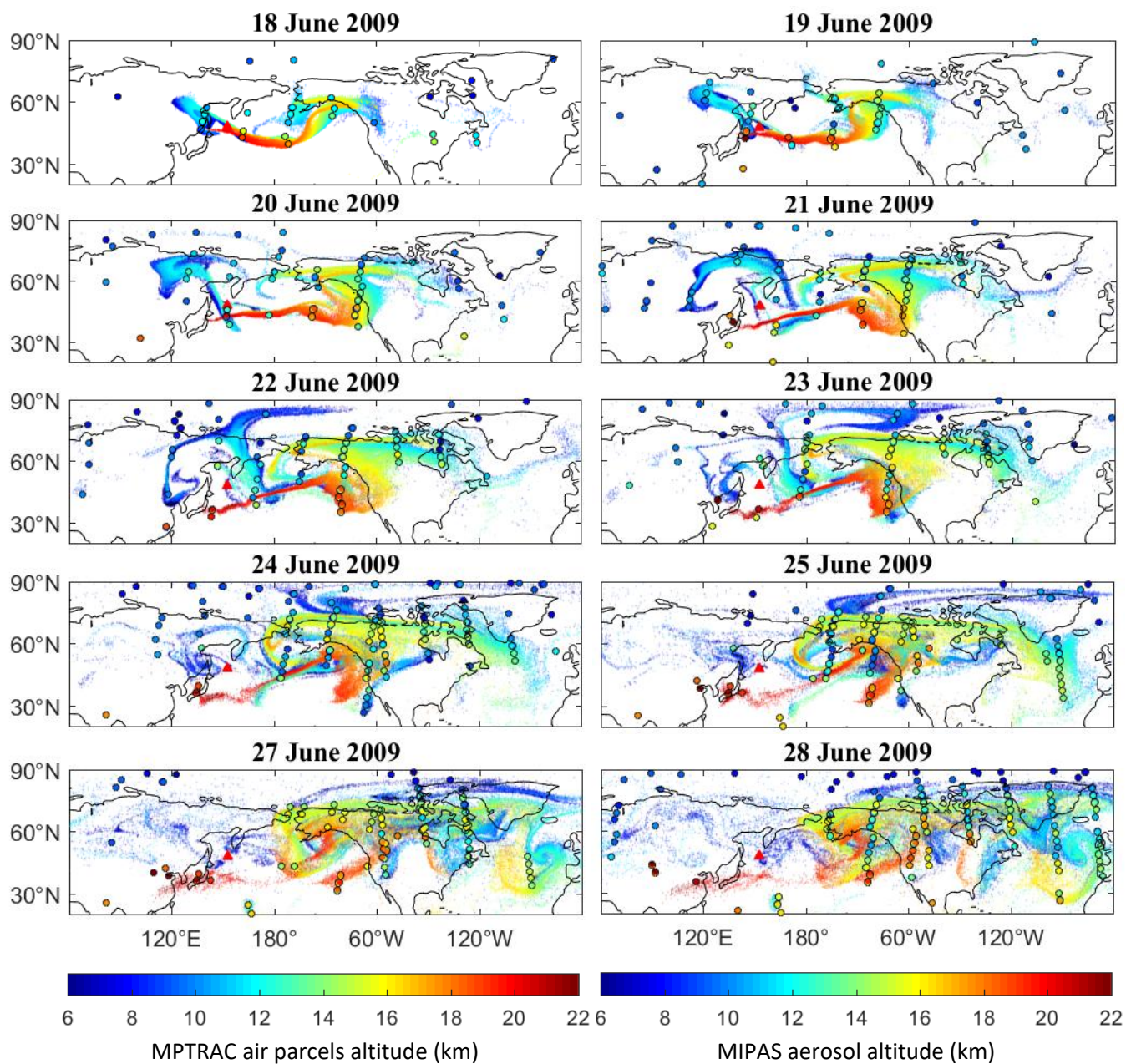


Figure 4: The evolution of SO₂ air parcel altitudes (shading) from MPTRAC simulations (shown for 0 UTC on selected days) and MIPAS aerosol detections within ± 6 hours (color-filled circles). The altitudes of all air parcels, regardless of their SO₂ values, are shown. The red triangle denotes the location of the Sarychev peak.

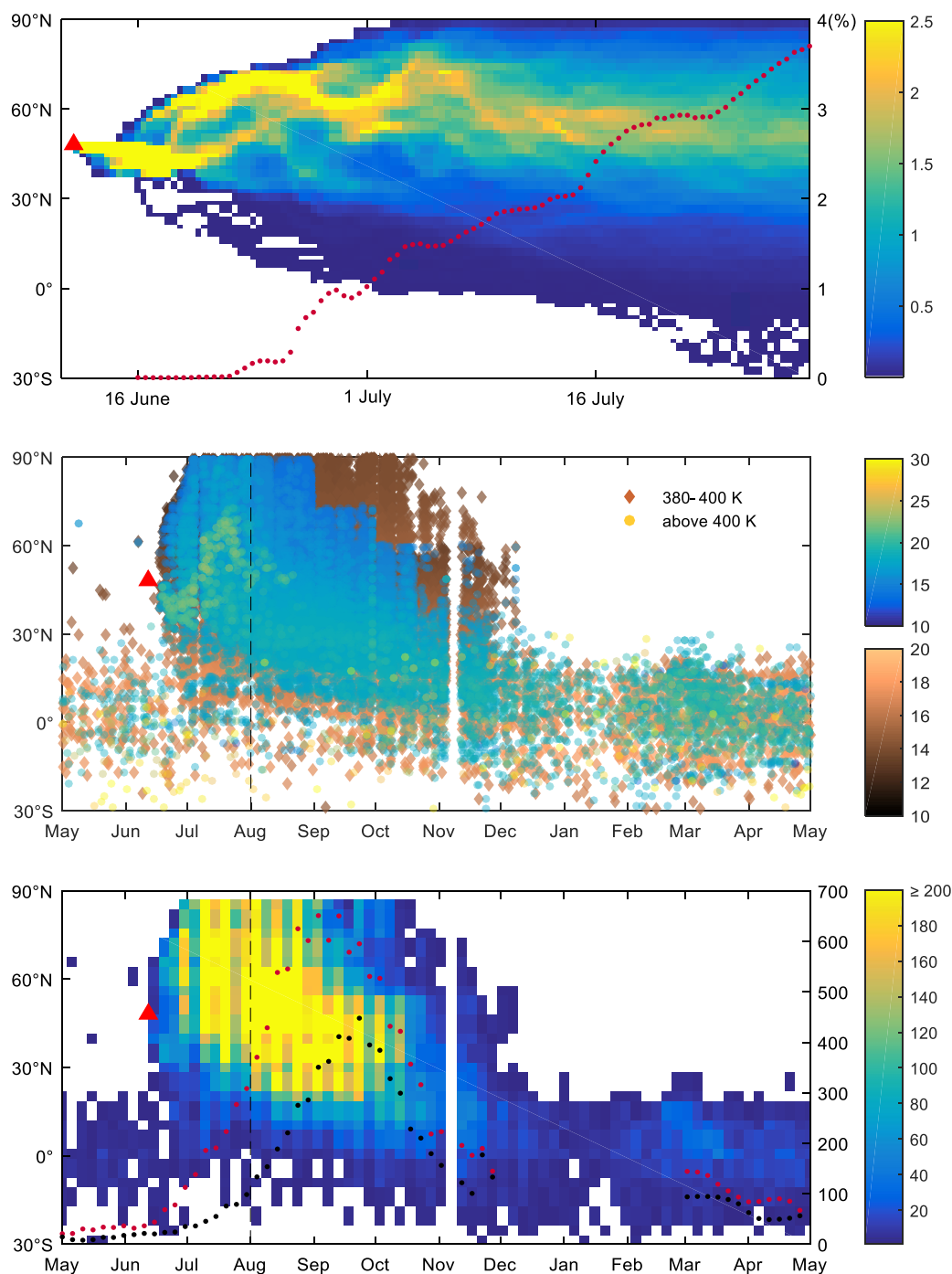


Figure 5: Top: Percentage (%) of air parcels above the 380 K isentropic surface from MPTRAC simulations, binned every 12 hours and 2° latitude. Red dots denote the percentage of air parcels above the 380 K isentropic surface between 30°N and 30°S. Middle: Altitudes (km) of MIPAS aerosol detections above the 380 K isentropic surface from May 2009 to April 2010. Bottom: Number of MIPAS aerosol detections above the 380 K isentropic surface from May 2009 to April 2010. Detections are binned every 5 days and 5° latitude. Red dots denote the number of the MIPAS aerosol detections above the 380 K isentropic surface between 30°N and 30°S. Black dots denote the number of the MIPAS aerosol detections above the 400 K isentropic surface between 30°N and 30°S. The number during the MIPAS data gap in 2009–2010 winter (Dec, Jan, and Feb) is omitted. The red triangle denotes the time and latitude of the first Sarychev eruption. Dashed lines in the middle and bottom panels indicate the time corresponding to the end of the MPTRAC simulation in the top panel, i.e., 31 July 2009.

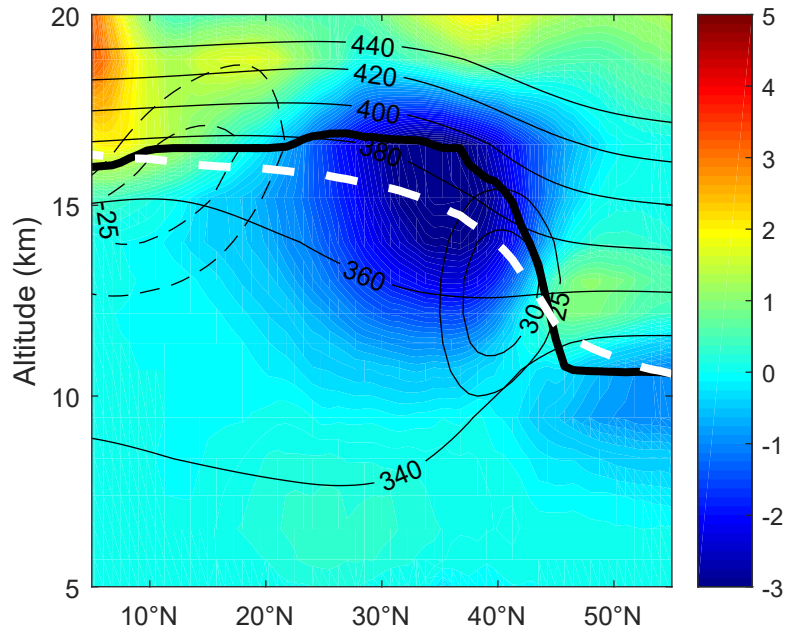


Figure 6: Meteorological conditions in the Asian monsoon anticyclone (based on ERA-Interim reanalysis). PV anomaly (shaded, unit: PVU) in the Asian monsoon anticyclone (40–120°E) with respect to the zonal mean, averaged over 2009 summer (June-August). Zonal wind (black solid lines indicating the westerlies and black dashed lines indicating the easterlies) is averaged between 40 and 120°E. The first thermal tropopause zonally averaged over 0 - 360°E is shown as dashed white line, averaged over 40 to 120°E as thick black line.

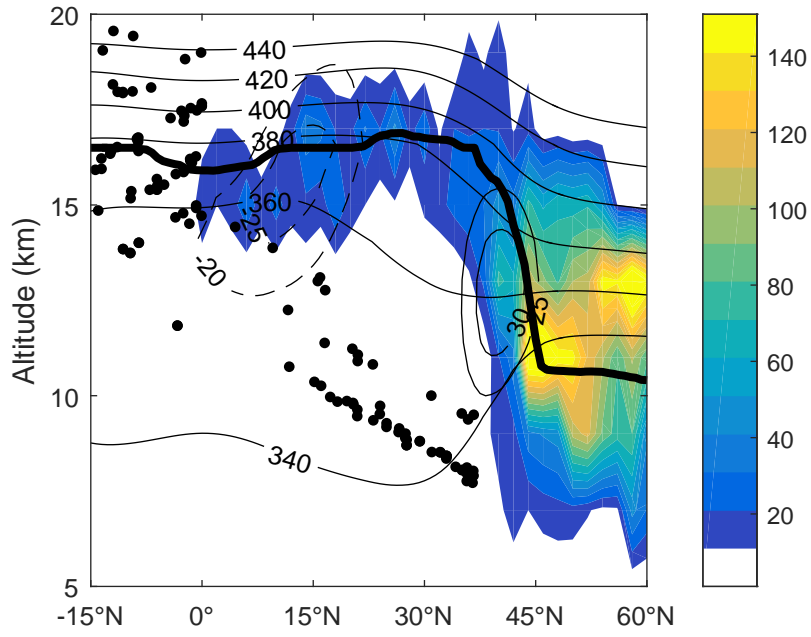


Figure 7: Number of MIPAS aerosol detections between 40°E and 120°E during June-August 2009 (binned every 2 km in altitude and 2° in latitude). Sparse detections (number of detections in each bin is smaller than 10 are shown with black dots). The tropopause, potential temperature, and zonal wind are the same as shown in Fig. 6.

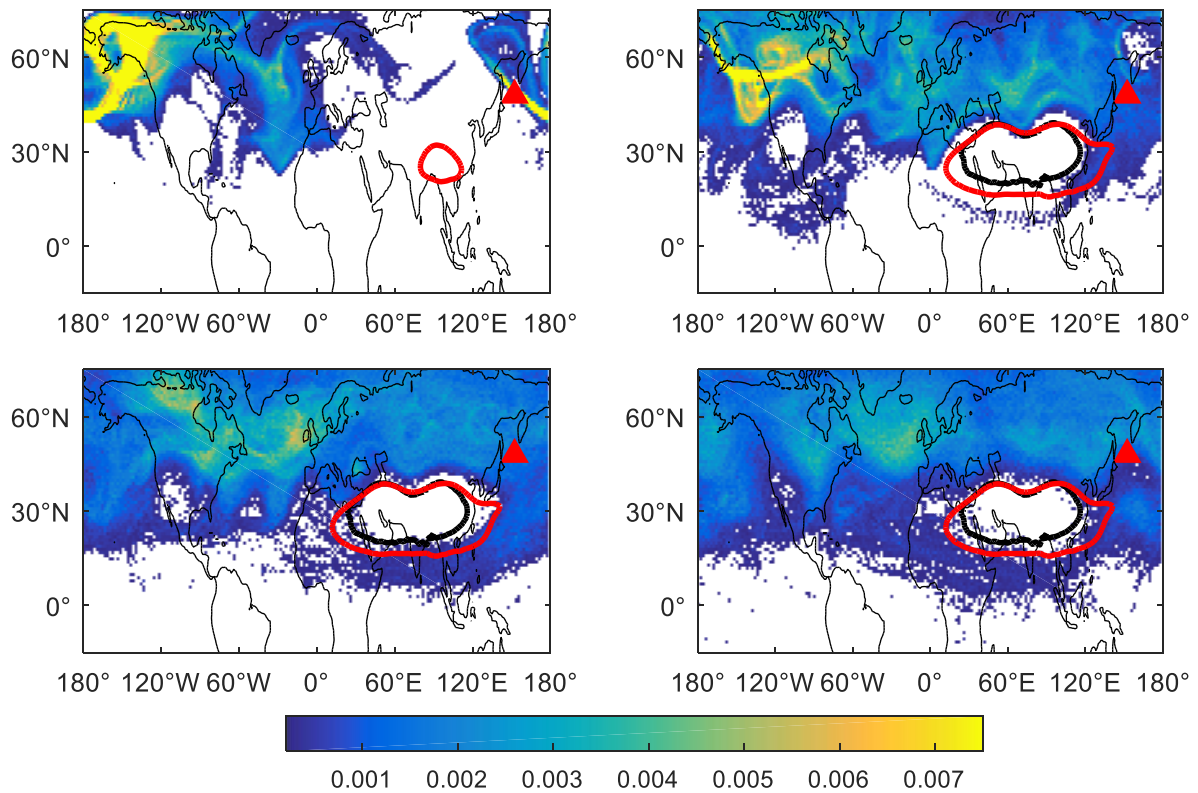


Figure 8: Percentage (%) of air parcels for 12–30 June (top left), 01–10 July (top right), 11–20 July (bottom left) and 21–31 July 2009 (bottom right) between isentropic surfaces of 360 and 400 K from MPTRAC simulations. Results are binned every 2° in longitude and 1° in latitude. The monthly mean 14,320 m geopotential height on the 150 hPa pressure surface is marked in red and the monthly mean PV-based barrier on the 370 K isentropic surface is marked in black. A PV-based barrier related to the Asian summer monsoon was not identified in June 2009. The red triangle denotes the location of the Sarychev volcano.

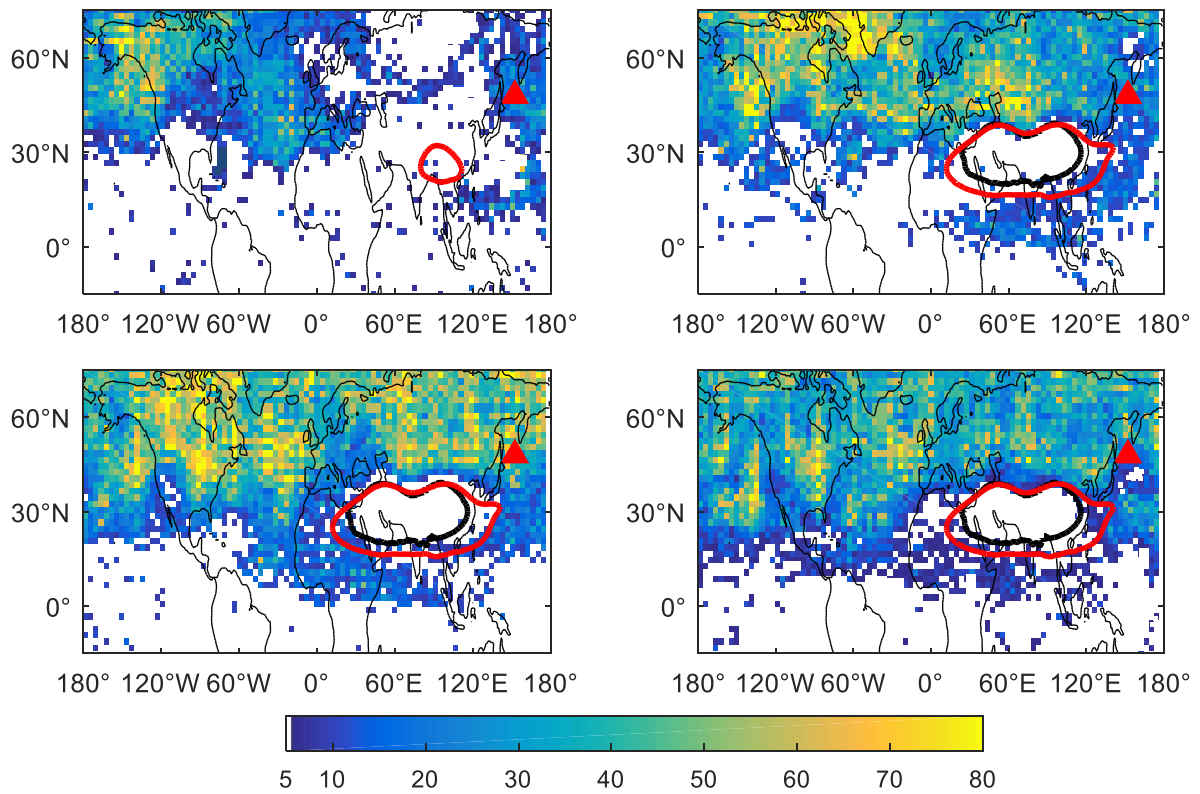


Figure 9: Number of aerosol data points generated with 1.5-day forward and 1.5-day backward trajectory calculation, for 12–30 June (top left), 01–10 July (top right), 11–20 July (bottom left) and 21–31 July 2009 (bottom right) between isentropic surfaces of 360 and 400 K. Results are binned every 4° in longitude and 2° in latitude. The 14,320 m geopotential height on the 150 hPa pressure surface is marked in red and the PV-based barrier on the 370 K isentropic surface is marked in black. The red triangle denotes the location of the Sarychev volcano.

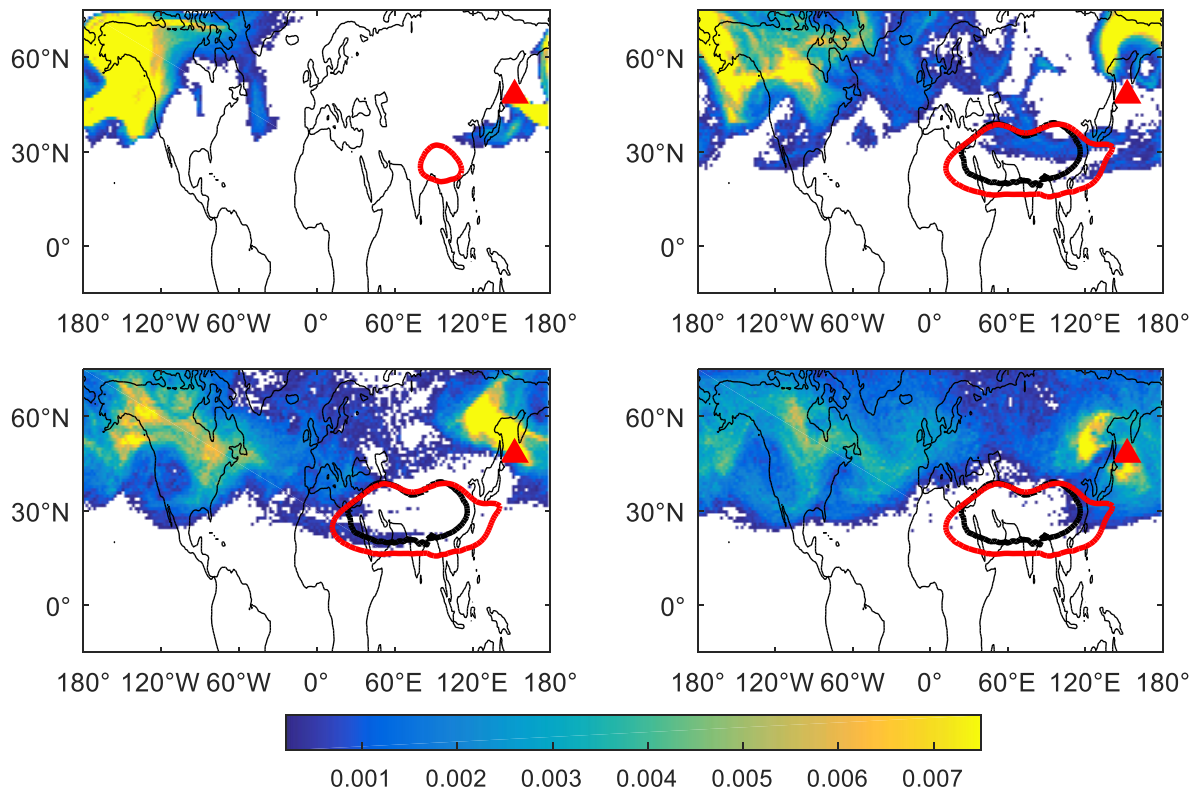


Figure 10: Same as Fig. 8 but for percentage (%) of total air parcels above the 400 K isentropic surface.

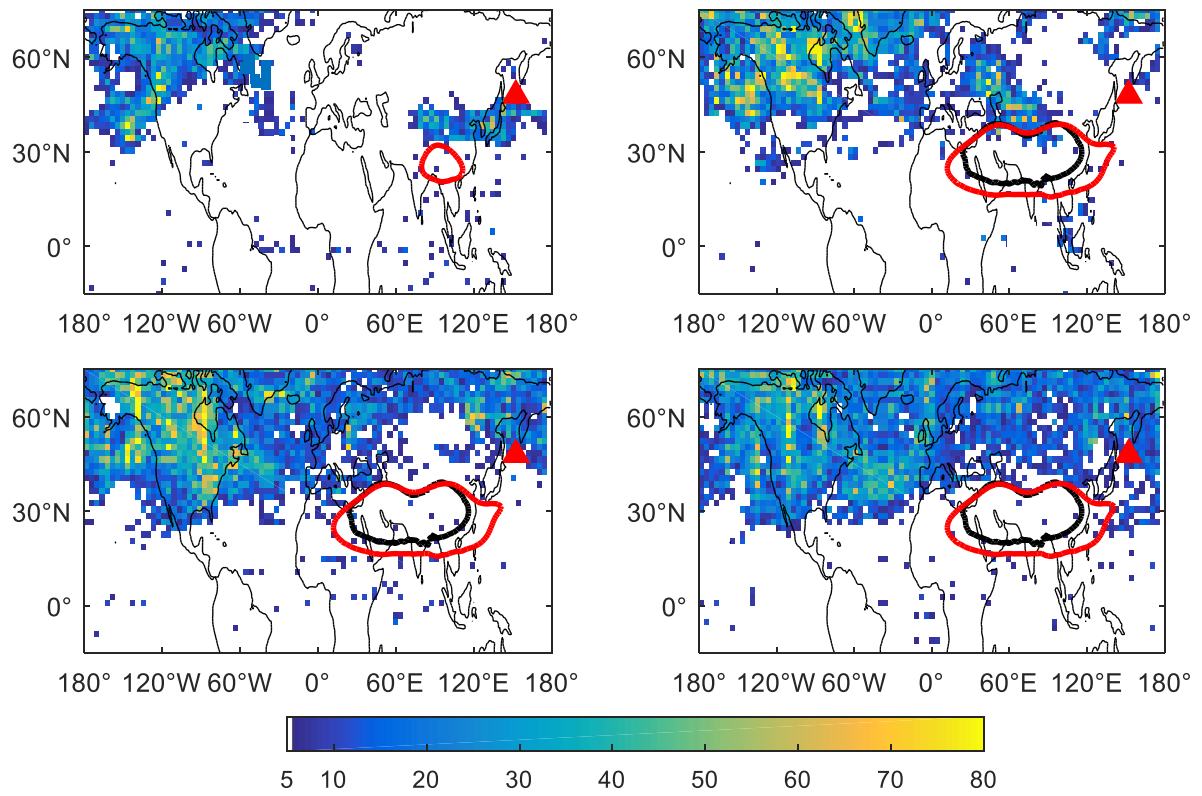


Figure 11: Same as Fig. 9, but for number of data points above the 400 K isentropic surface.

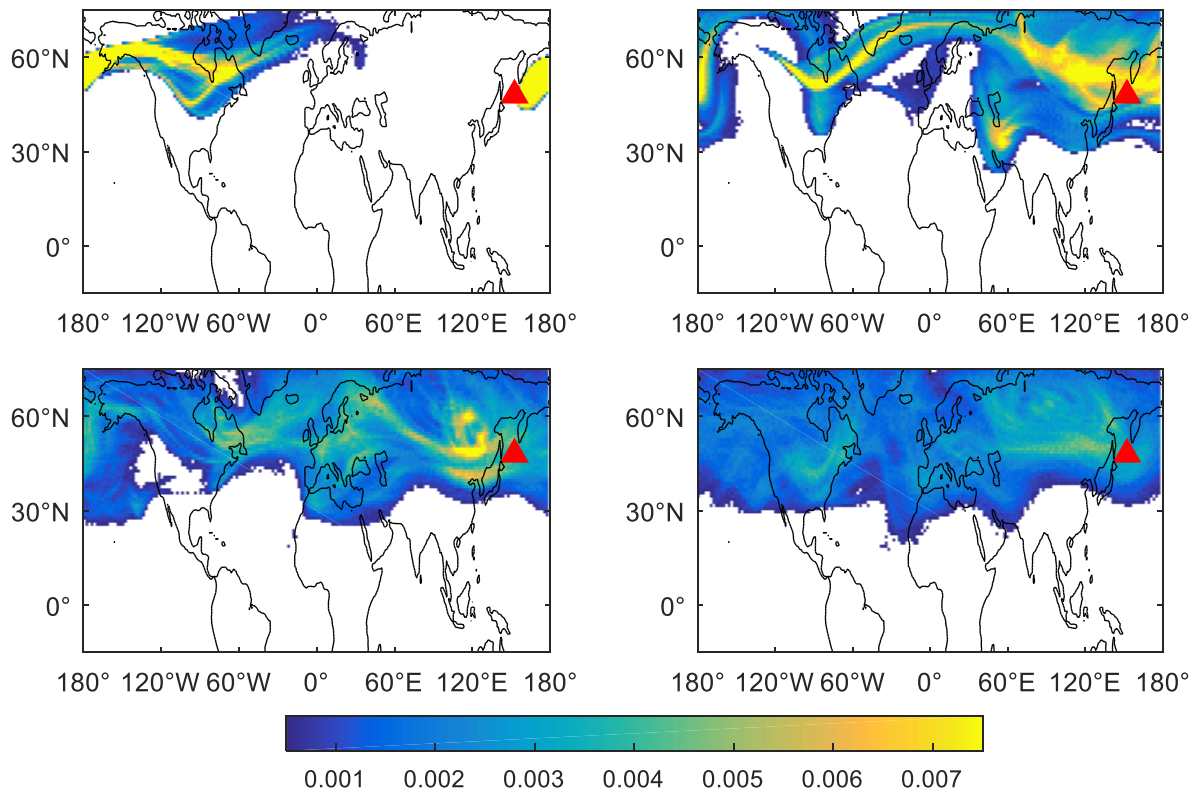


Figure 12: Percentage (%) of air parcels for the wintertime sensitivity study, on 10 January (top left), 20 January (top right), 31 January (bottom left) and 10 February 2009 (bottom right) from an MPTRAC simulation for a hypothetical eruption of the Sarychev **between isentropic surfaces of 360 and 400 K. Results are binned every 2° in longitude and 1° in latitude. The red triangle denotes the location of **the Sarychev volcano**.**

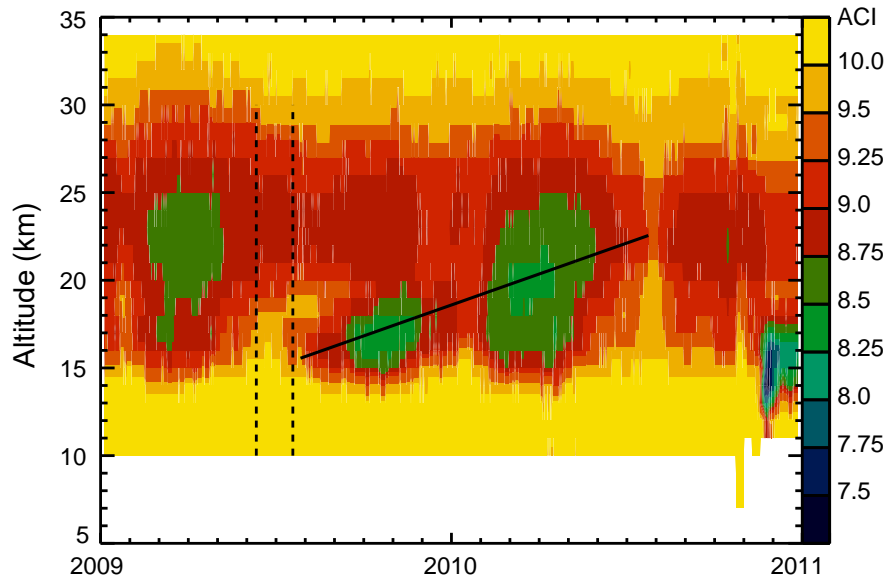


Figure 13: MIPAS nine-day running median of aerosol-cloud-index (ACI) between 10°N and 10°S (averaged along longitudes) from 2009 to 2010, overlaid with ascent speed of the water vapor tape recorder (solid line) derived with Aura Microwave Limb Sounder (MLS) water vapor mixing ratio from Glanville et al. (2017). Black dashed lines indicate the 12 June 2009 when the eruption started and 20 July 2009 when the simulations show first substantial aerosol transport to 10°N–10°S.